Therapeutic Targeting of Arteriogenesis Following Ischemic Stroke

Alexandra M. Kaloss

Dissertation submitted to the faculty of the
Virginia Polytechnic Institute and State University
in partial fulfillment of the requirements for the degree of

Doctor of Philosophy
In
Biomedical and Veterinary Sciences

Michelle Theus, Chair
John Chappell
William Huckle
Paul Morton

August 4, 2023
Blacksburg, Virginia

Keywords: Arteriogenesis, Pial Collateral, Ischemic Stroke, Endothelial Cell, Vasculotide

Therapeutic Targeting of Arteriogenesis Following Ischemic Stroke

Alexandra M. Kaloss

Abstract

Strokes are a leading cause of death and disability in the United States, predominantly caused by ischemic events. Ischemic strokes occur when a clot or other obstruction lodges in a blood vessel of the brain, restricting the movement of blood. Subsequent rapid cell death occurs and often leads to long term neurological deficits. Pial collaterals are a well-established determinant of patient outcome due to their unique ability to remodel into conductance arteries that can reroute blood back to the ischemic tissue. During development, pial collaterals arise within the pia mater and establish connections between distant arterioles of cerebral arteries. Under healthy conditions, these vessels are exposed to bidirectional blood flow, keeping them small and dormant. Following vascular obstruction, pial collaterals are exposed to unidirectional blood flow, triggering them to expand through an adaptive process termed, arteriogenesis, allowing for retrograde perfusion into the obstructed artery and its affected tissue. However, hyperacute arteriogenesis following ischemic stroke has been poorly investigated. The following dissertation aims to address this research gap and leverage the findings to develop therapeutics that enhance arteriogenesis. Previous research has revealed EphA4 restricts arteriogenesis through the Tie2 signaling axis, therefore this work sought to evaluate the endothelial cell (EC) specific role of the EphA4/Tie2 axis in acute arteriogenesis. EC-specific EphA4 KO mice displayed increased pial collateral size from 4.5 to 24-hours post-injury, which was associated with reduced tissue damage, improved cerebral blood flow, and enhanced motor function. Additionally, pharmaceutical stimulation of the Tie2 axis using Vasculotide, an angiopoietin-1 memetic peptide, replicates these findings. Administration of 3ug/kg Vasculotide to wildtype mice immediately after permanent middle cerebral artery occlusion leads to significantly larger pial collateral diameters, correlating with reduced tissue damage and improved functional recovery. Unlike Vasculotide, device stimulation using low intensity focused ultrasound failed to increase collateral diameter, despite resulting in profound neuroprotection. Taken together, this dissertation work demonstrates that the EphA4/Tie2 signaling pathway can be pharmacologically targeted to improve arteriogenesis following ischemic stroke.

Therapeutic Targeting of Arteriogenesis Following Ischemic Stroke

Alexandra M. Kaloss

General Audience Abstract

Worldwide, strokes are a leading cause of death and long-term disability with many cases being ischemic strokes, where a blood clot blocks blood flow to the brain. Without the critical oxygen and nutrients that the blood provides, cells in the affected region of the brain begin to rapidly die, leading to neurological deficits. While current treatments focus on removing the clot, it does not guarantee the restoration of blood flow to the damaged area. In contrast, our research focuses on pre-existing blood vessels in the brain, called pial collaterals, that can ease the loss of blood flow after stroke. These vessels, although relatively inactive under normal conditions, can enlarge after a stroke to reroute blood flow to the injured tissue. Thus, pial collateral growth is a critical process in the initial hours after stroke when this blood flow can prevent brain cells from dying. Previous work has shown EphA4, a receptor known for its role in nervous system development, restricts pial collateral size by inhibiting the Tie2 signaling pathway. Loss of EphA4 in endothelial cells allows for Tie2 receptor activation, increased pial collateral size, and decreased tissue damage. To explore therapeutic enhancement of pial collaterals, we administered Vasculotide, a drug that activates the Tie2 receptor, to wildtype mice expressing EphA4 after a stroke. The mice treated with Vasculotide displayed significantly larger pial collateral vessels one day after the stroke, compared to control mice. Moreover, Vasculotide-treated mice exhibited reduced tissue damage and performed better on behavioral assessments. In addition to pharmaceutical stimulation with Vasculotide, we also investigated the effects of low-intensity focused ultrasound (LIFU) on collateral size. LIFU treatment resulted in decreased tissue damage compared to untreated controls; however, it did not impact collateral size. These findings suggest that inhibiting EphA4 or stimulating Tie2 could serve as novel therapeutic targets to promote the expansion of pial collateral blood vessels, thereby restoring critical blood flow to injured areas of the brain.

Therapeutic Targeting of Arteriogenesis Following Ischemic Stroke

Alexandra M. Kaloss

Graphical Abstract

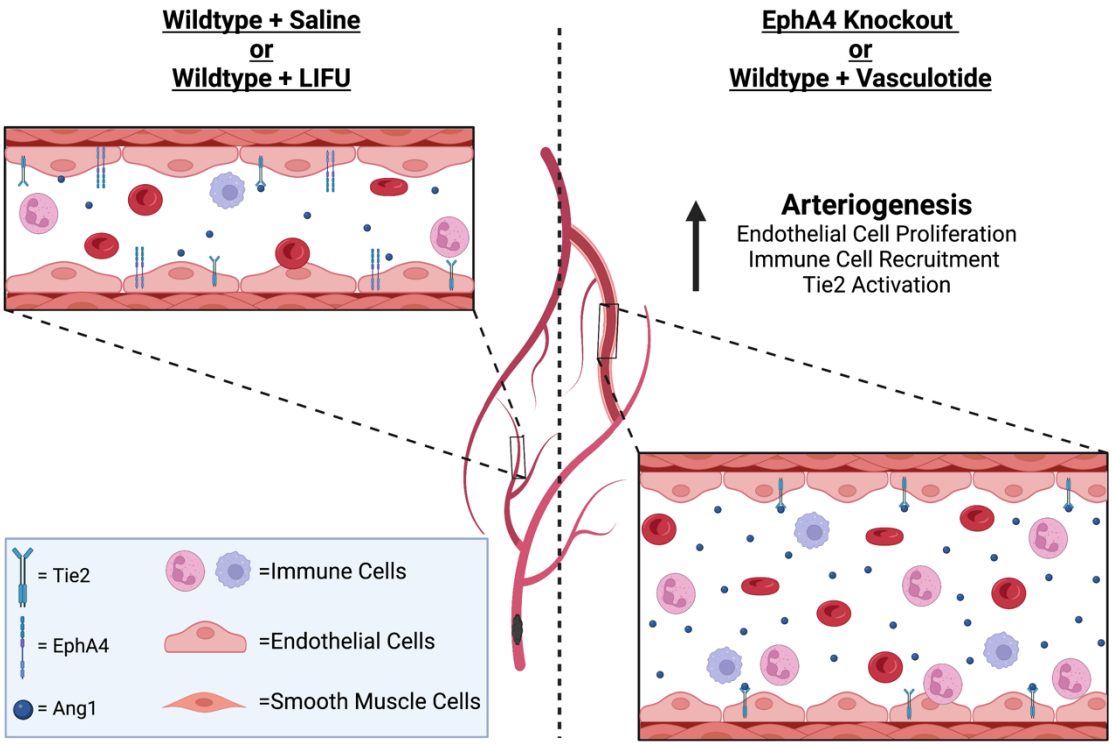

Dedication

To my parents, for turning me into the person I am today. None of this would have been possible without your unending love and support. Thank you for everything and may we always hope for the best.

Acknowledgements

Graduate school is by no means a solo endeavor and I am forever thankful to all the people who have supported me.

To God, for setting me on this journey and for being a light throughout it.

To my family, you have been an incredible support system that has given me the strength and inspiration to pursue this path. To my friends, especially Lauren, Amelia, Abbi, and Jake, thank you for all the chats, laughs, emotional support, and most importantly, for always reminding me of the value of a well-deserved break. To Ross, your patience, love, and support means more to me than you will ever know.

I am profoundly thankful to Dr. Michelle Theus; you are an extraordinary mentor. Your kindness, brilliance, passion, and support have shaped me into a true scientist and guided me through this program. Thank you for always listening to my ideas and supporting my goals. I will be forever grateful to have been a part of your team.

To Dr. Pickrell and Dr. Morton, this project would have never come to life without your help and willingness to share equipment. Thank you from the bottom of my heart.

To Dr. Chappell and Dr. Huckle, your scientific knowledge, feedback, and questions have shaped my project and helped me develop throughout my PhD work.

To my fellow lab mates and undergraduate students, you made these last four years immensely enjoyable. Thank you for your support, collaborative efforts, and the inspiration you provided along the way.

To the Life Science 1 staff and the RGS office, including Dr. Ahmed, Dr. Crawford, Andrea, and Monica, thank you for all the academic support and encouragement throughout my program. Thank you to the National Institute of Health (NIH) and BMVS program for funding and supporting this dissertation work.

Lastly to the many teachers, mentors, and club advisors that have brought me here. The life lessons you taught me have extended past the classroom and continue to shape the person I am today. I would not be where I am now, academically or personally, without you.

Table of Contents

Chapter 1: Introduction ……1
Chapter 2: Review of Literature ..……..4
Abstract
Introduction
The Unique Pial Collateral Vessel Niche
Influence of Fluid Shear Stress on Collateral Vessels
Mechanisms of Mechanosensing
Activation and Growth of Collateral Vessels
Activation of the Endothelium
Collateral Vessel Growth and Remodeling
Dual Role of Immune Modulation and LMA
Therapeutic Remodeling of LMA Remodeling
Vascular Endothelial Growth Factor
Colony Stimulating Factor
Statins
Physical Exercise
Conclusion
Chapter 3: Genetic and Pharmacological Targeting of The EphA4/Tie2 Axis Results in Improved Pial Collateral Response following Ischemic Stroke ……. 27
Abstract
Introduction
Results
Discussion
Methods
Figures
References
Chapter 4: Noninvasive Low-Intensity Focused Ultrasound Mediates Tissue Protection following Ischemic Stroke ..…….. 68
Abstract
Introduction
Results
Discussion
Methods
Figures
References
Chapter 5: Summary and Future Directions ……83

Chapter 1

Introduction

A stroke is the interruption of blood supply to the brain preventing oxygen and nutrients from reaching certain areas of the brain. Based on the cause of the blood flow disruption, strokes are divided into two categories: hemorrhagic and ischemic. Hemorrhagic strokes occur when a blood vessel in the brain begins leaking or bursts, leading to increased pressure on the surrounding brain tissue. Alternatively, ischemic strokes, which account for 87% of all stroke cases, result from a blood clot or other obstruction blocking the flow of blood through a brain supplying blood vessel [1]. Although a clot can lodge in any blood vessel within the brain, most often the clot lodges inside the middle cerebral artery (MCA) [2].

Within minutes of cessation of blood flow, brain cells begin to rapidly die, resulting in symptoms that range from mild and transient to severe and lethal. Despite their prevalence and potential severity, limited treatments exist for ischemic strokes and all focus on removal of the blood clot. Mechanical thrombectomy is a surgical intervention aimed at physically removing the clot and is most often utilized for large vessel occlusions [3-5]. Recombinant tissue plasminogen activator (rt-PA) is an infusion therapy that can break up clots but has a short window for administration and can lack efficacy for larger clots [6-8]. Successful removal of the blood clot using either treatment modality does not guarantee restoration of blood flow through the previously blocked-off vessel [9]. Therefore, novel therapeutics are needed for the treatment of ischemic strokes.

A promising direction for therapeutic development is targeting pial collaterals, or leptomeningeal anastomoses. Pial collaterals are direct arteriole connections between two conductance arteries, initially forming in utero and then undergo pruning to establish the adult pial collateral niche [10]. Under healthy conditions, these vessels experience bidirectional blood flow from their two connecting arteries and remain small and inactive. However, after an ischemic stroke, they can enlarge through a process termed arteriogenesis to reroute blood flow from the unaffected artery back to the starving tissue. The unique ability of these vessels to sustain the ischemic penumbra makes them a major predictor of patient outcome after an ischemic stroke, as an enhanced pial collateral niche is linked with improved prognosis [11].

Arteriogenesis is the process by which these pial collaterals enlarge in size to become major conductance arteries. Unlike angiogenesis, which is triggered by hypoxia, arteriogenesis is triggered by increased fluid shear stress (FSS), a mechanical stimulus [12]. The unidirectional blood flow that the pial collaterals experience after a blood clot becomes lodged in one of the connecting arteries increases FSS, activating arteriogenesis [13]. The mechanical stimulus is transferred into a chemical signal activating endothelial cells and smooth muscle cells to proliferate, peripheral immune cells are recruited, and the extracellular matrix is degraded to allow for outward expansion of the vessel [14]. This process occurs in the initial days to weeks following the ischemic stroke. However, despite it being well known that these vessels are critical in determining patient outcome, limited research has been conducted on how these vessels remodel in the initial hours after an ischemic stroke or how therapeutics impact their initial activation.

This dissertation focuses on identifying the temporal response of pial collaterals in the initial twenty-four hours following a stroke. It will also pursue multiple avenues for stimulation of these blood vessels with a focus on the role of endothelial cells (ECs). Previous research has implicated the EphA4/Tie2 axis in the regulation of collateral remodeling. Therefore, an endothelial cell-specific EphA4 KO model will be used to determine the contribution of EphA4 on these EC in negatively regulating arteriogenesis. Similarly, Vasculotide – an angiopoietin-1 memetic peptide and Tie2 agonist – will be employed to pharmacologically enhance collateral remodeling. Finally, low-intensity focused ultrasound (LIFU) will be explored for its use as a device driven therapeutic for collateral enhancement. These studies will further the knowledge of the cellular and molecular response in pial collateral vessels following large vessel occlusion and provide insight into numerous novel therapeutic options to stimulate these vessels.

1. Tsao, C.W., et al., *Heart Disease and Stroke Statistics-2023 Update: A Report From the American Heart Association.* Circulation, 2023. **147**(8): p. e93-e621.
2. Ng, Y.S., et al., *Comparison of clinical characteristics and functional outcomes of ischemic stroke in different vascular territories.* Stroke, 2007. **38**(8): p. 2309-14.
3. Campbell, B.C., et al., *Failure of collateral blood flow is associated with infarct growth in ischemic stroke.* J Cereb Blood Flow Metab, 2013. **33**(8): p. 1168-72.
4. Casetta, I., et al., *Endovascular Thrombectomy for Acute Ischemic Stroke Beyond 6 Hours From Onset: A Real-World Experience.* Stroke, 2020. **51**(7): p. 2051-2057.
5. Goyal, M., et al., *Randomized assessment of rapid endovascular treatment of ischemic stroke.* N Engl J Med, 2015. **372**(11): p. 1019-30.
6. Campbell, B.C.V., et al., *Tenecteplase versus Alteplase before Thrombectomy for Ischemic Stroke.* N Engl J Med, 2018. **378**(17): p. 1573-1582.
7. Hopkins, L.N., *Blazing the Frontiers of Stroke Therapy.* Neurosurgery, 2019. **85**(suppl_1): p. S1-S2.
8. Serna Candel, C., et al., *Recanalization of Emergent Large Intracranial Vessel Occlusion through Intravenous Thrombolysis: Frequency, Clinical Outcome, and Reperfusion Pattern.* Cerebrovasc Dis, 2019. **48**(3-6): p. 115-123.
9. Cho, T.H., et al., *Reperfusion within 6 hours outperforms recanalization in predicting penumbra salvage, lesion growth, final infarct, and clinical outcome.* Stroke, 2015. **46**(6): p. 1582-9.
10. Chalothorn, D. and J.E. Faber, *Formation and maturation of the native cerebral collateral circulation.* J Mol Cell Cardiol, 2010. **49**(2): p. 251-9.
11. Seker, F., et al., *Collateral Scores in Acute Ischemic Stroke : A retrospective study assessing the suitability of collateral scores as standalone predictors of clinical outcome.* Clin Neuroradiol, 2020. **30**(4): p. 789-793.
12. Heil, M., et al., *Arteriogenesis versus angiogenesis: similarities and differences.* J Cell Mol Med, 2006. **10**(1): p. 45-55.
13. Ma, T. and Y.P. Bai, *The hydromechanics in arteriogenesis.* Aging Med (Milton), 2020. **3**(3): p. 169-177.
14. Kaloss, A.M. and M.H. Theus, *Leptomeningeal anastomoses: Mechanisms of pial collateral remodeling in ischemic stroke.* WIREs Mech Dis, 2022. **14**(4): p. e1553.

Chapter 2

Leptomeningeal anastomoses: Mechanisms of pial collateral remodeling in ischemic stroke

Literature Review

This chapter is published as an advanced review in WIREs Mechanisms of Disease

Received: 1 October 2021 | Revised: 9 January 2022 | Accepted: 11 January 2022

DOI: 10.1002/wsbm.1553

ADVANCED REVIEW

WIREs MECHANISMS OF DISEASE WILEY

Leptomeningeal anastomoses: Mechanisms of pial collateral remodeling in ischemic stroke

Alexandra M. Kaloss[1] | **Michelle H. Theus**[1,2,3]

[1]Department of Biomedical Sciences and Pathobiology, Virginia-Maryland Regional College of Veterinary Medicine, Virginia Tech, Blacksburg, Virginia, USA

[2]School of Neuroscience, Virginia Tech, Blacksburg, Virginia, USA

[3]Center for Regenerative Medicine, Virginia-Maryland Regional College of Veterinary Medicine, Virginia Tech, Blacksburg, Virginia, USA

Correspondence
Michelle H. Theus, Department of Biomedical Sciences and Pathobiology, Virginia-Maryland Regional College of Veterinary Medicine, Virginia Tech, Blacksburg, VA 24061, USA.
Email: mtheus@vt.edu

Funding information
This work was supported by NS112541 (MHT).

Edited by: Michelle Olsen, Editor

Abstract

Arterial collateralization, as determined by leptomeningeal anastomoses or pial collateral vessels, is a well-established vital player in cerebral blood flow restoration and neurological recovery from ischemic stroke. A secondary network of cerebral collateral circulation apart from the Circle of Willis, exist as remnants of arteriole development that connect the distal arteries in the pia mater. Recent interest lies in understanding the cellular and molecular adaptations that control the growth and remodeling, or arteriogenesis, of these pre-existing collateral vessels. New findings from both animal models and human studies of ischemic stroke suggest a multi-factorial and complex, tempo-rospatial interplay of endothelium, immune and vessel-associated cell interactions may work in concert to facilitate or thwart arteriogenesis. These valuable reports may provide critical insight into potential predictors of the pial collateral response in patients with large vessel occlusion and may aid in therapeutics to enhance collateral function and improve recovery from stroke.

This article is categorized under:

Neurological Diseases > Molecular and Cellular Physiology

KEYWORDS

arteriogenesis, ischemic stroke, large vessel occlusion, leptomeningeal anastomoses, pial collateral

1 | INTRODUCTION

Stroke is a leading cause of death and long-term disability worldwide, with the majority of these stroke cases being ischemic strokes where a vascular obstruction prevents blood flow to areas of the brain. Globally, ischemic strokes accounted for over 3.3 million deaths in 2019 and in the United States impacts nearly 700,000 individuals annually (Benjamin et al., 2017; Virani et al., 2021). This vast case load creates a major medical and financial burden in the United States, with projected direct and indirect costs of ischemic strokes increasing from the $105.2 billion seen in 2010 to $240.7 billion in 2030 (Ovbiagele et al., 2013). To date, the development of ischemic stroke treatments has been limited to tissue plasmogen activator and mechanical thrombectomy (Powers et al., 2019). Recently, leptomeningeal anastomoses (LMA), also known as pial collateral vessels have garnered attention for their adaptive remodeling process, arteriogenesis, which makes them a critical determinant of stroke outcomes and an attractive therapeutic target.

Observational studies of collateral vessels date back to 1785 when Sir John Hunter, a Scottish anatomist discovered that if the external carotid artery of a male fallow deer was permanently ligated, the ipsilateral antler would become cool. However, a week post ligation the antler temperature and pulse would return to normal and was coupled with enlargement of smaller vessels around the ligation site (Murley, 1984). Nearly 100 years passed after Hunters experiments before LMAs were first reported by Heubner in 1874, then more extensively described by Van der Eecken and Adams (Heubner, 1874; Vander Eecken & Adams, 1953). Later, the term arteriogenesis was coined by Wolfgang Schaper and colleagues to distinguish the growth of pre-existing collateral vessels from angiogenesis, or the formation of new vessels (W. Schaper & Buschmann, 1999).

LMAs are a network of small arteriole-to-arteriole bypass vessels that connect the anterior, middle, and posterior cerebral arteries (ACA, MCA, PCA) in the pia mater (Liebeskind, 2003). The arteriole collateral vessel wall, is comprised of the tunica intima (endothelial cells, the basement membrane, internal elastic lamina), tunica media (smooth muscle cells, external elastic membrane), and tunica adventitia (connective tissue, nerve endings, and other vessel associated cells) (Martinez-Lemus, 2012). Under healthy conditions, no pressure gradient exists on the luminal side of the collateral vessel wall (Chalothorn & Faber, 2010). However, following vascular obstruction of the main MCA branch, a change in pressure that occurs in the occluded vessel, causes retrograde cerebral blood flow (CBF) through the LMAs into the territory of tissue served by the primary vessel (I. Buschmann & Schaper, 2000). This rescue of CBF can prevent neuronal loss and preserve the penumbra (Aoki et al., 2014). Poor collateral flow is associated with worse outcome and extensive infarct damage in patients with large vessel occlusion (LVO), most often occurring in the MCA (Bang et al., 2008; Bang et al., 2011; Campbell et al., 2013). On the other hand, the enhanced recruitment of these subsidiary networks of vessels can stabilize CBF and improve outcome from stroke (Christoforidis et al., 2005; Mohammad et al., 2008; Roberts et al., 2002). Therefore, understanding both the growth potential and limiting factors that dictate LMA circulation may offer insight into clinical management of these vessels that may provide neuroprotection prior to and/or following mechanical thrombectomy.

Interestingly, recent findings describe a phenomenon known as Willisian collateral failure (S. J. Lee et al., 2020). Willisian collateral vessels are primary collaterals that exist between major arteries of the Circle of Willis. Failure of these blood vessels to move adequate quantities of blood can contribute to increased speed of infarct growth and may be due to an incomplete Circle of Willis, with absent or hypoplastic communicating arteries (S. U. Lee et al., 2016). Willisian collateral failure can also result as a consequence of thrombus embolization, or detachment and movement of the original blood clot, to the ACA (Kurre et al., 2013) or distal embolization in the same territory (Mazur et al., 2016) during mechanical thrombectomy. Patients with collateral failure showed worse outcome under these conditions compared to those with collateral sparing (S. J. Lee et al., 2020). However, these are considered minor cases (~11%) that occur during endovascular recanalization of M1 occlusion resulting in ACA emboli and infarct that limit poststroke motor recovery (Kurre et al., 2013). These studies further highlight the importance of pial collateral circulation.

The time from onset of ischemic stroke to hospital entry and admission to treatment greatly influences infarct growth, with the majority of patients arriving at the hospital more than 3 h after symptoms for large vessel occlusion begin (E. J. Lee et al., 2021; Lees et al., 2010; Man et al., 2020; Tong et al., 2012). However, recent evidence has shown that greater penumbra salvaging is just as critical as time to treatment for effecting disability outcome after stroke (Kawano et al., 2017). LMAs are vital for maintaining the penumbra region, especially in the first 24-h after stroke onset (Agarwal et al., 2018; Cheng-Ching et al., 2015; Cheripelli et al., 2016; Christoforidis et al., 2017; Jung et al., 2013). Upon admission to the hospital, patients undergo imaging to determine their eligibility for revascularization therapy, as well as establish penumbra volume and collateral grade. Computed tomography angiography (CTA) is the most popular method for evaluating collateral status due to its wide availability and sensitivity, with dynamic CTA assessing extent and filling time of LMAs (Raymond & Schaefer, 2017). Analysis of penumbra volume, as well as collateral scoring, was the main outcome assessment used when extending the mechanical thrombectomy therapeutic window from 6 to 24 h after symptom onset, and may indicate extending this window further for eligible patients (Campbell et al., 2015; Casetta et al., 2020; Goyal et al., 2015). This shift toward using penumbra volume with support from collateral scoring assessments instead of time from symptom onset highlights the importance of LMAs and the critical need to improve our understanding of the mechanisms underlying their remodeling to therapeutically target this niche and improve treatment outcome.

1 | THE UNIQUE PIAL COLLATERAL VESSEL NICHE

Unlike adjacent distal arterioles, LMAs display near-zero net flow, with slow oscillations toward either end of the main artery branch from which they anastomose (Chalothorn & Faber, 2010; Toriumi et al., 2009; Traupe et al., 2013).
Additional factors contribute to the increased disturbed flow compared to other arteriole beds, including the nonphysiological angles of insertion of the collateral into the anastomosed trees and their hallmark tortuosity, which increases from in utero development through adulthood (Chalothorn & Faber, 2010). Recent findings suggest that although LMAs are exposed to continuous low flow/shear stress, which normally results in a cobble-stoned morphology of endothelial cells (ECs) elsewhere in the vasculature, LMA ECs remain tightly aligned with the vessel axis, have continuous coverage of smooth muscle cells and are less abundant in shear stress sensing cilia (Zhang, Chalothorn, & Faber, 2019). Thus, LMAs represent a specialized vascular niche that may respond differently to aberrant hemodynamic changes that occur following vascular obstruction including unidirectional high-speed flow, increased hematocrit, and perfusion pressure (van Royen et al., 2009; Zhang et al., 2020).During postnatal development, LMAs undergo pruning, where their numbers decrease as brain size increases, which reaches steady-state at postnatal (P) day 21. Additionally, the absolute diameter of LMAs increases during postnatal pruning (Chalothorn & Faber, 2010). Aging has been linked to collateral rarefaction, with regards to both LMA number and diameter. Rodent studies show that collateral reduction was found to occur in an age-dependent manner, with aged animals having significantly fewer LMAs than younger animals of the same strain (Faber et al., 2011; Hecht et al., 2012; Sonntag et al., 1997). Additionally, collateral rarefaction can be further exacerbated by cardiovascular risk factors, including hypertension, metabolic syndrome, diabetes mellitus, and obesity (Moore et al., 2015). The extent of pre-existing collateral rarefaction, and the acute LMA arteriogenic response to occlusion, contribute to patient prognosis. Those patients with poor collateral grade, such as elderly patients with collateral rarefaction, correlate with increased stroke severity, especially when coupled with failed or incomplete recanalization (Faber et al., 2011; Seker et al., 2020). Rarefaction of LMAs, in AD murine models, is suggested to be associated with increased markers of oxidative stress and inflammation in the aged endothelium (Zhang, Jin, & Faber, 2019). Although additional direct cellular analysis of the LMA vessel wall during aging is needed to elucidate changes in shear stress, EC alignment, immune cell recruitment, and smooth muscle cell coverage.

2 | INFLUENCE OF FLUID SHEER STRESS ON COLLATERAL VESSELS

Unlike angiogenesis, where hypoxic/ischemic conditions trigger sprouting of new capillaries, arteriogenesis is not driven by low oxygen (I. Buschmann et al., 2010; H. T. Yang et al., 1994). In fact, the LMA niche lies in an oxygen-rich environment separate from the ischemic tissue (Gray et al., 2007). Arteriogenesis is triggered by an increase in the mechanical forces on the collateral vessel wall (Heil & Schaper, 2004). Following the loss of pressure gradient after arterial occlusion, unidirectional blood flow from the nonoccluded artery flows at an accelerated rate through the nascent collateral vessel, which provides retrograde CBF to the blocked artery. This increase in unidirectional blood flow is directly proportional to increased fluid shear stress (FSS), the viscous drag exerted by the blood on the endothelium of the vessel (Roux et al., 2020). Due to the small size of the collateral vessels, FSS is very difficult to directly measure. As a result, it is often calculated using the blood flow (Q) and radius (r) of the vessel which are both more easily measured, and the equation $\tau = \frac{4\eta Q}{\pi r^3}$ where τ is FSS and η is blood viscosity (assumes Newtonian fluid dynamics; Helisch & Schaper, 2003). In preclinical models, collateral flow can be directly measured using two-photon laser scanning microscopy or laser speckle contrast imaging and indirectly through laser Doppler imaging (J. Ma et al., 2017; Okyere et al., 2020). In the clinical setting, collateral flow and grade is most commonly determined using computed tomographic angiography, but can also be measured indirectly using computed tomography perfusion or magnetic resonance imaging (Piedade et al., 2019).

Since FSS is inversely related to vessel diameter, as the collateral vessel wall undergoes outward expansion, FSS decreases. For this reason, collateral vessels are limited in growth to restore up to 35%–40% of the blood flow originally provided by occluded parent artery (Hoefer et al., 2001; W. Schaper et al., 1976). However, studies investigating the administration of growth factors and cytokines, including FGF-1, FGF-2, vascular endothelial growth factor (VEGF), and MCP-1, show increased collateral conductance to 50% of that provided by the original occluded artery (Arras et al., 1998; Henry et al., 2003; Lazarous et al., 1995; Unger et al., 1993). To date, increasing FSS on the collateral vessel wall, by utilizing an arteriovenous

shunt, has been the only effective way to fully restore and surpass the maximum conductance of the occluded parent vessel (Eitenmüller et al., 2006; Pipp et al., 2004). This inherent shortfall highlights the need to fully elucidate the mechanisms that govern arteriogenesis in the LMA niche to maximize their therapeutic potential to restore CBF following ischemic stroke and to overcome additional challenges that may exist as a consequence of age and chronic inflammatory conditions.

2.1 | Mechanisms of mechanosensing

A simple and eloquent explanation for transduction of mechanical signals is Ingber's "tensegrity" model. Tensegrity is a building principle first coined by Richard Buckminster Fuller in the 1980s, in which a structure is supported by continuous tension (Swanson 2nd, 2013). This principle also applies to the structure of a living cell. In Ingber's model, a cell is shaped by the cytoskeleton, which undergoes tensional forces generated by contractile microfilaments. Those tensional forces are balanced by tethers to the extracellular matrix through focal adhesions, such as integrins (Ingber, 2003). Not only does this design provide structural stabilization for the cell, but it allows for the transduction of external mechanical forces along integrins and load bearing cytoskeletal elements (Ingber, 2008).

In addition to mechanical signals entering the cell through integrins, there are numerous mechanoreceptors (Chatzizisis et al., 2007). One of the most commonly noted mechanoreceptor in arteriogenesis is a complex comprised of platelet endothelial cell adhesion molecule 1 (PECAM-1), vascular endothelial cadherin (VE-Cadherin), and VEGFR2 (T. Ma & Bai, 2020). PECAM-1 serves as the mechanosensor, forming a heparan sulfate stabilized complex with the Gq/G11 protein and couples with the adaptor protein VE-Cadherin to activate VEGFR2 and its subsequent signaling cascade (dela Paz et al., 2014). VEGFR2 activation is vital for EC proliferation and the release of von Willebrand Factor (vWF) from platelets in response to FSS induced extracellular RNA (Lasch et al., 2019). Studies using a hind limb occlusion model showed that reduction in VEGFR2 activity, vWF, or extracellular RNA through RNase treatment all interfered with arteriogenesis by impeding formation of platelet–neutrophil aggregates (Lasch et al., 2019). This complex also activates nuclear factor κB (NFκB) and protein kinase B (Akt), which are essential for expression of adhesion molecules, cytokines expression, and EC survival, respectively (Tzima et al., 2005).

Primary cilia are an immobile organelle that exist on the surface of almost all cell types, including LMA endothelial cells, and are well established for their role as mechanosensors in vascular beds. The primary cilia function through PC1/2 mechanosensitive ion channel complex to regulate nitric oxide production (Kathem et al., 2014; Nauli et al., 2008). In models of atherosclerosis, primary cilia are found in higher abundance on ECs exposed to low shear stress, and areas with more primary cilia tend to be prone to atherosclerotic plaque development (Van der Heiden et al., 2008). The increased concentration is thought to be a mechanism of sensitizing these vessels to mechanical changes (Hierck et al., 2008). Interestingly, LMAs which are normally exposed to low, oscillatory shear stress, have fewer primary cilia than distal arterioles (Zhang, Chalothorn, & Faber, 2019). This raises the questions of why LMA ECs have fewer primary cilia, how this phenotype may contribute to or limit the growth of LMAs in response to changes in shear stress and if they can be therapeutically sensitized following ischemic stroke.

Recent evidence suggests that ECs, from different vessel types, have a preferred level of FSS that determines remodeling. This "shear stress set point", where flow-induced stress is maintained through feedback mechanisms at an optimal point, ensures that aberrant inward or outward remodeling does not occur. Moreover, ECs that highly express VEGFR3, as part of a mechanoreceptor complex, tend to be more sensitive to shear stress, and therefore have a lower set point than those cells that express reduced VEGFR3 levels (Baeyens et al., 2015). Given that collateral ECs are morphologically distinct (Zhang, Chalothorn, & Faber, 2019), it may be postulated that their unique phenotype and by extension ability to remodel, may be governed by the density and properties of select mechanoreceptors. Interestingly, recent findings propose an alternative, flow-independent model to describe the growth of a small diameter vessel into large caliber arteries, involving endothelial cell enlargement. This mechanism proposes that soluble Flt1 controls precise titration of VEGF signaling at the arterial wall to influence the GEF trio in zebrafish and cell models (Klems et al., 2020). These studies highlight the potential level of influence on LMAs that will need further investigation in animal models of ischemic stroke.

3 | ACTIVATION AND GROWTH OF COLLATERALS VESSELS

3.1 | Activation of the endothelium

In response to increases in FSS, one of the first signs of endothelial cell activation is cell swelling. It has been observed in human coronary collaterals that flat endothelial cells lining the vessel become longitudinal bulges in response to the heightened FSS (Seiler, 2010). In an attempt to counteract this swelling, the endothelial cells activate ion channels, including the volume-regulated anion channel (VRAC). These channels allow for the efflux mainly of chloride ions, and permit entry of Ca^{2+} ions and movement of organic osmolytes, which drives a secondary efflux of water from the cell thereby decreasing its volume (Hoffmann et al., 2009). Blockade of these channels using mibefradil, which inhibits both VRACs and T-type calcium channels, resulting in decreased collateral growth in a hind limb occlusion model (Manolopoulos et al., 2000; Ziegelhoeffer et al., 2003). Therefore, shear stress-induced activation of ion channels is one of the first signs of endothelial cell activation. Although most RTKs are activated by shear stress (Chen et al., 1999), the Tie2 receptor, expressed predominately on endothelial cells, shows rapid and sustained, velocity-dependent phosphorylation that is correlated with Akt phosphorylation (H. J. Lee & Koh, 2003). These findings support recent studies that demonstrate the EphA4 RTK negatively regulates LMAs in ischemic stroke by suppressing Tie2/pAkt function and cell proliferation in the vessel wall (Okyere et al., 2020). Additionally, in models of hind limb and myocardial ischemia, both angiopoietin ligands have been implicated in supporting collateral growth and improving perfusion although the exact mechanisms of action have not been fully elucidated (Chae et al., 2000; Gluzman et al., 2007; Siddiqui et al., 2003; Tressel et al., 2008).

3.1.1 | Vasodilation

To date, the role of NO in arteriogenesis has remained paradoxical. When activated by shear stress, endothelial cells increase expression of eNOS, elevating the release of NO, a potent vasodilatory agent. However, as collateral vessels vasodilate and therefore increase in diameter, FSS is reduced, potentially serving as a negative regulator for arteriogenesis. In a mouse model of hind limb occlusion, mice overexpressing eNOS (eNOStg mice) had significantly improved blood flow immediately flowing occlusion compared to wild-type controls. Conversely, eNOS deficient mice had sustained decreases in blood flow. Interestingly, no difference was seen in collateral artery diameter between the groups after 3 weeks (Mees et al., 2007). This implies that NO is indispensable for initial vasodilation of collateral vessels, perhaps through increased dilation of arteries feeding the collateral upstream, but does not significantly impact arteriogenesis (Dai & Faber, 2010). Furthermore, inhaled NO (iNO) is being investigated for clinical applications to reduce ischemic brain damage and increase collateral flow through vasodilation. Studies in rodent and large animal models have shown the iNO treatment at moderate (10–40 ppm) but not high (80 ppm) concentrations following either transient or permanent models of ischemic stroke reduces tissue damage and increases collateral dilation and flow (Charriaut-Marlangue et al., 2012; Terpolilli et al., 2012). Although this treatment is beneficial when given during the ischemic period, when administered later it can cause negative effects by exacerbating oxidative stress and the formation of harmful nitrogen species (Charriaut-Marlangue et al., 2012; Joriot-Chekaf et al., 2010).

To combat the increase in oxidative stress that accompanies iNO, prostaglandins have emerged as an attractive target for improving acute vasodilation in collateral vessels following stroke due to their more delayed and moderate vasodilatory effects. Treatment with prostaglandin E1 in neonatal rats showed improvements in blood flow back to basal levels and significant reductions in lesion volume 2 days following injury in treated mice. The restoration in blood flow was thought to be due to increases in recruitment and blood flow through primary collaterals in the circle of Willis or through pial collaterals, although no direct analysis of the collateral vessels was performed (Bonnin et al., 2018). While this work sets the stage to solidify prostaglandin E1 as a potential therapy for stroke aimed at improving collateral vasodilation, more direct studies of LMAs are necessary.

Other pharmacological agents for enhancing vasodilation of collaterals have been found, such as leptin. Leptin increases collateral flow but does not impact cellular proliferation or collateral conductance when tested under maximum dilation, indicating no changes in vessel diameter occurred (Busch et al., 2011; Schirmer et al., 2004). Therefore, initial studies have shown the importance of taking advantage of collateral vessels for acute vasodilation and subsequent arteriogenesis to improve

blood flow restoration in ischemic stroke. From a clinical perspective, pharmacologically increasing vasodilation of collaterals could provide short-term improvements in tissue perfusion prior to recanalization. It could also help complement the on-going process of arteriogenesis, which may take additional time to allow for maximum vessel growth. The field would benefit from additional studies within the acute phase of ischemic stroke to determine the extent of vasodilation following occlusion and its relationship to early stages of arteriogenesis.

3.1.2 | Increased vascular permeability

Increases in vascular permeability during ischemic conditions have been described since the 1970s, when Schaper and colleagues found increased leakage of erythrocytes and plasma proteins in the wall of collateral vessels, as well as increased monocyte recruitment following induced cardiac ischemia (J. Schaper et al., 1972). Work by Yang et al reveals that NO and VE-Cadherin play a major role in regulating endothelial cell permeability and therefore likely contribute to the invasion of immune cells (B. Yang, Cai, et al., 2015). VE-cadherin is the transmembrane component of adherens junctions that are involved in cell–cell contacts. It is expressed in all vascular endothelial cells, with its function and organization controlled by numerous molecules, including NO. In endothelial cells exposed to laminar flow or in collaterals subjected to sham hind limb occlusion, endothelial cells highly express VE-cadherin with continuous expression along the junctions between endothelial cells (Miao et al., 2005; B. Yang, Cai, et al., 2015). However, in collateral vessels following occlusion of the femoral artery, VE-cadherin becomes significantly downregulated on collateral endothelial cells and form a broken, punctate pattern (B. Yang, Cai, et al., 2015). This is associated with disassembly of adherens junctions, increased vascular permeability, and modulates immune cell infiltration (Miyazaki et al., 2011; Zhao et al., 2021). This stark downregulation could be inhibited using L-NAME, a NO synthase inhibitor, or even further reduced using DETA NONOate, a NO donor (B. Yang, Cai, et al., 2015). This work indicates an important crosstalk between NO and VE-cadherin in regulating the permeability of the endothelium. This also suggests that permeability may allow for recruitment of key immune cells that participate and are required for the remodeling process.

Another contributor to vascular permeability is one of the hallmark regulators of collateral vessels, VEGF, with roles both in vascular development and in arteriogenesis after ischemic stroke. Following femoral artery ligation VEGF is upregulated in the FSS exposed endothelium, with isoform expression differing between mouse strains, potentially contributing to differences seen in arteriogenic capacity (Chalothorn et al., 2007). When disruption of VEGF signaling is performed using gene manipulation, inhibitors, anti-VEGF-A neutralizing antibodies, or soluble VEGFR traps, arteriogenesis is reduced (Clayton et al., 2008; Jacobi et al., 2004; Lloyd et al., 2005; Toyota et al., 2005). Downstream of VEGFR2, the guanine exchange factor Trio, activates RhoG and Rac1 inducing focal adhesions, F-actin remodeling, and actomyosin activity (Klems et al., 2020). Signaling through Trio has been shown to stabilize junctions between endothelial cells and prevent leakage during vascular remodeling (Timmerman et al., 2015).

3.2 | Collateral vessel growth and remodeling

In order for collateral vessels to enlarge into conductance arteries, the endothelium may expand through cellular proliferation, the mechanisms of which remain under investigation and may be organ specific. Following activation of mechanoreceptors, endothelial cells upregulate expression of matrix metalloproteinase (MMP)-2, MMP-9, tissue plasminogen activator (tPA), and urokinase plasminogen activator (uPA), which assist in the breakdown of extracellular matrix. The endothelium also upregulates the expression of chemoattractants and integrins to recruit leukocytes. These events are required for the remodeling of the vessel and monocyte invasion has been found to proceed vascular proliferation (Arras et al., 1998; Heil & Schaper, 2004). Under healthy conditions, ECs are quiescent, but following ischemic stroke must transition into a proliferative phenotype, allowing them to multiply and migrate as needed to grow the pial collaterals (Jin et al., 2017; Tzima et al., 2005). Intracellular signaling cascades involved in endothelial cell migration are also upregulated following activation, including focal adhesion kinase (FAK), integrin $\alpha5\beta1$, integrin $\alpha v\beta3$, and Erk1/2.

Activation and proliferation of the endothelium were first reported in the 1970s in canine coronary collaterals. DNA synthesis peaked in the canine collaterals 3 weeks following constriction of the coronary artery (W. Schaper et al., 1971). However, when proliferation was evaluated at more acute time points following occlusion, it was observed as early as 24 h, peaked at 3–7 days, and remained at 3 weeks (Scholz et al., 2000). This matches murine studies of LMA growth, where proliferation is visible as early as 24 h poststroke (Okyere et al., 2018; Okyere et al., 2020). The delay from occlusion to the start of cellular proliferation, may help emphasize the potential importance of collateral vasodilation in the early hours following stroke. However, given that the time of onset for large vessel occlusion until clinical admission can be several hours to days (E. J. Lee et al., 2021; Tong et al., 2012), it is likely that efficient LMA remodeling that includes endothelial cell activation, division, and remodeling may contribute to patients with good collateral function and stroke outcome.

In addition to EC proliferation, integration of endothelial progenitor cells (EPCs) could contribute to LMA expansion and remodeling. In ischemic stroke patients, EPCs are elevated compared to healthy controls and lower levels of circulating EPCs are a predictor of worse neurological outcome (Yip et al., 2008). Additionally, in myocardial infarction patients, reduced numbers of circulating EPCs were associated with poor collateral status (Lambiase et al., 2004). However, in LMAs following ischemic stroke, it remains controversial if these cells integrate into the collateral vessel wall, and if they do, how much of a role they play in total growth. In studies of hind limb ischemia, supplementation of EPCs or nanofibrillar scaffolds seeded with ECs enhanced arteriogenesis (Nakayama et al., 2015; Zhou et al., 2017). Although these studies are limited as they looked at total vascular volume instead of direct measurements of the collateral vessel wall, as integration of the EPCs was not demonstrated. In a murine, hind limb ischemia model, integration of bone marrow-derived EPCs was shown using a chimeric mouse containing GFP labeled bone marrow. However, the GFP labeling was not colocalized to the collateral endothelial or smooth muscle cell layer, instead the GFP-positive cells surrounded the abluminal wall (Ziegelhoeffer et al., 2004). This could indicate a role for EPCs and bone marrow-derived cells in paracrine signaling of growth factors and chemokines that support arteriogenesis (Kinnaird et al., 2004; Rehman et al., 2003).

4 | DUAL ROLE OF IMMUNE MODULATION AND LMA

When activated by shear stress, the endothelium has been shown to mediate the process of recruiting peripheral immune cells to the collateral vessel, where they help create the balanced inflammatory environment required for arteriogenesis. Unfortunately, most of the research regarding immune cell attraction, adhesion, and activation in collaterals have not been performed in animal models of stroke. Due to the unique niche properties of LMAs, further investigation could assist in uncovering the role of immune mediators and lead to the discovery of pro-arteriogenic immune cell types that may benefit stroke patients.

Studies in hind limb ischemia, have shown that monocytes accumulate by 12 h and recruitment peaks between 1 and 3 days after occlusion (Heil et al., 2002). Depletion of these monocytes through op/op knockout mice or treatment with 5-fluorouracil and other agents resulted in severely impaired arteriogenesis (Bergmann et al., 2006; Heil et al., 2002; Millenaar et al., 2013; Pipp et al., 2003). Conversely, studies using clodronate liposome and cyclophosphamide did not show negative results on arteriogenesis, with the authors hypothesizing that resident macrophages may play a more prominent role than circulating cells in the early stages of collateral growth (Jetten et al., 2013; Khmelewski et al., 2004). Work by Schirmer, found 244 genes that were differentially expressed in circulating monocytes from patients with poor vs good coronary collateral circulation and development. They observed that genes related to type 1 interferons were overexpressed in the patients that had poor collateral networks, also highlighting the importance of looking at monocyte-specific pathways in the regulation of LMAs (Schirmer et al., 2008).

One of the most well-regarded chemo attractants in LMA remodeling is monocyte chemoattractant protein 1 (MCP1), with the ability to attract immune cells, especially monocytes, to the collateral arteriole. In human patients, high levels of MCP-1 were associated with good collateral grade before treatment for ischemic stroke (Mechtouff et al., 2020). A later study, found no significant difference in MCP-1 levels of human stroke patients with different collateral grades (Yu et al., 2021). This discrepancy could be due to the difference in collateral scoring technique, samples size, or blood collection time. In addition, Apelin-17, an endogenous apelin receptor agonist which plays a role in vascular health and immune modulation (Y. Yang, Lv, et al., 2015), was positively associated with human ischemic stroke patients that had good collateral circulation (Jiang et al.,

2019). Apelin can be secreted by many cell types, including endothelial cells and peripheral immune cells, and the main apelin receptor is most highly expressed on endothelial cells (Helker et al., 2020). These findings indicate that the peripheral immune response may play a vital role in LMAs, although additional research is needed.

Importantly, collateral circulation may play a key role in the broad immunological response to stroke. In stroke patients, it was found that even though the extent of collateral circulation did not impact the concentration of leukocytes circulating in the blood after LVO (Tarkanyi et al., 2020), the extent of collateral circulation was an indicator of how well immune cells were able to infiltrate into the ischemic tissue of the brain (Strinitz et al., 2021). The extent of LMAs coincident with immune status, also predicts hemorrhagic complications, with patients admitted with leukopenia showing poor collateral status coupled are more at risk for intracerebral hemorrhage (Semerano et al., 2019).

5 | THERAPEUTIC TARGETING OF LMA REMODELING

Extensive research has vastly improved our fundamental understanding of the development and function of collateral remodeling in stroke. However, to date, the ability for preclinical therapies to be translated into ischemic stroke treatments or therapeutic enhancement of collateral growth has been limited. In the experimental setting, there have been numerous compounds targeting endothelial and smooth muscle growth or monocyte recruitment. Once in clinical trials, these compounds led to disappointing results, mostly centered on safety concerns (Table 1).

5.1 | Vascular endothelial growth factor

The role of VEGF-A has been widely studied in endothelial activation and growth. As earlier discussed, while it is highly regarded as a strong promoter of angiogenesis, its exact role in arteriogenesis remains under debate. In contrast to its promising potential for both modes of vascular growth in preclinical studies and success of small patient studies, a larger controlled clinical trial failed to show improvements. The VEGF in Ischemia for Vascular Angiogenesis (VIVA) investigated stimulation of angiogenesis, but failed to show improvements in walking time between patients given the treatment and the placebo (Henry et al., 2003). Clinical investigations into VEGF as a biomarker for ischemic stroke and transient ischemic attacks also revealed increased VEGF serum concentrations were associated with increased incidence and severity of these ischemic events (Bhasin et al., 2019; Pikula et al., 2013).

5.2 | Colony-stimulating factors

Granulocyte-macrophage colony-stimulating factor (GM-CSF) and granulocyte colony-stimulating factor (G-CSF) are released by the endothelium following increased shear stress and are noted for their ability to mobilize progenitor cells from the bone marrow (Just et al., 1993; Klein et al., 1982; Kosaki et al., 1998). They can also support the survival, proliferation, and differentiation of hematopoietic cells, such as monocytes. In preclinical models, treatment with GM-CSF or GCSF showed improvements in collateral artery growth (I. R. Buschmann et al., 2003; Duelsner et al., 2012; Sugiyama et al., 2011; Todo et al., 2008) and was even more promising for its anti-atherogenic properties unlike other potential therapeutic compounds, such as MCP-1. An initial study on the pro-arteriogenic effects of GM-CSF on patients with coronary artery disease showed promising results, but a later study saw safety concerns with two of seven treated patients having acute coronary syndrome vs none in the placebo control group (Seiler et al., 2001; S. Zbinden et al., 2005). The effects of GM-CSF were also tested in peripheral artery disease but no improvements were seen in the primary endpoint (van Royen et al., 2005). Alternatively, G-CSF was tested in acute ischemic stroke patients and while it showed safety and feasibility in small clinical trials (Floel et al., 2011; Moriya et al., 2013; Schäbitz et al., 2010), it failed to show significant improvements to patient outcomes in larger controlled trials (Mizuma et al., 2016; Ringelstein et al., 2013).

5.3 | Statins

Statins are classically known for their ability to lower lipid concentrations in the blood, but they can also exhibit cholesterol-independent effects by directly improving endothelial function through increased NO production. In arteriogenesis, statins may serve as a therapeutic to improve collateral vessel function by improving EPC mobilization and monocyte function (Landmesser et al., 2004). Preclinical data shows a decrease in the efficacy of monocytes in arteriogenesis during hypercholesterolemia and that it could be reversed with statin administration (Czepluch et al., 2007). Clinical trials have shown positive results in stroke patients indicating statins as a potential pharmacological approach to treat stroke (Table 1). However, the effects of statins on augmenting arteriogenesis are less clear. Multiple clinical trials have shown a positive correlation between statin treatment and collateral score (Dincer et al., 2006; Pourati et al., 2003). However, a larger study in patients with coronary artery disease found no effects of collaterals on arteriogenesis when looking at functional collateral flow index measurements (S. Zbinden, Brunner, et al., 2004). Further highlighting the need to understand the collateral remodeling niche response in a site-specific fashion across multiple preclinical models.

5.4 | Physical exercise

An alternative to pharmacological rescue is physical exercise, which may provide a natural method for improving collateral function. Physical exercise has been shown to promote arteriogenesis through increased FSS across the endothelium and accumulation of macrophages to the collaterals with increased expression of iNOS and eNOS (Dopheide

TABLE 1 Biomarker detection and therapeutic targeting of LMC remodeling

	Author	Disease	n-value	Treatment duration	Major findings
VEGF	Henry et al., 2003	Exertional angina	178	Day 0, 3, 6, and 9	Recombinant human VEGF (rhVEGF) was safe. No significant improvements in myocardial perfusion or quality of life in the first at day 60 in rhVEGF treated compared to controls. High dose rhVEGF improved angina class compared to controls, no difference in low rhVEGF treated group.
	Bhasin et al., 2019	Acute ischemic stroke	250	N/A	VEGF is upregulated in the blood of patients with severe stroke compared to healthy controls. At 3 months poststroke when coupled with clinical scores, VEGF as a biomarker is a predictor of stroke severity and patient functional outcome.
	Pikula et al., 2013	Incident stroke/ ischemic attack	3440	N/A	Higher serum concentrations of VEGF associated with increased risk of transient ischemic event.
Colony Stimulating Factor	Seiler et al., 2001	Coronary artery disease	21	14 days	Coronary collateral flow was measured using invasive collateral flow index (CFI). Treatment with GM-CSF in severe CAD patients resulted in significantly improved CFI compared to the placebo group.
	Zbinden et al., 2005	Coronary artery disease	14	14 days	CAD patients treated with GM-CSF had significantly improved CFI. In the GM-CSF treated group, two of seven patients experience acute coronary syndrome, bringing into question the safety of treatment.

	van Royen et al., 2005	Peripheral artery disease	40	14 days	Collateral flow measured indirectly using laser Doppler flowmetry. No difference in walking time (primary endpoint) was seen between treatment and control patients. GM-CSF treatment did not result in improvements of microcirculatory flow reserve.
	Floel et al., 2011	Chronic ischemic stroke with concomitant vascular disease	41	10 days	No significant improvement in hand motor function seen in G-CSF treated patients. G-CSF resulted in more frequent mild or moderate adverse outcomes compared to controls, demonstrating reasonable safety and tolerability.
	Moriya et al., 2013	Acute and subacute ischemic stroke	18	5 days	No severe adverse outcomes noted, indicating safety and tolerability of low dose G-CSF.
	Schäbitz et al., 2010	Acute ischemic stroke	44	3 days	G-CSF demonstrated safety and tolerability at low and high doses. No improvement in clinical outcome was seen with G-CSF treatment.

(Continues)

TABLE 1 (Continued)

	Author	Disease	n-value	Treatment duration	Major findings
	Mizuma et al., 2016	Acute ischemic stroke	49		G-CSF was well tolerated but did not improve functional recovery or decrease infarct volume 3 months following stroke.
	Ringelstein et al., 2013	Acute ischemic stroke	328	3 days	No improvement was seen in patient outcome or imaging biomarkers in patients treated with G-CSF poststroke.
Statins	Dincer et al., 2006	Diabetes mellitus	149	Variable	Coronary collaterals were graded using Cohen–Rentrop method. Treatment with statins was associated with better coronary collateral score.
	Pourati et al., 2003	Major coronary artery occlusion or stenosis	94	Variable	Coronary collaterals were graded using Cohen–Rentrop method. Patients receiving statins had significantly higher collateral score and left ventricular ejection fraction compared to patients not taking statins.
	Zbinden, Brunner, et al., 2004	Coronary artery disease	500	Variable (avg 9.5 months)	No difference in CFI with statin use and the number of patients with insufficient collaterals was significantly greater in the group taking statins.
Physical exercise	Möbius-Winkler et al., 2016	Coronary artery disease	60	4 Weeks	CFI was significantly increased in patients receiving either high or moderate-intensity exercise compared to controls. Exercise improved peak VO_2 and ischemic threshold compared to patients in control group.

	Togni et al., 2010	Coronary artery disease	30	1 Treatment	CFI of coronary collaterals doubles in patients during supine bicycle exercise compared with resting state.
	Zbinden et al., 2007	Coronary artery disease undergoing percutaneous coronary intervention	40	3 Months	CFI increased in arteries undergoing and in normal vessels of the exercise group patients compared to controls. The increase in collateral flow correlated with exercise capacity gained (VO_{2Max} and Watt).
	Zbinden, Zbinden, et al., 2004	Healthy Control	Case study	25+ years	The left descending coronary artery was occluded for 1 min. CFI increased 60% in response to endurance training compared to baseline.
Petrovic et al., 2020		Coronary Artery Disease	32	2 Weeks + Heparin	Collateral score using CTA, myocardial ischemia, and angina class improved significantly in group receiving exercise and heparin compared to the exercise only group.

et al., 2017; Schirmer et al., 2015). It has also been shown to reduce collateral rarefaction during aging in an animal model (McMullan et al., 2016). FSS rises during physical exercise because of the increase in heart rate and blood pressure needed to maintain cellular function (Duncker & Bache, 2008). The heightened NO can then act on the endothelial and smooth muscle cells to improve collateral vasodilation and growth. Multiple clinical trials using collateral flow index have shown a significant relationship with exercise and collateral blood flow, indicating the use of exercise in a clinical setting to improve arteriogenesis (Table 1; Möbius-Winkler et al., 2016; Togni et al., 2010; R. Zbinden et al., 2007; R. Zbinden, Zbinden, et al., 2004). The effects of physical exercise on collaterals can also be improved when coupled with pharmacological treatments. A recent clinical trial investigating myocardial ischemia found that patients that received heparin in addition to exercise had improved collateral flow compared to patients in the exercise alone group (Petrovic et al., 2020).

6 | CONCLUSION

LMAs are a vital determinant of ischemic stroke outcome, but their niche properties and mechanism of remodeling remain under intense investigation. Substantial research has been done in other collateral beds, especially the hind limb; however, more work is underway to correlate these findings with LMA niche regulation. This knowledge gap could limit the development of precision therapeutics targeted at LMAs, as their unique characteristics have not yet been fully elucidated. This may also contribute to the poor translational capacity of pro-arteriogenic compounds from preclinical to clinical models. To combat this, more research emphasis is being placed on determining the molecular pathways that propel human arteriogenesis in the LMAs of the brain, as the biological mechanisms driving this critical adaptive response have to remain under-investigated and may differ from animal models. Additionally, the mechanism for arteriogenesis elucidated in preclinical models has been predominantly unsubstantiated in humans. The lack of investigation into human arteriogenesis is largely due to the difficulties in identifying and accessing pial collateral vessels.

An additional factor that could contribute to the disappointing translatability is the lack of a clear definition of what constitutes remodeling. Most studies utilize collateral diameter to indicate remodeling. Currently, the classical definition of arteriogenesis focuses on the cellular remodeling of the LMAs, not on the vessels' ability to dilate or the potential for endothelial cell enlargement; therefore, a clearer definition for what constitutes the full extent of LMA remodeling needs to be further established. Work investigating the cellular changes in the LMAs during the acute phase of ischemic stroke may shed

light on how these vessels initially react to changes in blood flow and help establish the temporospatial characteristics of the remodeling process.

Finally, while these specialized vessels harbor numerous differences from distal arterioles, little work has been done on how these differences impact vessel function, notably in the response to mechanical stimuli. What expression patterns exist for VEGFR3 on LMAs, compared to other vessel types, and how does this contribute to their mechanosensing complex? How does the density of primary cilia influence LMAs and does this limit their capacity to fully respond to appropriate changes in shear stress? Are these differences influenced by immune status, age and are they linked to patient collateral scoring? Understanding the basic mechanisms for mechanosensing, specifically in the LMAs given their unique niche properties, opens the door to potential therapeutic enhancement of their growth. Since LMA remodeling will likely have to be targeted poststroke in a combinatory fashion, mechanosensing is a promising target. Numerous studies have shown that increasing FSS results in collaterals with the highest conductance (Eitenmüller et al., 2006; Pipp et al., 2004). Additional emphasis should be placed on understanding how we can sensitize LMAs to small changes in FSS, potentially allowing for the large increase in conductance capacity, without needing to therapeutically shunt additional blood into the LMAs. This priming of the LMAs may also be beneficial as a prophylactic for patients at unusually high risk for having an ischemic stroke. Therefore, additional research into LMA remodeling will aid future investigation aimed at improving novel therapeutic development for ischemic stroke.

ACKNOWLEDGMENT
We recognize The Center for Engineered Health for grant support.

CONFLICT OF INTEREST
The authors have declared no conflicts of interest for this article.

AUTHOR CONTRIBUTIONS
Alexandra M. Kaloss: Conceptualization (equal). Michelle H. Theus: Conceptualization (equal).

DATA AVAILABILITY STATEMENT
Data sharing is not applicable to this article as no new data were created or analyzed in this study.

ORCID
Alexandra M. Kaloss https://orcid.org/0000-0002-2054-2320
Michelle H. Theus https://orcid.org/0000-0001-6485-2104

RELATED WIREs ARTICLE
In vivo visualization of macrophage infiltration and activity in inflammation using magnetic resonance imaging

REFERENCES

Agarwal, S., Bivard, A., Warburton, E., Parsons, M., & Levi, C. (2018). Collateral response modulates the time-penumbra relationship in proximal arterial occlusions. Neurology, 90(4), e316–e322. https://doi.org/10.1212/WNL.0000000000004858

Aoki, J., Tateishi, Y., Cummings, C. L., Cheng-Ching, E., Ruggieri, P., Hussain, M. S., & Uchino, K. (2014). Collateral flow and brain changes on computed tomography angiography predict infarct volume on early diffusion-weighted imaging. Journal of Stroke and Cerebrovascular Diseases, 23(10), 2845–2850. https://doi.org/10.1016/j.jstrokecerebrovasdis.2014.07.015

Arras, M., Ito, W. D., Scholz, D., Winkler, B., Schaper, J., & Schaper, W. (1998). Monocyte activation in angiogenesis and collateral growth in the rabbit hindlimb. The Journal of Clinical Investigation, 101(1), 40–50. https://doi.org/10.1172/JCI119877

Baeyens, N., Nicoli, S., Coon, B. G., Ross, T. D., van den Dries, K., Han, J., Lauridsen, H. M., Mejean, C. O., Eichmann, A., Thomas, J. L., Humphrey, J. D., & Schwartz, M. A. (2015). Vascular remodeling is governed by a VEGFR3-dependent fluid shear stress set point. eLife, 4, e04645. https://doi.org/10.7554/eLife.04645

Bang, O. Y., Saver, J. L., Buck, B. H., Alger, J. R., Starkman, S., Ovbiagele, B., Kim, D., Jahan, R., Duckwiler, G. R., Yoon, S. R., Viñuela, F., Liebeskind, D. S., & UCLA Collateral Investigators. (2008). Impact of collateral flow on tissue fate in acute ischaemic stroke. Journal of Neurology, Neurosurgery, and Psychiatry, 79(6), 625–629. https://doi.org/10.1136/jnnp.2007.132100

Bang, O. Y., Saver, J. L., Kim, S. J., Kim, G. M., Chung, C. S., Ovbiagele, B., Lee, K. H., & Liebeskind, D. S. (2011). Collateral flow predicts response to endovascular therapy for acute ischemic stroke. Stroke, 42(3), 693–699. https://doi.org/10.1161/STROKEAHA.110.595256

Benjamin, E. J., Blaha, M. J., Chiuve, S. E., Cushman, M., Das, S. R., Deo, R., de Ferranti, S. D., Floyd, J., Fornage, M., Gillespie, C., Isasi, C. R., Jiménez, M. C., Jordan, L. C., Judd, S. E., Lackland, D., Lichtman, J. H., Lisabeth, L., Liu, S., Longenecker, C. T., … American Heart Association Statistics Committee and Stroke Statistics Subcommittee. (2017). Heart disease and Stroke Statistics-2017 update: A report from the American Heart Association. Circulation, 135(10), e146–e603. https://doi.org/10.1161/CIR.0000000000000485

Bergmann, C. E., Hoefer, I. E., Meder, B., Roth, H., van Royen, N., Breit, S. M., Jost, M. M., Aharinejad, S., Hartmann, S., & Buschmann, I. R. (2006). Arteriogenesis depends on circulating monocytes and macrophage accumulation and is severely depressed in op/op mice. Journal of Leukocyte Biology, 80(1), 59–65. https://doi.org/10.1189/jlb.0206087

Bhasin, A., Srivastava, M. V. P., Vivekanandhan, S., Moganty, R., Talwar, T., Sharma, S., Kuthiala, N., Kumaran, S., & Bhatia, R. (2019). Vascular endothelial growth factor as predictive biomarker for Stroke severity and outcome; an evaluation of a new clinical module in acute ischemic Stroke. Neurology India, 67(5), 1280–1285. https://doi.org/10.4103/0028-3886.271241

Bonnin, P., Pansiot, J., Baud, O., & Charriaut-Marlangue, C. (2018). Prostaglandin E1-mediated collateral recruitment is delayed in a neonatal rat Stroke model. International Journal of Molecular Sciences, 19(10), 2995. https://doi.org/10.3390/ijms19102995

Busch, H. J., Schirmer, S. H., Jost, M., van Stijn, S., Peters, S. L., Piek, J. J., Bode, C., Buschmann, I. R., & Mies, G. (2011). Leptin augments cerebral hemodynamic reserve after three-vessel occlusion: Distinct effects on cerebrovascular tone and proliferation in a nonlethal model of hypoperfused rat brain. Journal of Cerebral Blood Flow and Metabolism, 31(4), 1085–1092. https://doi.org/10.1038/jcbfm.2010.192

Buschmann, I., Pries, A., Styp-Rekowska, B., Hillmeister, P., Loufrani, L., Henrion, D., Shi, Y., Duelsner, A., Hoefer, I., Gatzke, N., Wang, H., Lehmann, K., Ulm, L., Ritter, Z., Hauff, P., Hlushchuk, R., Djonov, V., van Veen, T., & le Noble, F. (2010). Pulsatile shear and Gja5 modulate arterial identity and remodeling events during flow-driven arteriogenesis. Development, 137(13), 2187–2196. https://doi.org/10.1242/dev.045351

Buschmann, I., & Schaper, W. (2000). The pathophysiology of the collateral circulation (arteriogenesis). The Journal of Pathology, 190(3), 338–342. https://doi.org/10.1002/(SICI)1096-9896(200002)190:3<338::AID-PATH594>3.0.CO;2-7

Buschmann, I. R., Busch, H. J., Mies, G., & Hossmann, K. A. (2003). Therapeutic induction of arteriogenesis in hypoperfused rat brain via granulocyte-macrophage colony-stimulating factor. Circulation, 108(5), 610–615. https://doi.org/10.1161/01.CIR.0000074209.17561.99

Campbell, B. C., Christensen, S., Tress, B. M., Churilov, L., Desmond, P. M., Parsons, M. W., Barber, P. A., Levi, C. R., Bladin, C., Donnan, G. A., Davis, S. M., & EPITHET Investigators. (2013). Failure of collateral blood flow is associated with infarct growth in ischemic stroke. Journal of Cerebral Blood Flow and Metabolism, 33(8), 1168–1172. https://doi.org/10.1038/jcbfm.2013.77

Campbell, B. C., Mitchell, P. J., Kleinig, T. J., Dewey, H. M., Churilov, L., Yassi, N., Yan, B., Dowling, R. J., Parsons, M. W., Oxley, T. J., Wu, T. Y., Brooks, M., Simpson, M. A., Miteff, F., Levi, C. R., Krause, M., Harrington, T. J., Faulder, K. C., Steinfort, B. S., … EXTENDIA Investigators. (2015). Endovascular therapy for ischemic stroke with perfusion-imaging selection. The New England Journal of Medicine, 372(11), 1009–1018. https://doi.org/10.1056/NEJMoa1414792

Casetta, I., Fainardi, E., Saia, V., Pracucci, G., Padroni, M., Renieri, L., Nencini, P., Inzitari, D., Morosetti, D., Sallustio, F., Vallone, S., Bigliardi, G., Zini, A., Longo, M., Francalanza, I., Bracco, S., Vallone, I. M., Tassi, R., Bergui, M., … Italian Registry of Endovascular Treatment in Acute Stroke. (2020). Endovascular thrombectomy for acute ischemic Stroke beyond 6 hours from onset: A real-world experience. Stroke, 51(7), 2051–2057. https://doi.org/10.1161/STROKEAHA.119.027974

Chae, J. K., Kim, I., Lim, S. T., Chung, M. J., Kim, W. H., Kim, H. G., & Koh, G. Y. (2000). Coadministration of angiopoietin-1 and vascular endothelial growth factor enhances collateral vascularization. Arteriosclerosis, Thrombosis, and Vascular Biology, 20(12), 2573–2578. https://doi.org/10.1161/01.atv.20.12.2573

Chalothorn, D., Clayton, J. A., Zhang, H., Pomp, D., & Faber, J. E. (2007). Collateral density, remodeling, and VEGF-A expression differ widely between mouse strains. Physiological Genomics, 30(2), 179–191. https://doi.org/10.1152/physiolgenomics.00047.2007

Chalothorn, D., & Faber, J. E. (2010). Formation and maturation of the native cerebral collateral circulation. Journal of Molecular and Cellular Cardiology, 49(2), 251–259. https://doi.org/10.1016/j.yjmcc.2010.03.014

Charriaut-Marlangue, C., Bonnin, P., Gharib, A., Leger, P. L., Villapol, S., Pocard, M., Gressens, P., Renolleau, S., & Baud, O. (2012). Inhaled nitric oxide reduces brain damage by collateral recruitment in a neonatal stroke model. Stroke, 43(11), 3078–3084. https://doi.org/10.1161/STROKEAHA.112.664243

Chatzizisis, Y. S., Coskun, A. U., Jonas, M., Edelman, E. R., Feldman, C. L., & Stone, P. H. (2007). Role of endothelial shear stress in the natural history of coronary atherosclerosis and vascular remodeling: Molecular, cellular, and vascular behavior. Journal of the American College of Cardiology, 49(25), 2379–2393. https://doi.org/10.1016/j.jacc.2007.02.059

Chen, K. D., Li, Y. S., Kim, M., Li, S., Yuan, S., Chien, S., & Shyy, J. Y. (1999). Mechanotransduction in response to shear stress. Roles of receptor tyrosine kinases, integrins, and Shc. The Journal of Biological Chemistry, 274(26), 18393–18400. https://doi.org/10.1074/jbc.274.26.18393

Cheng-Ching, E., Frontera, J. A., Man, S., Aoki, J., Tateishi, Y., Hui, F. K., Wisco, D., Ruggieri, P., Hussain, M. S., & Uchino, K. (2015). Degree of collaterals and not time is the determining factor of Core infarct volume within 6 hours of Stroke onset. AJNR. American Journal of Neuroradiology, 36(7), 1272–1276. https://doi.org/10.3174/ajnr.A4274

Cheripelli, B. K., Huang, X., McVerry, F., & Muir, K. W. (2016). What is the relationship among penumbra volume, collaterals, and time since onset in the first 6 h after acute ischemic stroke? International Journal of Stroke, 11(3), 338–346. https://doi.org/10.1177/1747493015620807

Christoforidis, G. A., Mohammad, Y., Kehagias, D., Avutu, B., & Slivka, A. P. (2005). Angiographic assessment of pial collaterals as a prognostic indicator following intra-arterial thrombolysis for acute ischemic stroke. American Journal of Neuroradiology, 26(7), 1789–1797.

Christoforidis, G. A., Vakil, P., Ansari, S. A., Dehkordi, F. H., & Carroll, T. J. (2017). Impact of Pial collaterals on infarct growth rate in experimental acute ischemic Stroke. AJNR. American Journal of Neuroradiology, 38(2), 270–275. https://doi.org/10.3174/ajnr.A5003

Clayton, J. A., Chalothorn, D., & Faber, J. E. (2008). Vascular endothelial growth factor-a specifies formation of native collaterals and regulates collateral growth in ischemia. Circulation Research, 103(9), 1027–1036. https://doi.org/10.1161/CIRCRESAHA.108.181115

Czepluch, F. S., Bergler, A., & Waltenberger, J. (2007). Hypercholesterolaemia impairs monocyte function in CAD patients. Journal of Internal Medicine, 261(2), 201–204. https://doi.org/10.1111/j.1365-2796.2006.01753.x

Dai, X., & Faber, J. E. (2010). Endothelial nitric oxide synthase deficiency causes collateral vessel rarefaction and impairs activation of a cell cycle gene network during arteriogenesis. Circulation Research, 106(12), 1870–1881. https://doi.org/10.1161/CIRCRESAHA.109.212746

dela Paz, N. G., Melchior, B., Shayo, F. Y., & Frangos, J. A. (2014). Heparan sulfates mediate the interaction between platelet endothelial cell adhesion molecule-1 (PECAM-1) and the Galphaq/11 subunits of heterotrimeric G proteins. The Journal of Biological Chemistry, 289(11), 7413–7424. https://doi.org/10.1074/jbc.M113.542514

Dincer, I., Ongun, A., Turhan, S., Ozdol, C., Ertas, F., & Erol, C. (2006). Effect of statin treatment on coronary collateral development in patients with diabetes mellitus. The American Journal of Cardiology, 97(6), 772–774. https://doi.org/10.1016/j.amjcard.2005.09.124 Dopheide, J. F., Rubrech, J., Trumpp, A., Geissler, P., Zeller, G. C., Schnorbus, B., Schmidt, F., Gori, T., Münzel, T., & Espinola-Klein, C. (2017). Supervised exercise training in peripheral arterial disease increases vascular shear stress and profunda femoral artery diameter. European Journal of Preventive Cardiology, 24(2), 178–191. https://doi.org/10.1177/2047487316665231

Duelsner, A., Gatzke, N., Glaser, J., Hillmeister, P., Li, M., Lee, E. J., Lehmann, K., Urban, D., Meyborg, H., Stawowy, P., Busjahn, A., Nagorka, S., Persson, A. B., Laage, R., Schneider, A., & Buschmann, I. R. (2012). Granulocyte colony-stimulating factor improves cerebrovascular reserve capacity by enhancing collateral growth in the circle of Willis. Cerebrovascular Diseases, 33(5), 419–429. https://doi.org/10.1159/000335869

Duncker, D. J., & Bache, R. J. (2008). Regulation of coronary blood flow during exercise. Physiological Reviews, 88(3), 1009–1086. https://doi.org/10.1152/physrev.00045.2006

Eitenmüller, I., Volger, O., Kluge, A., Troidl, K., Barancik, M., Cai, W. J., Heil, M., Pipp, F., Fischer, S., Horrevoets, A. J., SchmitzRixen, T., & Schaper, W. (2006). The range of adaptation by collateral vessels after femoral artery occlusion. Circulation Research, 99(6), 656–662. https://doi.org/10.1161/01.RES.0000242560.77512.dd

Faber, J. E., Zhang, H., Lassance-Soares, R. M., Prabhakar, P., Najafi, A. H., Burnett, M. S., & Epstein, S. E. (2011). Aging causes collateral rarefaction and increased severity of ischemic injury in multiple tissues. Arteriosclerosis, Thrombosis, and Vascular Biology, 31(8), 1748– 1756. https://doi.org/10.1161/ATVBAHA.111.227314

Floel, A., Warnecke, T., Duning, T., Lating, Y., Uhlenbrock, J., Schneider, A., Vogt, G., Laage, R., Koch, W., Knecht, S., & Schäbitz, W. R. (2011). Granulocyte-colony stimulating factor (G-CSF) in stroke patients with concomitant vascular disease—A randomized controlled trial. PLoS One, 6(5), e19767. https://doi.org/10.1371/journal.pone.0019767

Gluzman, Z., Koren, B., Preis, M., Cohen, T., Tsaba, A., Cosset, F. L., Shofti, R., Lewis, B. S., Virmani, R., & Flugelman, M. Y. (2007). Endothelial cells are activated by angiopoeitin-1 gene transfer and produce coordinated sprouting in vitro and arteriogenesis in vivo. Biochemical and Biophysical Research Communications, 359(2), 263–268. https://doi.org/10.1016/j.bbrc.2007.05.097

Goyal, M., Demchuk, A. M., Menon, B. K., Eesa, M., Rempel, J. L., Thornton, J., Roy, D., Jovin, T. G., Willinsky, R. A., Sapkota, B. L., Dowlatshahi, D., Frei, D. F., Kamal, N. R., Montanera, W. J., Poppe, A. Y., Ryckborst, K. J., Silver, F. L., Shuaib, A., Tampieri, D., … ESCAPE Trial Investigators. (2015). Randomized assessment of rapid endovascular treatment of ischemic stroke. The New England Journal of Medicine, 372(11), 1019–1030. https://doi.org/10.1056/NEJMoa1414905

Gray, C., Packham, I. M., Wurmser, F., Eastley, N. C., Hellewell, P. G., Ingham, P. W., & Chico, T. J. (2007). Ischemia is not required for arteriogenesis in zebrafish embryos. Arteriosclerosis, Thrombosis, and Vascular Biology, 27(10), 2135–2141. https://doi.org/10.1161/ATVBAHA.107.143990

Hecht, N., He, J., Kremenetskaia, I., Nieminen, M., Vajkoczy, P., & Woitzik, J. (2012). Cerebral hemodynamic reserve and vascular remodeling in C57/BL6 mice are influenced by age. Stroke, 43(11), 3052–3062. https://doi.org/10.1161/STROKEAHA.112.653204

Heil, M., & Schaper, W. (2004). Influence of mechanical, cellular, and molecular factors on collateral artery growth (arteriogenesis). Circulation Research, 95(5), 449–458. https://doi.org/10.1161/01.RES.0000141145.78900.44

Heil, M., Ziegelhoeffer, T., Pipp, F., Kostin, S., Martin, S., Clauss, M., & Schaper, W. (2002). Blood monocyte concentration is critical for enhancement of collateral artery growth. American Journal of Physiology. Heart and Circulatory Physiology, 283(6), H2411–H2419. https://doi.org/10.1152/ajpheart.01098.2001

Helisch, A., & Schaper, W. (2003). Arteriogenesis: The development and growth of collateral arteries. Microcirculation, 10(1), 83–97. https://doi.org/10.1038/sj.mn.7800173

Helker, C. S., Eberlein, J., Wilhelm, K., Sugino, T., Malchow, J., Schuermann, A., Baumeister, S., Kwon, H. B., Maischein, H. M., Potente, M., Herzog, W., & Stainier, D. Y. (2020). Apelin signaling drives vascular endothelial cells toward a pro-angiogenic state. eLife, 9, e55589. https://doi.org/10.7554/eLife.55589

Henry, T. D., Annex, B. H., McKendall, G. R., Azrin, M. A., Lopez, J. J., Giordano, F. J., Shah, P. K., Willerson, J. T., Benza, R. L., Berman, D. S., Gibson, C. M., Bajamonde, A., Rundle, A. C., Fine, J., McCluskey, E., & VIVA Investigators. (2003). The VIVA trial: Vascular endothelial growth factor in ischemia for vascular angiogenesis. Circulation, 107(10), 1359–1365. https://doi.org/10.1161/01.cir.0000061911.47710.8a Heubner, O. (1874). Die luetischen erkankungen der hirnarterien (pp. 170–214). FC Vogel.

Hierck, B. P., van der Heiden, K., Alkemade, F. E., van de Pas, S., van Thienen, J., Groenendijk, B. C., Bax, W. H., van der Laarse, A., Deruiter, M. C., Horrevoets, A. J., & Poelmann, R. E. (2008). Primary cilia sensitize endothelial cells for fluid shear stress. Developmental Dynamics, 237(3), 725–735. https://doi.org/10.1002/dvdy.21472

Hoefer, I. E., van Royen, N., Buschmann, I. R., Piek, J. J., & Schaper, W. (2001). Time course of arteriogenesis following femoral artery occlusion in the rabbit. Cardiovascular Research, 49(3), 609–617. https://doi.org/10.1016/s0008-6363(00)00243-1

Hoffmann, E. K., Lambert, I. H., & Pedersen, S. F. (2009). Physiology of cell volume regulation in vertebrates. Physiological Reviews, 89(1), 193–277. https://doi.org/10.1152/physrev.00037.2007

Ingber, D. E. (2003). Tensegrity I. cell structure and hierarchical systems biology. Journal of Cell Science, 116(Pt 7), 1157–1173. https://doi.org/10.1242/jcs.00359

Ingber, D. E. (2008). Tensegrity and mechanotransduction. Journal of Bodywork and Movement Therapies, 12(3), 198–200. https://doi.org/10.1016/j.jbmt.2008.04.038

Jacobi, J., Tam, B. Y., Wu, G., Hoffman, J., Cooke, J. P., & Kuo, C. J. (2004). Adenoviral gene transfer with soluble vascular endothelial growth factor receptors impairs angiogenesis and perfusion in a murine model of hindlimb ischemia. Circulation, 110(16), 2424–2429. https://doi.org/10.1161/01.CIR.0000145142.85645.EA

Jetten, N., Donners, M. M., Wagenaar, A., Cleutjens, J. P., van Rooijen, N., de Winther, M. P., & Post, M. J. (2013). Local delivery of polarized macrophages improves reperfusion recovery in a mouse hind limb ischemia model. PLoS One, 8(7), e68811. https://doi.org/10.1371/journal.pone.0068811

Jiang, W., Hu, W., Ye, L., Tian, Y., Zhao, R., du, J., Shen, B., & Wang, K. (2019). Contribution of Apelin-17 to collateral circulation following cerebral ischemic Stroke. Translational Stroke Research, 10(3), 298–307. https://doi.org/10.1007/s12975-018-0638-7

Jin, Y., Muhl, L., Burmakin, M., Wang, Y., Duchez, A. C., Betsholtz, C., Arthur, H. M., & Jakobsson, L. (2017). Endoglin prevents vascular malformation by regulating flow-induced cell migration and specification through VEGFR2 signalling. Nature Cell Biology, 19(6), 639–652. https://doi.org/10.1038/ncb3534

Joriot-Chekaf, S., Sfeir, R., Riou, Y., Gressens, P., Vallee, L., Bordet, R., & Vamecq, J. (2010). Evaluation of inhaled NO in a model of rat neonate brain injury caused by hypoxia-ischaemia. Injury, 41(5), 517–521. https://doi.org/10.1016/j.injury.2009.03.046

Jung, S., Gilgen, M., Slotboom, J., el-Koussy, M., Zubler, C., Kiefer, C., Luedi, R., Mono, M. L., Heldner, M. R., Weck, A., Mordasini, P., Schroth, G., Mattle, H. P., Arnold, M., Gralla, J., & Fischer, U. (2013). Factors that determine penumbral tissue loss in acute ischaemic stroke. Brain, 136(Pt 12), 3554–3560. https://doi.org/10.1093/brain/awt246

Just, U., Friel, J., Heberlein, C., Tamura, T., Baccarini, M., Tessmer, U., Klingler, K., & Ostertag, W. (1993). Upregulation of lineage specific receptors and ligands in multipotential progenitor cells is part of an endogenous program of differentiation. Growth Factors, 9(4), 291– 300. https://doi.org/10.3109/08977199308991589

Kathem, S. H., Mohieldin, A. M., Abdul-Majeed, S., Ismail, S. H., Altaei, Q. H., Alshimmari, I. K., Alsaidi, M. M., Khammas, H., Nauli, A. M., Joe, B., & Nauli, S. M. (2014). Ciliotherapy: A novel intervention in polycystic kidney disease. Journal of Geriatric Cardiology, 11(1), 63–73. https://doi.org/10.3969/j.issn.1671-5411.2014.01.001

Kawano, H., Bivard, A., Lin, L., Ma, H., Cheng, X., Aviv, R., O'Brien, B., Butcher, K., Lou, M., Zhang, J., Jannes, J., Dong, Q., Levi, C. R., & Parsons, M. W. (2017). Perfusion computed tomography in patients with stroke thrombolysis. Brain, 140(3), 684–691. https://doi.org/10.1093/brain/aww338

Khmelewski, E., Becker, A., Meinertz, T., & Ito, W. D. (2004). Tissue resident cells play a dominant role in arteriogenesis and concomitant macrophage accumulation. Circulation Research, 95(6), E56–E64. https://doi.org/10.1161/01.RES.0000143013.04985.E7

Kinnaird, T., Stabile, E., Burnett, M. S., Lee, C. W., Barr, S., Fuchs, S., & Epstein, S. E. (2004). Marrow-derived stromal cells express genes encoding a broad spectrum of arteriogenic cytokines and promote in vitro and in vivo arteriogenesis through paracrine mechanisms. Circulation Research, 94(5), 678–685. https://doi.org/10.1161/01.RES.0000118601.37875.AC

Klein, B., Le Bousse-Kerdiles, C., Smadja-Joffe, F., Pragnell, I., Ostertag, W., & Jasmin, C. (1982). A study of added GM-CSF independent granulocyte and macrophage precursors in mouse spleen infected with myeloproliferative sarcoma virus (MPSV). Experimental Hematology, 10(4), 373–382.

Klems, A., van Rijssel, J., Ramms, A. S., Wild, R., Hammer, J., Merkel, M., Derenbach, L., Préau, L., Hinkel, R., Suarez-Martinez, I., SchulteMerker, S., Vidal, R., Sauer, S., Kivelä, R., Alitalo, K., Kupatt, C., van Buul, J., & le Noble, F. (2020). The GEF trio controls endothelial cell size and arterial remodeling downstream of Vegf signaling in both zebrafish and cell models. Nature Communications, 11(1), 5319. https://doi.org/10.1038/s41467-020-19008-0

Kosaki, K., Ando, J., Korenaga, R., Kurokawa, T., & Kamiya, A. (1998). Fluid shear stress increases the production of granulocytemacrophage colony-stimulating factor by endothelial cells via mRNA stabilization. Circulation Research, 82(7), 794–802. https://doi.org/10.1161/01.res.82.7.794

Kurre, W., Vorlaender, K., Aguilar-Perez, M., Schmid, E., Bazner, H., & Henkes, H. (2013). Frequency and relevance of anterior cerebral artery embolism caused by mechanical thrombectomy of middle cerebral artery occlusion. AJNR. American Journal of Neuroradiology, 34(8), 1606–1611. https://doi.org/10.3174/ajnr.A3462

Lambiase, P. D., Edwards, R. J., Anthopoulos, P., Rahman, S., Meng, Y. G., Bucknall, C. A., Redwood, S. R., Pearson, J. D., & Marber, M. S. (2004). Circulating humoral factors and endothelial progenitor cells in patients with differing coronary collateral support. Circulation, 109(24), 2986–2992. https://doi.org/10.1161/01.CIR.0000130639.97284.EC

Landmesser, U., Engberding, N., Bahlmann, F. H., Schaefer, A., Wiencke, A., Heineke, A., Spiekermann, S., Hilfiker-Kleiner, D., Templin, C., Kotlarz, D., Mueller, M., Fuchs, M., Hornig, B., Haller, H., & Drexler, H. (2004). Statin-induced improvement of endothelial progenitor cell mobilization, myocardial neovascularization, left ventricular function, and survival after experimental myocardial infarction requires endothelial nitric oxide synthase. Circulation, 110(14), 1933–1939. https://doi.org/10.1161/01.CIR.0000143232.67642.7A

Lasch, M., Kleinert, E. C., Meister, S., Kumaraswami, K., Buchheim, J. I., Grantzow, T., Lautz, T., Salpisti, S., Fischer, S., Troidl, K., Fleming, I., Randi, A. M., Sperandio, M., Preissner, K. T., & Deindl, E. (2019). Extracellular RNA released due to shear stress controls natural bypass growth by mediating mechanotransduction in mice. Blood, 134(17), 1469–1479. https://doi.org/10.1182/blood.2019001392

Lazarous, D. F., Scheinowitz, M., Shou, M., Hodge, E., Rajanayagam, S., Hunsberger, S., Robison, W. G., Jr., Stiber, J. A., Correa, R., & Epstein, S. E. (1995). Effects of chronic systemic administration of basic fibroblast growth factor on collateral development in the canine heart. Circulation, 91(1), 145–153. https://doi.org/10.1161/01.cir.91.1.145

Lee, E. J., Kim, S. J., Bae, J., Lee, E. J., Kwon, O. D., Jeong, H. Y., Kim, Y., & Jeong, H. B. (2021). Impact of onset-to-door time on outcomes and factors associated with late hospital arrival in patients with acute ischemic stroke. PLoS One, 16(3), e0247829. https://doi.org/10.1371/journal.pone.0247829

Lee, H. J., & Koh, G. Y. (2003). Shear stress activates Tie2 receptor tyrosine kinase in human endothelial cells. Biochemical and Biophysical Research Communications, 304(2), 399–404. https://doi.org/10.1016/s0006-291x(03)00592-8

Lee, S. J., Hwang, Y. H., Hong, J. M., Choi, J. W., Kang, D. H., Kim, Y. W., Kim, Y. S., Hong, J. H., Yoo, J., Kim, C. H., Ovbiagele, B., Demchuk, A., Sohn, S. I., & Lee, J. S. (2020). Predictors and prognoses of Willisian collateral failure during mechanical thrombectomy. Scientific Reports, 10(1), 20874. https://doi.org/10.1038/s41598-020-77946-7

Lee, S. U., Hong, J. M., Kim, S. Y., Bang, O. Y., Demchuk, A. M., & Lee, J. S. (2016). Differentiating carotid terminus occlusions into two distinct populations based on Willisian collateral status. Journal of Stroke, 18(2), 179–186. https://doi.org/10.5853/jos.2015.01529

Lees, K. R., Bluhmki, E., von Kummer, R., Brott, T. G., Toni, D., Grotta, J. C., Albers, G. W., Kaste, M., Marler, J. R., Hamilton, S. A., Tilley, B. C., Davis, S. M., Donnan, G. A., Hacke, W., ECASS, ATLANTIS, NINDS and EPITHET rt-PA Study Group, Allen, K., Mau, J., Meier, D., del Zoppo, G., ... Byrnes, G. (2010). Time to treatment with intravenous alteplase and outcome in stroke: An updated pooled analysis of ECASS, ATLANTIS, NINDS, and EPITHET trials. Lancet, 375(9727), 1695–1703. https://doi.org/10.1016/S0140-6736(10) 60491-6

Liebeskind, D. S. (2003). Collateral circulation. Stroke, 34(9), 2279–2284. https://doi.org/10.1161/01.STR.0000086465.41263.06

Lloyd, P. G., Prior, B. M., Li, H., Yang, H. T., & Terjung, R. L. (2005). VEGF receptor antagonism blocks arteriogenesis, but only partially inhibits angiogenesis, in skeletal muscle of exercise-trained rats. American Journal of Physiology. Heart and Circulatory Physiology, 288(2), H759–H768. https://doi.org/10.1152/ajpheart.00786.2004

Ma, J., Ma, Y., Dong, B., Bandet, M. V., Shuaib, A., & Winship, I. R. (2017). Prevention of the collapse of pial collaterals by remote ischemic perconditioning during acute ischemic stroke. Journal of Cerebral Blood Flow and Metabolism, 37(8), 3001–3014. https://doi.org/10.1177/0271678X16680636

Ma, T., & Bai, Y. P. (2020). The hydromechanics in arteriogenesis. Aging Medicine (Milton), 3(3), 169–177. https://doi.org/10.1002/agm2.12101

Man, S., Xian, Y., Holmes, D. N., Matsouaka, R. A., Saver, J. L., Smith, E. E., Bhatt, D. L., Schwamm, L. H., & Fonarow, G. C. (2020). Association between thrombolytic door-to-needle time and 1-year mortality and readmission in patients with acute ischemic Stroke. JAMA, 323(21), 2170–2184. https://doi.org/10.1001/jama.2020.5697

Manolopoulos, V. G., Liekens, S., Koolwijk, P., Voets, T., Peters, E., Droogmans, G., Lelkes, P. I., de Clercq, E., & Nilius, B. (2000). Inhibition of angiogenesis by blockers of volume-regulated anion channels. General Pharmacology, 34(2), 107–116. https://doi.org/10.1016/s0306-3623(00)00052-5

Martinez-Lemus, L. A. (2012). The dynamic structure of arterioles. Basic & Clinical Pharmacology & Toxicology, 110(1), 5–11. https://doi.org/10.1111/j.1742-7843.2011.00813.x

Mazur, M. D., Kilburg, C., Park, M. S., & Taussky, P. (2016). Patterns and clinical impact of Angiographically visible distal emboli during Thrombectomy with solitaire for acute ischemic Stroke. Neurosurgery, 78(2), 242–250. https://doi.org/10.1227/NEU.0000000000001135

McMullan, R. C., Kelly, S. A., Hua, K., Buckley, B. K., Faber, J. E., Pardo-Manuel de Villena, F., & Pomp, D. (2016). Long-term exercise in mice has sex-dependent benefits on body composition and metabolism during aging. Physiological Reports, 4(21), e13011. https://doi.org/10.14814/phy2.13011

Mechtouff, L., Bochaton, T., Paccalet, A., Crola da Silva, C., Buisson, M., Amaz, C., Derex, L., Ong, E., Berthezene, Y., Eker, O. F., Dufay, N., Mewton, N., Ovize, M., Cho, T. H., & Nighoghossian, N. (2020). Matrix Metalloproteinase-9 and monocyte chemoattractant Protein-1 are associated with collateral status in acute ischemic Stroke with large vessel occlusion. Stroke, 51(7), 2232–2235. https://doi.org/10.1161/STROKEAHA.120.029395

Mees, B., Wagner, S., Ninci, E., Tribulova, S., Martin, S., van Haperen, R., Kostin, S., Heil, M., de Crom, R., & Schaper, W. (2007). Endothelial nitric oxide synthase activity is essential for vasodilation during blood flow recovery but not for arteriogenesis. Arteriosclerosis, Thrombosis, and Vascular Biology, 27(9), 1926–1933. https://doi.org/10.1161/ATVBAHA.107.145375

Miao, H., Hu, Y. L., Shiu, Y. T., Yuan, S., Zhao, Y., Kaunas, R., Wang, Y., Jin, G., Usami, S., & Chien, S. (2005). Effects of flow patterns on the localization and expression of VE-cadherin at vascular endothelial cell junctions: In vivo and in vitro investigations. Journal of Vascular Research, 42(1), 77–89. https://doi.org/10.1159/000083094

Millenaar, D. N., Degen, A., Boehm, M., Laufs, U., & Schirmer, S. H. (2013). Macrohage depletion using clodronate liposomes delays exercise-induced collateral artery growth. European Heart Journal, 34, 116–116.

Miyazaki, T., Taketomi, Y., Takimoto, M., Lei, X. F., Arita, S., Kim-Kaneyama, J. R., Arata, S., Ohata, H., Ota, H., Murakami, M., & Miyazaki, A. (2011). M-Calpain induction in vascular endothelial cells on human and mouse atheromas and its roles in VE-cadherin disorganization and atherosclerosis. Circulation, 124(23), 2522–2532. https://doi.org/10.1161/CIRCULATIONAHA.111.021675

Mizuma, A., Yamashita, T., Kono, S., Nakayama, T., Baba, Y., Itoh, S., Asakura, K., Niimi, Y., Asahi, T., Kanemaru, K., Mutoh, T., Kuroda, S., Kinouchi, H., Abe, K., & Takizawa, S. (2016). Phase II trial of intravenous low-dose granulocyte Colony-stimulating factor in acute ischemic Stroke. Journal of Stroke and Cerebrovascular Diseases, 25(6), 1451–1457. https://doi.org/10.1016/j.jstrokecerebrovasdis.2016.01.022

Möbius-Winkler, S., Uhlemann, M., Adams, V., Sandri, M., Erbs, S., Lenk, K., Mangner, N., Mueller, U., Adam, J., Grunze, M., Brunner, S., Hilberg, T., Mende, M., Linke, A. P., & Schuler, G. (2016). Coronary collateral growth induced by physical exercise: Results of the impact of intensive exercise training on coronary collateral circulation in patients with stable coronary artery disease (EXCITE) trial. Circulation, 133(15), 1438–1448; discussion 1448. https://doi.org/10.1161/CIRCULATIONAHA.115.016442

Mohammad, Y. M., Christoforidis, G. A., Bourekas, E. C., & Slivka, A. P. (2008). Qureshi grading scheme predicts subsequent volume of brain infarction following intra-arterial thrombolysis in patients with acute anterior circulation ischemic stroke. Journal of Neuroimaging, 18(3), 262–267. https://doi.org/10.1111/j.1552-6569.2007.00233.x

Moore, S. M., Zhang, H., Maeda, N., Doerschuk, C. M., & Faber, J. E. (2015). Cardiovascular risk factors cause premature rarefaction of the collateral circulation and greater ischemic tissue injury. Angiogenesis, 18(3), 265–281. https://doi.org/10.1007/s10456-015-9465-6

Moriya, Y., Mizuma, A., Uesugi, T., Ohnuki, Y., Nagata, E., Takahashi, W., Kobayashi, H., Kawada, H., Ando, K., Takagi, S., & Takizawa, S. (2013). Phase I study of intravenous low-dose granulocyte colony-stimulating factor in acute and subacute ischemic stroke. Journal of Stroke and Cerebrovascular Diseases, 22(7), 1088–1097. https://doi.org/10.1016/j.jstrokecerebrovasdis.2012.08.002

Murley, R. (1984). John Hunter, velvet and vascular surgery. Annals of the Royal College of Surgeons of England, 66(3), 214–218.

Nakayama, K. H., Hong, G., Lee, J. C., Patel, J., Edwards, B., Zaitseva, T. S., Paukshto, M. V., Dai, H., Cooke, J. P., Woo, Y. J., & Huang, N. F. (2015). Aligned-braided Nanofibrillar scaffold with endothelial cells enhances Arteriogenesis. ACS Nano, 9(7), 6900–6908. https://doi.org/10.1021/acsnano.5b00545

Nauli, S. M., Kawanabe, Y., Kaminski, J. J., Pearce, W. J., Ingber, D. E., & Zhou, J. (2008). Endothelial cilia are fluid shear sensors that regulate calcium signaling and nitric oxide production through polycystin-1. Circulation, 117(9), 1161–1171. https://doi.org/10.1161/CIRCULATIONAHA.107.710111

Okyere, B., Creasey, M., Lebovitz, Y., & Theus, M. H. (2018). Temporal remodeling of pial collaterals and functional deficits in a murine model of ischemic stroke. Journal of Neuroscience Methods, 293, 86–96. https://doi.org/10.1016/j.jneumeth.2017.09.010

Okyere, B., Mills, W. A., 3rd, Wang, X., Chen, M., Chen, J., Hazy, A., Qian, Y., Matson, J. B., & Theus, M. H. (2020). EphA4/Tie2 crosstalk regulates leptomeningeal collateral remodeling following ischemic stroke. The Journal of Clinical Investigation, 130(2), 1024–1035. https://doi.org/10.1172/JCI131493

Ovbiagele, B., Goldstein, L. B., Higashida, R. T., Howard, V. J., Johnston, S. C., Khavjou, O. A., Lackland, D. T., Lichtman, J. H., Mohl, S., Sacco, R. L., Saver, J. L., Trogdon, J. G., & American Heart Association Advocacy Coordinating Committee and Stroke Council. (2013). Forecasting the future of stroke in the United States: A policy statement from the American Heart Association and American Stroke Association. Stroke, 44(8), 2361–2375. https://doi.org/10.1161/STR.0b013e31829734f2

Petrovic, M. T., Djordjevic-Dikic, A., Giga, V., Boskovic, N., Vukcevic, V., Cvetic, V., Mladenovic, A., Radmili, O., Markovic, Z., Dobric, M., Aleksandric, S., Tesic, M., Juricic, S., Nedeljkovic Beleslin, B., Stojkovic, S., Ostojic, M. C., Beleslin, B., & Picano, E. (2020). The coronary ARteriogenesis with combined heparin and EXercise therapy in chronic refractory angina (CARHEXA) trial: A double-blind, randomized, placebo-controlled stress echocardiographic study. European Journal of Preventive Cardiology, 28, 1452–1459. https://doi.org/10.1177/2047487320915661

Piedade, G. S., Schirmer, C. M., Goren, O., Zhang, H., Aghajanian, A., Faber, J. E., & Griessenauer, C. J. (2019). Cerebral collateral circulation: A review in the context of ischemic Stroke and mechanical Thrombectomy. World Neurosurgery, 122, 33–42. https://doi.org/10.1016/j.wneu.2018.10.066

Pikula, A., Beiser, A. S., Chen, T. C., Preis, S. R., Vorgias, D., DeCarli, C., Au, R., Kelly-Hayes, M., Kase, C. S., Wolf, P. A., Vasan, R. S., & Seshadri, S. (2013). Serum brain-derived neurotrophic factor and vascular endothelial growth factor levels are associated with risk of stroke and vascular brain injury: Framingham study. Stroke, 44(10), 2768–2775. https://doi.org/10.1161/STROKEAHA.113.001447

Pipp, F., Boehm, S., Cai, W. J., Adili, F., Ziegler, B., Karanovic, G., Ritter, R., Balzer, J., Scheler, C., Schaper, W., & Schmitz-Rixen, T. (2004). Elevated fluid shear stress enhances postocclusive collateral artery growth and gene expression in the pig hind limb. Arteriosclerosis, Thrombosis, and Vascular Biology, 24(9), 1664–1668. https://doi.org/10.1161/01.ATV.0000138028.14390.e4

Pipp, F., Heil, M., Issbrücker, K., Ziegelhoeffer, T., Martin, S., van den Heuvel, J., Weich, H., Fernandez, B., Golomb, G., Carmeliet, P., Schaper, W., & Clauss, M. (2003). VEGFR-1-selective VEGF homologue PlGF is arteriogenic: Evidence for a monocyte-mediated mechanism. Circulation Research, 92(4), 378–385. https://doi.org/10.1161/01.RES.0000057997.77714.72

Pourati, I., Kimmelstiel, C., Rand, W., & Karas, R. H. (2003). Statin use is associated with enhanced collateralization of severely diseased coronary arteries. American Heart Journal, 146(5), 876–881. https://doi.org/10.1016/S0002-8703(03)00413-7

Powers, W. J., Rabinstein, A. A., Ackerson, T., Adeoye, O. M., Bambakidis, N. C., Becker, K., Biller, J., Brown, M., Demaerschalk, B. M., Hoh, B., Jauch, E. C., Kidwell, C. S., Leslie-Mazwi, T. M., Ovbiagele, B., Scott, P. A., Sheth, K. N., Southerland, A. M., Summers, D. V., & Tirschwell, D. L. (2019). Guidelines for the early Management of Patients with Acute Ischemic Stroke: 2019 update to the 2018 guidelines for the early Management of Acute Ischemic Stroke: A guideline for healthcare professionals from the American Heart Association/American Stroke Association. Stroke, 50(12), e344–e418. https://doi.org/10.1161/STR.0000000000000211

Raymond, S. B., & Schaefer, P. W. (2017). Imaging brain collaterals: Quantification, scoring, and potential significance. Topics in Magnetic Resonance Imaging, 26(2), 67–75. https://doi.org/10.1097/RMR.0000000000000123

Rehman, J., Li, J., Orschell, C. M., & March, K. L. (2003). Peripheral blood "endothelial progenitor cells" are derived from monocyte/macrophages and secrete angiogenic growth factors. Circulation, 107(8), 1164–1169. https://doi.org/10.1161/01.cir.0000058702.69484.a0

Ringelstein, E. B., Thijs, V., Norrving, B., Chamorro, A., Aichner, F., Grond, M., & Investigators, A. (2013). Granulocyte colony-stimulating factor in patients with acute ischemic stroke: Results of the AX200 for ischemic stroke trial. Stroke, 44(10), 2681–2687. https://doi.org/10.1161/STROKEAHA.113.001531

Roberts, H. C., Dillon, W. P., Furlan, A. J., Wechsler, L. R., Rowley, H. A., Fischbein, N. J., Higashida, R. T., Kase, C., Schulz, G. A., Lu, Y., & Firszt, C. M. (2002). Computed tomographic findings in patients undergoing intra-arterial thrombolysis for acute ischemic stroke due to middle cerebral artery occlusion: Results from the PROACT II trial. Stroke, 33(6), 1557–1565. https://doi.org/10.1161/01.str.0000018011.66817.41

Roux, E., Bougaran, P., Dufourcq, P., & Couffinhal, T. (2020). Fluid shear stress sensing by the endothelial layer. Frontiers in Physiology, 11, 861. https://doi.org/10.3389/fphys.2020.00861

Schäbitz, W. R., Laage, R., Vogt, G., Koch, W., Kollmar, R., Schwab, S., Schneider, A., Hamann, G. F., Rosenkranz, M., Veltkamp, R., Fiebach, J. B., Hacke, W., Grotta, J. C., Fisher, M., & Schneider, A. (2010). AXIS: A trial of intravenous granulocyte colony-stimulating factor in acute ischemic stroke. Stroke, 41(11), 2545–2551. https://doi.org/10.1161/STROKEAHA.110.579508

Schaper, J., Borgers, M., & Schaper, W. (1972). Ultrastructure of ischemia-induced changes in the precapillary anastomotic network of the heart. The American Journal of Cardiology, 29(6), 851–859. https://doi.org/10.1016/0002-9149(72)90506-1

Schaper, W., & Buschmann, I. (1999). Arteriogenesis, the good and bad of it. Cardiovascular Research, 43(4), 835–837. https://doi.org/10.1016/s0008-6363(99)00191-1

Schaper, W., De Brabander, M., & Lewi, P. (1971). DNA synthesis and mitoses in coronary collateral vessels of the dog. Circulation Research, 28(6), 671–679. https://doi.org/10.1161/01.res.28.6.671

Schaper, W., Flameng, W., Winkler, B., Wüsten, B., Türschmann, W., Neugebauer, G., Carl, M., & Pasyk, S. (1976). Quantification of collateral resistance in acute and chronic experimental coronary occlusion in the dog. Circulation Research, 39(3), 371–377. https://doi.org/10.1161/01.res.39.3.371

Schirmer, S. H., Buschmann, I. R., Jost, M. M., Hoefer, I. E., Grundmann, S., Andert, J. P., Ulusans, S., Bode, C., Piek, J. J., & van Royen, N. (2004). Differential effects of MCP-1 and leptin on collateral flow and arteriogenesis. Cardiovascular Research, 64(2), 356–364. https://doi.org/10.1016/j.cardiores.2004.06.022

Schirmer, S. H., Fledderus, J. O., Bot, P. T., Moerland, P. D., Hoefer, I. E., Baan, J., Jr., Henriques, J. P., van der Schaaf, R., Vis, M. M., Horrevoets, A. J., Piek, J. J., & van Royen, N. (2008). Interferon-beta signaling is enhanced in patients with insufficient coronary collateral artery development and inhibits arteriogenesis in mice. Circulation Research, 102(10), 1286–1294. https://doi.org/10.1161/CIRCRESAHA.108.171827

Schirmer, S. H., Millenaar, D. N., Werner, C., Schuh, L., Degen, A., Bettink, S. I., Lipp, P., van Rooijen, N., Meyer, T., Böhm, M., & Laufs, U. (2015). Exercise promotes collateral artery growth mediated by monocytic nitric oxide. Arteriosclerosis, Thrombosis, and Vascular Biology, 35(8), 1862–1871. https://doi.org/10.1161/ATVBAHA.115.305806

Scholz, D., Ito, W., Fleming, I., Deindl, E., Sauer, A., Wiesnet, M., Busse, R., Schaper, J., & Schaper, W. (2000). Ultrastructure and molecular histology of rabbit hind-limb collateral artery growth (arteriogenesis). Virchows Archiv, 436(3), 257–270. https://doi.org/10.1007/s004280050039

Seiler, C. (2010). The human coronary collateral circulation. European Journal of Clinical Investigation, 40(5), 465–476. https://doi.org/10.1111/j.1365-2362.2010.02282.x

Seiler, C., Pohl, T., Wustmann, K., Hutter, D., Nicolet, P. A., Windecker, S., Eberli, F. R., & Meier, B. (2001). Promotion of collateral growth by granulocyte-macrophage colony-stimulating factor in patients with coronary artery disease: A randomized, double-blind, placebocontrolled study. Circulation, 104(17), 2012–2017. https://doi.org/10.1161/hc4201.097835

Seker, F., Pereira-Zimmermann, B., Pfaff, J., Purrucker, J., Gumbinger, C., Schönenberger, S., Bendszus, M., & Möhlenbruch, M. A. (2020). Collateral scores in acute ischemic stroke: A retrospective study assessing the suitability of collateral scores as standalone predictors of clinical outcome. Clinical Neuroradiology, 30(4), 789–793. https://doi.org/10.1007/s00062-019-00858-1

Semerano, A., Laredo, C., Zhao, Y., Rudilosso, S., Renú, A., Llull, L., Amaro, S., Obach, V., Planas, A. M., Urra, X., & Chamorro, A. (2019). Leukocytes, collateral circulation, and reperfusion in ischemic Stroke patients treated with mechanical Thrombectomy. Stroke, 50(12), 3456–3464. https://doi.org/10.1161/STROKEAHA.119.026743

Siddiqui, A. J., Blomberg, P., Wardell, E., Hellgren, I., Eskandarpour, M., Islam, K. B., & Sylven, C. (2003). Combination of angiopoietin-1 and vascular endothelial growth factor gene therapy enhances arteriogenesis in the ischemic myocardium. Biochemical and Biophysical Research Communications, 310(3), 1002–1009. https://doi.org/10.1016/j.bbrc.2003.09.111

Sonntag, W. E., Lynch, C. D., Cooney, P. T., & Hutchins, P. M. (1997). Decreases in cerebral microvasculature with age are associated with the decline in growth hormone and insulin-like growth factor 1. Endocrinology, 138(8), 3515–3520. https://doi.org/10.1210/endo.138.8.5330

Strinitz, M., Pham, M., März, A. G., Feick, J., Weidner, F., Vogt, M. L., Essig, F., Neugebauer, H., Stoll, G., Schuhmann, M. K., & Kollikowski, A. M. (2021). Immune cells invade the collateral circulation during human Stroke: Prospective replication and extension. International Journal of Molecular Sciences, 22(17), 9161. https://doi.org/10.3390/ijms22179161

Sugiyama, Y., Yagita, Y., Oyama, N., Terasaki, Y., Omura-Matsuoka, E., Sasaki, T., & Kitagawa, K. (2011). Granulocyte colony-stimulating factor enhances arteriogenesis and ameliorates cerebral damage in a mouse model of ischemic stroke. Stroke, 42(3), 770–775. https://doi.org/10.1161/STROKEAHA.110.597799

Swanson, R. L., 2nd. (2013). Biotensegrity: A unifying theory of biological architecture with applications to osteopathic practice, education, and research—A review and analysis. The Journal of the American Osteopathic Association, 113(1), 34–52. https://doi.org/10.7556/jaoa.2013.113.1.34

Tarkanyi, G., Karadi, Z. N., Szabo, Z., Szegedi, I., Csiba, L., & Szapary, L. (2020). Relationship between leukocyte counts and large vessel occlusion in acute ischemic stroke. BMC Neurology, 20(1), 440. https://doi.org/10.1186/s12883-020-02017-3

Terpolilli, N. A., Kim, S. W., Thal, S. C., Kataoka, H., Zeisig, V., Nitzsche, B., Klaesner, B., Zhu, C., Schwarzmaier, S., Meissner, L., Mamrak, U., Engel, D. C., Drzezga, A., Patel, R. P., Blomgren, K., Barthel, H., Boltze, J., Kuebler, W. M., & Plesnila, N. (2012). Inhalation of nitric oxide prevents ischemic brain damage in experimental stroke by selective dilatation of collateral arterioles. Circulation Research, 110(5), 727–738. https://doi.org/10.1161/CIRCRESAHA.111.253419

Timmerman, I., Heemskerk, N., Kroon, J., Schaefer, A., van Rijssel, J., Hoogenboezem, M., van Unen, J., Goedhart, J., Gadella, T. W., Jr., Yin, T., Wu, Y., Huveneers, S., & van Buul, J. (2015). A local VE-cadherin and trio-based signaling complex stabilizes endothelial junctions through Rac1. Journal of Cell Science, 128(16), 3041–3054. https://doi.org/10.1242/jcs.168674

Todo, K., Kitagawa, K., Sasaki, T., Omura-Matsuoka, E., Terasaki, Y., Oyama, N., Yagita, Y., & Hori, M. (2008). Granulocyte-macrophage colony-stimulating factor enhances leptomeningeal collateral growth induced by common carotid artery occlusion. Stroke, 39(6), 1875– 1882. https://doi.org/10.1161/STROKEAHA.107.503433

Togni, M., Gloekler, S., Meier, P., de Marchi, S. F., Rutz, T., Steck, H., Traupe, T., & Seiler, C. (2010). Instantaneous coronary collateral function during supine bicycle exercise. European Heart Journal, 31(17), 2148–2155. https://doi.org/10.1093/eurheartj/ ehq202

Tong, D., Reeves, M. J., Hernandez, A. F., Zhao, X., Olson, D. M., Fonarow, G. C., Schwamm, L. H., & Smith, E. E. (2012). Times from symptom onset to hospital arrival in the get with the guidelines–Stroke program 2002 to 2009: Temporal trends and implications. Stroke, 43(7), 1912–1917. https://doi.org/10.1161/STROKEAHA.111.644963

Toriumi, H., Tatarishvili, J., Tomita, M., Tomita, Y., Unekawa, M., & Suzuki, N. (2009). Dually supplied T-junctions in arteriolo-arteriolar anastomosis in mice: Key to local hemodynamic homeostasis in normal and ischemic states? Stroke, 40(10), 3378–3383. https://doi.org/10.1161/STROKEAHA.109.558577

Toyota, E., Warltier, D. C., Brock, T., Ritman, E., Kolz, C., O'Malley, P., Rocic, P., Focardi, M., & Chilian, W. M. (2005). Vascular endothelial growth factor is required for coronary collateral growth in the rat. Circulation, 112(14), 2108–2113. https://doi.org/10.1161/CIRCULATIONAHA.104.526954

Traupe, T., Ortmann, J., Stoller, M., Baumgartner, I., de Marchi, S. F., & Seiler, C. (2013). Direct quantitative assessment of the peripheral artery collateral circulation in patients undergoing angiography. Circulation, 128(7), 737–744. https://doi.org/10.1161/CIRCULATIONAHA.112.000516

Tressel, S. L., Kim, H., Ni, C. W., Chang, K., Velasquez-Castano, J. C., Taylor, W. R., Yoon, Y. S., & Jo, H. (2008). Angiopoietin-2 stimulates blood flow recovery after femoral artery occlusion by inducing inflammation and arteriogenesis. Arteriosclerosis, Thrombosis, and Vascular Biology, 28(11), 1989–1995. https://doi.org/10.1161/ATVBAHA.108.175463

Tzima, E., Irani-Tehrani, M., Kiosses, W. B., Dejana, E., Schultz, D. A., Engelhardt, B., Cao, G., DeLisser, H., & Schwartz, M. A. (2005). A mechanosensory complex that mediates the endothelial cell response to fluid shear stress. Nature, 437(7057), 426–431. https://doi.org/10.1038/nature03952

Unger, E. F., Banai, S., Shou, M., Jaklitsch, M., Hodge, E., Correa, R., Jaye, M., & Epstein, S. E. (1993). A model to assess interventions to improve collateral blood flow: Continuous administration of agents into the left coronary artery in dogs. Cardiovascular Research, 27(5),

785–791. https://doi.org/10.1093/cvr/27.5.785

van der Heiden, K., Hierck, B. P., Krams, R., de Crom, R., Cheng, C., Baiker, M., Pourquie, M. J., Alkemade, F. E., DeRuiter, M., Gittenberger-de Groot, A. C., & Poelmann, R. E. (2008). Endothelial primary cilia in areas of disturbed flow are at the base of atherosclerosis. Atherosclerosis, 196(2), 542–550. https://doi.org/10.1016/j.atherosclerosis.2007.05.030

van Royen, N., Piek, J. J., Schaper, W., & Fulton, W. F. (2009). A critical review of clinical arteriogenesis research. Journal of the American College of Cardiology, 55(1), 17–25. https://doi.org/10.1016/j.jacc.2009.06.058

van Royen, N., Schirmer, S. H., Atasever, B., Behrens, C. Y., Ubbink, D., Buschmann, E. E., Voskuil, M., Bot, P., Hoefer, I., Schlingemann, R. O., Biemond, B. J., Tijssen, J. G., Bode, C., Schaper, W., Oskam, J., Legemate, D. A., Piek, J. J., & Buschmann, I. (2005). START trial: A pilot study on STimulation of ARTeriogenesis using subcutaneous application of granulocyte-macrophage colonystimulating factor as a new treatment for peripheral vascular disease. Circulation, 112(7), 1040–1046. https://doi.org/10.1161/ CIRCULATIONAHA.104.529552

Vander Eecken, H. M., & Adams, R. D. (1953). The anatomy and functional significance of the meningeal arterial anastomoses of the human brain. Journal of Neuropathology and Experimental Neurology, 12(2), 132–157. https://doi.org/10.1097/00005072-195304000-00002

Virani, S. S., Alonso, A., Aparicio, H. J., Benjamin, E. J., Bittencourt, M. S., Callaway, C. W., Carson, A. P., Chamberlain, A. M., Cheng, S., Delling, F. N., Elkind, M. S. V., Evenson, K. R., Ferguson, J. F., Gupta, D. K., Khan, S. S., Kissela, B. M., Knutson, K. L., Lee, C. D., Lewis, T. T., ... American Heart Association Council on Epidemiology and Prevention Statistics Committee and Stroke Statistics Subcommittee. (2021). Heart disease and Stroke Statistics-2021 update: A report from the American Heart Association. Circulation, 143(8), e254– e743. https://doi.org/10.1161/CIR.0000000000000950

Yang, B., Cai, B., Deng, P., Wu, X., Guan, Y., Zhang, B., Cai, W., Schaper, J., & Schaper, W. (2015). Nitric oxide increases arterial endotheial permeability through mediating VE-cadherin expression during arteriogenesis. PLoS One, 10(7), e0127931. https://doi.org/10.1371/journal.pone.0127931

Yang, H. T., Ogilvie, R. W., & Terjung, R. L. (1994). Peripheral adaptations in trained aged rats with femoral artery stenosis. Circulation Research, 74(2), 235–243. https://doi.org/10.1161/01.res.74.2.235

Yang, Y., Lv, S. Y., Lyu, S. K., Wu, D., & Chen, Q. (2015). The protective effect of apelin on ischemia/reperfusion injury. Peptides, 63, 43–46. https://doi.org/10.1016/j.peptides.2014.11.001

Yip, H. K., Chang, L. T., Chang, W. N., Lu, C. H., Liou, C. W., Lan, M. Y., Liu, J. S., Youssef, A. A., & Chang, H. W. (2008). Level and value of circulating endothelial progenitor cells in patients after acute ischemic stroke. Stroke, 39(1), 69–74. https://doi.org/10.1161/STROKEAHA.107.489401

Yu, F., Feng, X., Li, X., Liu, Z., Liao, D., Luo, Y., Wei, M., Huang, Q., Zhang, L., & Xia, J. (2021). Association of Plasma Metabolic Biomarker Sphingosine-1-phosphate with cerebral collateral circulation in acute ischemic Stroke. Frontiers in Physiology, 12, 720672. https://doi.org/10.3389/fphys.2021.720672

Zbinden, R., Zbinden, S., Meier, P., Hutter, D., Billinger, M., Wahl, A., Schmid, J. P., Windecker, S., Meier, B., & Seiler, C. (2007). Coronary collateral flow in response to endurance exercise training. European Journal of Cardiovascular Prevention and Rehabilitation, 14(2), 250– 257. https://doi.org/10.1097/HJR.0b013e3280565dee

Zbinden, R., Zbinden, S., Windecker, S., Meier, B., & Seiler, C. (2004). Direct demonstration of coronary collateral growth by physical endurance exercise in a healthy marathon runner. Heart, 90(11), 1350–1351. https://doi.org/10.1136/hrt.2003.023267

Zbinden, S., Brunner, N., Wustmann, K., Billinger, M., Meier, B., & Seiler, C. (2004). Effect of statin treatment on coronary collateral flow in patients with coronary artery disease. Heart, 90(4), 448–449. https://doi.org/10.1136/hrt.2003.017871

Zbinden, S., Zbinden, R., Meier, P., Windecker, S., & Seiler, C. (2005). Safety and efficacy of subcutaneous-only granulocyte-macrophage colony-stimulating factor for collateral growth promotion in patients with coronary artery disease. Journal of the American College of Cardiology, 46(9), 1636–1642. https://doi.org/10.1016/j.jacc.2005.01.068

Zhang, H., Chalothorn, D., & Faber, J. E. (2019). Collateral vessels have unique endothelial and smooth muscle cell phenotypes. International Journal of Molecular Sciences, 20(15), 3608. https://doi.org/10.3390/ijms20153608

Zhang, H., Jin, B., & Faber, J. E. (2019). Mouse models of Alzheimer's disease cause rarefaction of pial collaterals and increased severity of ischemic stroke. Angiogenesis, 22(2), 263–279. https://doi.org/10.1007/s10456-018-9655-0

Zhang, H., Rzechorzek, W., Aghajanian, A., & Faber, J. E. (2020). Hypoxia induces de novo formation of cerebral collaterals and lessens the severity of ischemic stroke. Journal of Cerebral Blood Flow and Metabolism, 40(9), 1806–1822. https://doi.org/10.1177/0271678X20924107

Zhao, Y., Li, J., Ting, K. K., Chen, J., Coleman, P., Liu, K., Wan, L., Moller, T., Vadas, M. A., & Gamble, J. R. (2021). The VE-Cadherin/βcatenin signalling axis regulates immune cell infiltration into tumours. Cancer Letters, 496, 1–15. https://doi.org/10.1016/j.canlet.2020. 09.026

Zhou, P., Tan, Y. Z., Wang, H. J., & Wang, G. D. (2017). Hypoxic preconditioning-induced autophagy enhances survival of engrafted endothelial progenitor cells in ischaemic limb. Journal of Cellular and Molecular Medicine, 21(10), 2452–2464. https://doi.org/10.1111/jcmm.13167

Ziegelhoeffer, T., Fernandez, B., Kostin, S., Heil, M., Voswinckel, R., Helisch, A., & Schaper, W. (2004). Bone marrow-derived cells do not incorporate into the adult growing vasculature. Circulation Research, 94(2), 230–238. https://doi.org/10.1161/01.RES.0000110419.50982.1C

Ziegelhoeffer, T., Scholz, D., Friedrich, C., Helisch, A., Wagner, S., Fernandez, B., & Schaper, W. (2003). Inhibition of collateral artery growth by mibefradil: Possible role of volume-regulated chloride channels. Endothelium, 10(4–5), 237–246. https://doi.org/10.1080/ 10623320390246423

Chapter 3

Genetic and Pharmacological Targeting of The EphA4/Tie2 Axis Results in Improved Pial Collateral Response following Ischemic Stroke

Genetic and Pharmacological Targeting of the EphA4/Tie2 Axis Results in Improved Pial Collateral Response following Ischemic Stroke

Alexandra M. Kaloss[1], Kennedie Lyles[2], Nathalie A. Groot[1], Jackie Zhu[7], Yu Lin[6], Hehuang Xie[1,3,5,6], John B. Matson[7], and Michelle H. Theus*[1,2,3,4]

[1]Department o f Biomedical Sciences and Pathobiology, Virginia Tech, Blacksburg, VA 24061, USA
[2]School of Neuroscience, Virginia Tech, Blacksburg VA 24061, USA
[3]Center for engineered Health, VT, Blacksburg, Virginia, 24061, USA,
[4]Neurotrauma Research Program, Blacksburg, VA, 24061, USA
[5]Genetics, Bioinformatics and Computational Biology Program, Blacksburg, VA 24061, USA
[6]Epigenomics and Computational Biology Lab, Fralin Life Sciences Institute, Blacksburg, VA, 24061 USA
[7]Department of Chemistry, Virginia Tech, Blacksburg, VA 24061, USA

Running Title: Collateral Enhancement by EphA4/Tie2 Targeting

***Keywords*:** Ischemic Strike, EphA4, Tie2, angiopoietin, Vasculotide, arteriogenesis, neuroprotection

***Corresponding author:**
Michelle Theus, PhD
Co-Director Translational Biology Medicine and Health graduate program
Associate Professor, Biomedical Sciences and Pathobiology, Virginia Tech
Associate Professor, Health Sciences, Virginia Tech
Affiliate, VT-Biomedical Engineering and School of Neuroscience
970 Washington Street SW
Life Sciences I; rm 249 (MC0910)
Blacksburg, VA 24061
Tel. 540-231-0909; Fax 540-231-7425; E-mail: **mtheus@vt.edu**

Abbreviations: WT, wildtype; KO, knockout; tKD, Tie2 knockdown; dKD, double Tie2/EphA4 knockdown; pMCAO, permanent middle cerebral artery occlusion; MCA, middle cerebral artery; ACA, anterior cerebral artery; PCA, posterior cerebral artery; CBF, cerebral blood flow; EC, endothelial cells; SMC, smooth muscle cell; SMA, smooth muscle actin; Ang, angiopoietin; VT, Vasculotide.

Conflict of interest statement: The authors have declared that no conflict of interest exists.

Author Contribution: A.M.K., K.L., N.A.G., Y.L., H.X., and M.H.T. performed research and analyzed data. A.M.K., J.Z., H.X., J.B.M., and M.H.T contributed reagents/analytic tools. A.M.K. and M.H.T. designed research, wrote and edited paper.

Acknowledgments: We recognize the Biomedical and Veterinary Sciences Program (BMVS). We thank Dr. John Chappell for the generous gift of *VeCadherin-CreERT2* mice and Dr. Joachim R. Göthert for the generous gift of *Tie2*$^{fl/fl}$ mice. Thank you to Xiguang Xu and the Fralin Life Sciences Genomic Sequencing Center for assistance with RNA quality testing. This work was supported by the National Institute of Neurological Disorders and Stroke of the National Institutes of Health, R01NS112541 (MHT).

Abstract

Background: Pial collaterals are a major determinant of patient outcome following ischemic stroke, however, targeted treatments for enhancing these blood vessels remain elusive. EphA4, a receptor tyrosine kinase, has been found to restrict the growth of these vessels, potentially through modulation of the Tie2 signaling pathway. The present study assessed the endothelial cell (EC)-specific role of EphA4 in arteriogenesis and the therapeutic potential of Vasculotide, a Tie2 agonist, after ischemic stroke.

Methods: EC-specific EphA4 knockout mice and wildtype controls, as well as wildtype mice treated with vehicle or Vasculotide, were subjected to a permanent middle cerebral artery model of stroke. Infarct volume and functional recovery were assessed. Vessel painting coupled with immunohistochemistry was employed to assess collateral size and cellular changes. Bulk RNA sequencing of the pial surface was performed to identify unique transcriptional changes.

Results: Deletion of EphA4 in ECs resulted in increased collateral size and accelerated cellular remodeling, which correlated with reduced infarct volume, enhanced CBF recovery, and improved performance on behavioral assessments. These effects could be replicated in wildtype mice through the administration of 3μg/kg Vasculotide immediately following stroke. Treatment with 150μg/kg Vasculotide provided neuroprotection and increased collateral size but lacked the robust improvements in CBF recovery and motor recovery seen in the 3μg/kg treated group. Additionally, pial surfaces from 3μg/kg Vasculotide and EphA4 KO mice showed significant changes in mRNA transcripts associated with the Krt5/Krt14 pathway compared to WT controls.

Conclusion: The EphA4/Tie2 signaling axis mediates collateral growth and can be successfully therapeutically targeted by Vasculotide.

Introduction

Ischemic strokes remain a significant global cause of mortality and morbidity. Loss of cerebral blood flow (CBF) after the vascular obstruction leads to cell death and neurological impairments. It has been well documented that leptomeningeal anastomoses or pial collaterals can function to partially restore CBF to vulnerable neural tissue [1]. This retrograde perfusion is imperative for preserving the penumbral tissue and reducing the damage of an ischemic stroke, making the extent of collateral vessels present a major determinant of patient outcome following ischemic stroke [2]. Under healthy conditions, these specialized pre-existing arterioles are fed by two arteries resulting in bidirectional blood flow. This coupled with the high tortuosity and non-physiological angles of insertion provides these vessels and their associated cells with a unique hemodynamic environment, as they are continuously exposed to disturbed flow [3]. Following an ischemic stroke, where one of the feeding arteries is blocked, these pial collateral vessels become exposed to unidirectional flow via the non-obstructed artery. This change in blood flow leads to an increase in fluid shear stress, the viscous drag force of the blood along the vessel wall, and triggers arteriogenesis, the remodeling process of these pial collaterals into conductance arteries [4].

The process of arteriogenesis requires endothelial and smooth muscle cell proliferation, immune cell recruitment, and degradation of the extracellular matrix to allow for the outward expansion of the collateral vessel [5]. However, temporal cellular remodeling of the pial collaterals following ischemic stroke has not been fully established. Importantly, it remains unclear how early after occlusion these changes are evident and whether outward remodeling contributes to collateral size and redistribution of CBF. This gap in knowledge of the acute remodeling capacity of these vessels could hinder the development of targeted therapeutics that enhance arteriogenesis or the vasodilatory capacity of the pial collateral vessels.

Eph receptors, the largest family of receptor tyrosine kinases, and their ephrin ligands have been implicated in vascular differentiation and endothelial cell health. The ephrinB2 ligand is expressed on

arterial endothelial cells, while the EphB4 receptor is expressed on venous-fated endothelial cells [6, 7]. Additionally, EphA4 and ephrinA1 are upregulated in endothelial cells following oxygen-glucose deprivation *in vitro* [8]. In murine stroke models, EphA4 has been implicated as a negative regulator of collateral formation and arteriogenesis [9, 10]. In this study, we report a marked improvement in pial collateral vessel response and functional recovery using EC-specific EphA4 knockout (KO) mice. This response was associated with increased Tie2 and Angiopeotin-1 protein expression in the KO mice and could be recapitulated in wildtype mice by a single dose of Vasculotide, an ang-1 mimetic peptide. Taken together, we conclude that the EphA4/Tie2 axis can dictate collateral response and be successfully therapeutically targeted to enhance collateral growth following ischemic stroke.

Results

Loss of Endothelial Cell-Specific EphA4 Confers Neuroprotection and Improves Functional Recovery

Evidence from previous studies has implicated EphA4 in exacerbating tissue loss and functional recovery after ischemic stroke [10]. In the present investigation, we employed EC-specific knockout mice ($EphA4^{fl/fl}$/VECadherin-Cre^{ERT2}; KO) and wildtype controls ($EphA4^{fl/fl}$; WT) to evaluate how the cell-specific expression of EphA4 influences ischemic stroke outcomes. Infarct volume, as a measure of tissue loss, was assessed using cresyl violet (Nissl) stained serial cryo-sectioned slides. A reduction in infarct volume was observed in the KO mice (14.31 ± 2.52 mm^3) compared to WT controls (24.04 ± 1.69 mm^3) at one-day post-pMCAO (Fig 1A-1C). This correlated with improved CBF perfusion in KO mice measured by laser speckle contrast imaging from 1- to 4-days post-injury compared to WT control mice.

EC-specific EphA4 KO mice also displayed marked improvements in behavioral recovery after ischemic stroke compared to WT counterparts. In the rotarod assessment of motor function, KO mice performed significantly better than WT mice at 3-days (67.31 ± 3.45% vs 78.77 ± 2.12%) and 7-days post-injury (76.84 ± 2.76% vs 88.77 ± 2.89%) (Fig 1F). Similarly, KO mice showed improvements beyond WT mice

– as demonstrated by significantly lower modified neurological severity scores – at 3 (5.69 ± 0.29 vs 4.28 ± 0.21) and 7 days post-pMCAO (5.08 ± 0.18 vs 4.31 ± 0.17) (Fig 1G). Furthermore, assessing adhesive tape removal using asymmetry score revealed that KO mice performed significantly better than WT controls at all timepoints following injury (1, 3, 7, 14, 21, and 28 days) (Fig 1H). These findings suggest that EC-specific expression of EphA4 exacerbates tissue loss, dampens recovery of CBF, and reduces functionality after injury.

Increased Size in the MCA-ACA Pial Niche of EC-Specific EphA4 Knockout Mice During the Hyperacute Phase of Ischemic Stroke

Pial collateral density and remodeling capacity are the main indicators of ischemic stroke outcomes in patients. In naïve mice, no differences were observed between WT and KO pial collateral size or number (Supplementary Fig 1A-D). To determine how EC-specific EphA4 influenced the hyperacute response of pial collateral vessels to vascular obstruction, vessel painting was performed at 4.5-, 6-, and 24-hours post-pMCAO. As early as 4.5 hours after stroke, KO mice had significantly larger MCA-ACA ipsilateral pial collaterals (32.41 ± 0.77 μm) compared to WT controls (27.31 ± 0.58 μm) and this enhancement continued through 6-hours (WT: 29.41 ± 0.60 μm; KO: 33.70 ± 0.61 μm) and 24-hours (WT: 31.14 ± 0.84 μm; KO: 36.73 ± 0.89 μm) post-pMCAO (Fig 2A-2E). Conversely, no differences were seen between WT and KO mice in the MCA-PCA connecting collateral bed at any timepoint (4.5-hours: 25.16 ± 1.11 μm vs 27.69 ± 1.34 μm; 6-hours: 27.50 ± 0.64 μm vs 30.93 ± 0.89 μm; 24-hours: 30.00 ± 1.30 μm vs 32.77 ± 1.23 μm, respectively) (Supplementary Fig 2H). Total MCA intercollaterals, including both previously mentioned collateral niches, displayed the same trends seen in that of the MCA-ACA collaterals, with significantly larger diameter pial collaterals seen in the ipsilateral hemisphere of KO mice at all timepoints compared to WT controls (Supplementary Fig. 2I). Regarding collateral density, no changes were observed in MCA-ACA connecting collateral or total MCA intercollateral number across the timepoints

between WT and KO mice (Fig 2F; Supplementary Fig 2J). A breakdown of the MCA-ACA collateral distribution showed KO mice had a larger percentage (55%) of ipsilateral collaterals with a diameter greater than 31 μm at 4.5 hours, this percent then increased to 70% and 73% at 6-hours and 24-hours post-pMCAO, respectively. Comparatively, WT mice only had 36%, 39%, and 54% of collaterals over 31 μm at 4.5-, 6-, and 24-hours post-pMCAO, respectively (Supplementary Fig 2E-2G). These results suggest that loss of EC-specific EphA4 enhances MCA-ACA pial collateral diameter as early as 4.5-hours post-pMCAO and that this heightened response is sustained through 24-hours post-injury.

EphA4 functions through forward signaling to restrict collateral expansion

Eph-ephrin signaling is unique because the ephrin ligand is membrane bound, which allows not only classical forward signaling through the eph receptor cell but also reverse signaling in the ligand-containing cell [11]. To investigate if restriction of pial collateral growth we see in WT mice is due to forward or reverse signaling, we employed clustered (cl) EphA4-Fc. In KO mice, clEphA4-Fc was delivered in a bolus IV injection immediately following MCA occlusion to stimulate the ephrin ligands. No changes were seen in collateral vessel size or number 24-hours following stroke, indicating that the negative effects of EphA4 on collateral size occurs through forward signaling (Supplemental Figure 2).

Nitric Oxide Induced Vasodilation Does Not Fully Account for Increased Pial Collateral Size in Knockout Mice

Collateral blood vessels can increase in size due to two major modes of action: vasodilation or cellular remodeling. Nitric oxide (NO) is a free radical that serves as a potent vasodilator known to be released after ischemic stroke and impact collateral circulation [12]. To begin investigating if the increased diameter seen in KO MCA-ACA pial collateral vessels was due to nitric oxide-induced vasodilation, L-NAME – a NO synthase inhibitor – was given to mice in their drinking water at 1g/L for 24-hours post-

pMCAO. Both WT and KO mice treated with L-NAME had significantly reduced serum nitrate/nitrite levels, confirming the efficacy of this treatment regime (Fig 2I). No difference was seen between genotypes or in drinking water treatment (plain water/vehicle vs L-NAME) in the MCA-ACA pial collaterals of the contralateral hemisphere (Vehicle: 22.34 ± 0.75 μm vs 23.45 ± 0.58 μm; L-NAME: 21.63 ± 0.95 μm vs 22.28 ± 0.97 μm) (Fig 2G). However, in the ipsilateral hemisphere, the pial collaterals of L-NAME treated WT (25.23 ± 0.78 μm vs 29.95 ± 0.67 μm) and KO mice were significantly smaller than their respective plain water controls (31.48 ± 0.91 μm vs 37.69 ± 1.19 μm). Interestingly, MCA-ACA collateral diameter remained elevated in the L-NAME treated KO group compared to the L-NAME treated WT collaterals (Fig 2H). These findings suggest that in WT but not KO mice, NO-induced vasodilation accounts for the increase in pial collateral vessel size within the first 24-hours post-injury.

Knockout Mice Exhibit Increased Immune Cell Recruitment and EC Proliferation but No Changes in Smooth Muscle Cell Phenotype

Following vascular occlusion, pial collateral vessels undergo cellular remodeling events to expand into conductance arteries. To uncover the temporal nature of these cellular changes in MCA-ACA connecting pial collateral vessels, immunolabeling was performed using various markers. CD11b and Iba1 were used to investigate the number and population of immune cells recruited to the collateral (CD11b: a marker of monocytes/macrophages, granulocytes, and natural killer cells; Iba1: a marker for monocytes/macrophages), PCNA for endothelial cell proliferation, and smooth muscle actin (SMA) for smooth muscle cell (SMC).

At 4.5-hours post-pMCAO no differences were seen in CD11b+ immune cell recruitment between WT and KO mice (Supplementary Fig 3A-3C). Interestingly, by 6-hours KO mice have significantly higher total CD11b+ immune cell recruitment compared to WT controls (WT: 0.95 ± 0.21 cells/100μm; KO: 2.37 ± 0.35 cells/100μm) (Fig 3C). KO mice also display higher recruitment of CD11b+/Iba1+

monocytes/macrophages (WT: 0.71 ± 0.14 cells/100μm; KO: 1.63 ± 0.32 cells/100μm) and CD11b+/Iba1- other immune cell types compared to their WT counterparts (WT: 0.24 ± 0.08 cells/100μm; KO: 0.73 ± 0.15 cells/100μm) (Fig 3D-3E). At 24-hours post-pMCAO, KO mice maintain significantly higher total CD11b+ immune cell recruitment to collateral vessels (WT: 1.80 ± 0.19 cells/100μm; KO: 3.1 ± 0.61 cells/100μm), but no differences are seen in CD11b+/Iba1+ monocytes/macrophages (WT: 1.08 ± 0.12 cells/100μm; KO: 1.55 ± 0.32 cells/100μm) or CD11b+/Iba1- (WT: 0.71 ± 0.14 cells/100μm; KO: 1.55± 0.69 cells/100μm) subpopulations compared to WT mice (Fig 3F-3H).

Analysis of confocal images of the MCA-ACA pial collateral vessels indicated that at 6-hours, no changes were seen in the number of proliferating DiI+/PCNA+ endothelial cells within the collateral wall of WT vs KO mice (Fig 3M). Conversely, at 24-hours post-pMCAO, KO mice displayed significantly more proliferative DiI+/PCNA+ endothelial cells (8.34 ± 1.42 cells/100μm) in the MCA-ACA pial collateral vessel walls compared to WT mice (2.16 ± 0.64 cells/100μm) (Fig 3I-3L, 3N).

Percent coverage of SMA was utilized to determine if SMC reorganization was occurring. At 24-hours post-pMCAO, no difference was observed in SMA percent coverage in the ipsilateral hemisphere of WT and KO mice (Supplementary Fig 3D-3F).

EphA4 Functions Through Restriction of the Tie2 Signaling Pathway

It has previously been shown that blockade of the Tie2 receptor using soluble Tie2-Fc reverses the protective effects seen in an EphA4-Tie2Cre KO mouse model after stroke [10]. Protein analysis of WT and KO cortex 24-hours post-pMCAO shows increased Tie2, p-Tie2, and angiopoietin-1 expression in KO mice compared to WT controls. However, no differences were seen in the expression of Angiopoietin-2, a classical antagonist of the Tie2 receptor. To provide further insight into the link between EphA4 and Tie2,

EC-specific Tie2 deficient knockdown (tKD) and double Tie2/EphA4 deficient KD (dKD) mice were generated on a mixed background (Fig 4F). No differences were seen in the ipsilateral MCA-ACA collateral diameters or in MCA-ACA collateral number in either genotype compared to WT controls (Fig 4G-4I). Similarly, no change was seen in infarct volume among the genotypes (Fig 4L). The lack of change in collateral diameter or tissue loss between genotypes indicates EphA4 is primarily exerting its restrictive effects on collateral growth through the constraint of the Tie2 pathway.

Pharmacological Targeting of the Tie2 receptor increases EC response to injury in vitro.

To investigate if stimulation of the Tie2 receptor could overcome the negative regulation of EphA4 on pial collaterals, Vasculotide – an angiopoietin-1 memetic peptide – was employed (Supplementary Fig 4A). *In vitro,* Vasculotide was tested in two forms: a dimer and a tetramer, capable of binding to two or four Tie2 receptors, respectively. Treatment on primary, wildtype endothelial cells with the dimer Vasculotide construct resulted in no improvements in wound healing, regardless of the concentration, within the first 48-hours post-scratch (Supplementary Fig 4B-4E). However, the tetramer configuration of Vasculotide resulted in improved wound healing at 10nM and 500nM concentrations 24-hours post-scratch compared to vehicle treated cells (Vehicle: 40.20 ± 4.96%; 10nM: 67.36 ± 4.85%; and 500nM: 62.18 ± 4.76%). These improvements were not seen at 12- and 48-hours post-scratch. (Supplementary Fig 4B, 4F-4H). Additionally, protein analysis showed significantly higher pTie2 relative to Tie2 in cells treated with 10nM Vasculotide for five minutes compared to vehicle treated cells (Supplementary Fig 4I-4J). Collectively, these findings suggest the tetramer, but not the dimer, construct of Vasculotide can activate Tie2 and improve EC response *in vitro*.

Vasculotide Induced Tie2 Stimulation in WT Mice Results in Neuroprotection and Improved Functional Recovery

To evaluate if activation of Tie2 would recapitulate results seen through genetic deletion of EC-specific EphA4, we treated mice with one dose of Vasculotide (either 3μg/kg or 150μg/kg) via the tail vein immediately following pMCAO. At 24-hours post-injury, mice treated with either dose of Vasculotide exhibited decreased infarct volume compared to vehicle treated controls (Vehicle: 18.73 ± 1.58mm^3; 3μg/kg: 9.09 ± 0.76 mm^3; 150μg/kg: 11.42 ± 1.33 mm^3) (Fig 5A-5D). This reduction in tissue damage correlated with increased CBF recovery in 3μg/kg Vasculotide treated mice at days 1-4 post-pMCAO compared to control treated mice. Alternatively, 150μg/kg Vasculotide treated mice only exhibited improved CBF recovery compared to vehicle treated mice at 1- and 2-days post-injury (Fig 5E-5F).

Vasculotide and vehicle treated mice then underwent a series of behavioral tests to determine how a single dose of the peptide could alter long-term recovery. Mice receiving one bolus dose of 3μg/kg-VT performed significantly better on rotarod than vehicle controls at 3- (Vehicle: 65.00 ± 2.94%; 3μg/kg-VT: 84.67 ± 4.72%) and 7-days post-pMCAO (Vehicle: 76.09 ± 3.48%; 3μg/kg-VT: 92.42 ± 3.46%). The 150μg/kg-VT group had significantly improved performance on the rotarod only at 3-days post-injury (79.00 ± 60%) (Fig 5G). When assessed using the modified neurological severity scoring system, the 3μg/kg-VT group had significantly lower score, indicative of improved recovery, at 1-21-days post-injury, compared to vehicle controls. Meanwhile, the 150μg/kg-VT group only showed significant improvement over vehicle controls at 7-21 days post-pMCAO (Fig 5H). Lastly, mice underwent the adhesive tape test and compared to vehicle controls, mice treated with one 3μg/kg dose of Vasculotide showed significantly lower asymmetry scores at 1-28-days post-pMCAO, while mice treated with 150μg/kg-VT displayed lower scores only at 7-days post-injury (Fig 5I). Taken together these findings indicate Vasculotide is neuroprotective following stroke and that low dose treatment at 3μg/kg confers superior functional recovery after permanent artery occlusion.

Collateral Size and EC Proliferation can be altered with Vasculotide Treatment in vivo

To determine if the previously noted decrease in tissue damage and improved functional recovery were connected to enhanced pial collateral response, Vasculotide or vehicle control treated mice were vessel painted. Mice receiving either dose of Vasculotide exhibited significantly larger ipsilateral MCA-ACA pial collaterals 24-hours post-stroke compared to vehicle controls (Vehicle: 29.60 ± 0.80 μm; 3μg/kg: 37.16 ± 0.64 μm; 150μg/kg: 34.94 ± 0.98 μm) (Fig 6A-6D). However, Vasculotide treatment did not influence ipsilateral MCA-PCA collateral size (Vehicle: 28.46 ± 0.56 μm; 3μg/kg: 29.83 ± 1.06 μm; 150μg/kg: 30.74 ± 1.21 μm) or total MCA intercollateral number (Vehicle: 18.45 ± 1.08; 3μg/kg: 16.09 ± 1.06 μm; 150μg/kg: 18.22 ± 1.31) (Fig 6E-6F). Lastly, we found that Vasculotide treatment increased PCNA+/DiI+ proliferating ECs in MCA-ACA collateral vessels compared to vehicle treated controls (Vehicle: 1.94 ± 0.41; 3μg/kg: 3.92 ± 0.70; 150μg/kg: 4.22 ± 0.56) (Fig 6G-6J). These findings suggest pharmacological targeting of Tie2 can be a novel pathway for enhancing pial collateral response.

EphA4 KO and Vasculotide Treatment Mice Display Similar Alterations Pial Surface Transcriptome Following pMCAO

To improve our understanding of the underlying changes in the pial surface after ischemic stroke, mice were perfused with RNAlater and Evans blue, then frozen. The pial surface was later isolated for RNA extraction (Fig 7A) and bulk RNA sequencing was performed on pooled samples (pial surface from 4 hemispheres/sample). Comparative RNA sequencing analysis of ipsilateral vs contralateral pial surface yielded 2004 upregulated genes and 1240 downregulated genes that were shared between all groups. Mice treated with 3μg/kg Vasculotide had the highest number of uniquely differentially expressed genes after stroke with 466 upregulated and 714 downregulated, compared to 330 upregulated and 547 downregulated in WT-Vehicle and 214 upregulated and 547 downregulated in KO-Vehicle pial surfaces (Fig 7B-7C). When comparing the top differentially expressed genes in the ipsilateral hemisphere of each group, we

find *Krt5, Krt14, Col17a1,* and *Pgam1-ps1* to be differentially regulated in both KO and Vasculotide treated mice compared to WT-Vehicle controls (Fig 7D-H, Table 1). Keratins 5 and 14 dimerize to form keratin intermediate filaments that support stable desmosomes. Together, these findings indicate that activation of Tie2 or loss of EphA4 in endothelial cells can generate similar responses, upregulating genes in the *Krt5/Krt14* pathway, after stroke.

Discussion

The significance of pial collateral vessels in determining patient outcomes after an ischemic stroke is well known. However, limited research has focused on understanding how these vessels respond in the critical, clinically relevant first 24 hours post-stroke. The current study assessed temporal remodeling in the pial collateral vessels and further evaluated the previously implicated EphA4/Tie2 axis in this remodeling process.

EphA4 is a member of the largest family of receptor tyrosine kinases and plays a pivotal role in neurodevelopment [11]. In adulthood, EphA4 has been implicated in numerous disease and injury processes. Previous work in stroke models, have shown that EphA4 activation exacerbates brain edema and reduces functional recovery [13], while inhibiting EphA4 could confer neuroprotection and enhance collateral response [10]. Nevertheless, the outcomes of experiments using EphA4 inhibitors have been inconsistent. KYL increased collateral size in both MCA-ACA and MCA-PCA collateral niches [10], however, EphA4 inhibitor APY failed to show improved functional recovery [14] and inhibitors of molecules downstream EphA4, such as ROCK, have failed to show neuroprotection in stroke models [15]. The differences seen in the above experiments are likely due two factors, firstly, these inhibitors often have poor specificity for EphA4, interacting with other receptors in the Eph/Ephrin family. Secondly, EphA4 is widely expressed in the brain and these inhibitors are unable to target specific cell types that may be beneficial.

Here we find that conditional knockout of EphA4 on ECs led to neuroprotection and improved functional outcomes. These improvements are accompanied by an increase in MCA-ACA collateral size and cellular remodeling within the first 24-hours post-pMCAO. In cortex tissue 1-day post stroke, KO mice exhibit increased Tie2, pTie2 and Ang-1 protein expression. It should be noted that collaterals make up an exceedingly small portion of a cortex sample and analysis of their collateral specific expression could be further evaluated using spatial RNA sequencing coupled with IHC. To strengthen the link between EphA4 and Tie2, conditional EC-specific Tie2 and Tie2/EphA4 knockdown mice were used, and the knockdown of Tie2 nullified the effects of EphA4 ablation on collateral vessel growth.

Due to the high expression of Ang-1 in KO cortex tissue, stimulation of the Tie2 receptor was done by administering an angiopoietin-1 memetic peptide, Vasculotide. Several improvements observed in the EphA4 knockout model were replicated with a single low dose (3ug/kg) of Vasculotide, including enhanced tissue and functional outcomes, along with increased MCA-ACA pial collateral vessel size. This study is not the first to evaluate Vasculotide in a stroke model. Work done with diabetic rats given 3μg/kg Vasculotide i.p. 30 minutes prior to stroke, plus 8 and 24-hours post stroke show decreased infarct volume and improved functional recovery [16]. When Vasculotide usage is delayed until 24-hours post-stroke and given daily for 14 days, treatment improved white matter recovery and increased vascular density at the ischemic boarder [17]. Further work is still needed to evaluate if a single dose of Vasculotide can be given at a later timepoint post-stroke (i.e. 6-12 hours) to make treatment with this peptide more clinically relevant.

Furthermore, significant transcriptomic changes were observed in the pial surface of EphA4 KO and Vasculotide treated mice compared to WT controls, specifically involving the *Krt5-Krt14-Col17a1* pathway. Both EphA4 KO and Vasculotide treated mice displayed elevated expression of these genes in their ipsilateral hemisphere compared to WT+Vehicle controls. Although Keratin-5 and Keratin-14 are typically associated with stratified squamous endothelium rather than meningeal tissue, recent evidence

has shown their expression in neural tissue and association with neurological diseases. Keratin 9 has been shown to be upregulated in the cerebral spinal fluid of patients with Alzheimer's disease, multiple sclerosis, and neuromyelitis optica [18, 19]. On the other hand, Krt5 has been shown to be expressed in the choroid plexus of normal rodent brains [20]. In mouse models of chronic alcohol consumption, Krt5 mRNA expression was increased in the hippocampus and decreased in the striatum compared to healthy controls [21]. The mechanism underlying Tie2 activation and its role in upregulating Krt5 expression requires further investigation.

In conclusion, our findings provide evidence of crosstalk between EphA4 and Tie2 in endothelial cells and offer insights into the initial cellular changes in pial collateral vessels. Understanding the mechanisms of collateral growth is crucial for developing targeted therapeutics to enhance arteriogenesis, and our results indicate that activation of Tie2 signaling represents a promising novel therapeutic strategy.

Methods

Animals

All mice were housed in a virus/antigen free, AALAC accredited facility on a 12h light/dark cycle and provided with standard rodent chow and water ad libitum. Mice were used for experiments at 8-12 weeks of age. For EC-specific EphA4 experiments, wild type ($EphA4^{fl/fl}$; WT) and EC-Specific knockout mice ($EphA4^{fl/fl}$/VECadherin-Cre^{ERT2}; KO) were bred on a CD1 background. For Tie2 genetic deletion experiments, wildtype ($Tie2^{+/+}EphA4^{+/+}$/VECahherin-Cre^{ERT2}; WT), Tie2 knockdown ($Tie2^{fl/fl}$/VECaherin-Cre^{ERT2}; tKD), and double EphA4/Tie2 knockdown mice ($Tie2^{fl/fl}EphA4^{fl/fl}$/VECaherin-$Cre^{ERT2}$; dKD) were generated on a mixed CD1/C57Bl6 background. All experiments were performed in accordance with the NIH Guide for the Care and Use of Laboratory Animals and under the approval of the Virginia Tech Institutional Animal Care and Use Committee (IACUC; #21-056) and the Virginia-Maryland College of Veterinary Medicine.

Tamoxifen Injections

Adult male WT, KO, tKD, and dKD mice were intraperitoneally injected at eight weeks of age with 2mg/kg of tamoxifen (Sigma Aldrich; St Louis, MO, USA) diluted in corn oil for five consecutive days. Two weeks following the final injection, tail snips were taken to perform genotyping using the five-primer system as previously described [10]. Briefly, following digestion and centrifugation, 1µl of supernatant, primers (0.2µM), and GoTaq Green Master Mix were used in the PCR reaction per the manufactures protocol (Promega, USA). Tie2 knockdown was confirmed by IHC on serial sectioned tissue from all experimental mice (WT, tKD, and dKD).

Surgical Procedures and Treatments.

Ischemic stroke was induced in adult mice via permanent middle cerebral artery occlusion as previously described [10]. Briefly, mice were anesthetized with 2.5%isolfulane-30% oxygen and received Buprenorphine-SR (3.25mg/kg; EthiqaXR, Fidelis Animal Health, USA). Following hair removal and skin preparation, an incision was made, and a craniectomy performed to expose the left middle cerebral artery. The main distal branch and two bifurcating branches were cauterized. Sham control animals received the same procedure, including exposure of the middle cerebral artery, without ligation. For clEphA4-Fc experiments,

mice received via tail vein injection either clustered 1mg/kg clEphA4-Fc or 0.34mg/kg of soluble human Fc control, immediately following pMCAO. Mice were euthanized at 24-hours and vessel painted for collateral analysis. For Vasculotide experiments, immediately following sham or pMCAO surgery, mice received either saline (vehicle control), 3µg/kg Vasculotide, or 150µg/kg Vasculotide via tail vein injection.

Infarct volume

Fresh frozen or perfused brains were embedded in OCT, frozen, and serial sectioned into 30um slices, 990um apart using a cryostat. Sections were stained with 0.2% cresyl violet (Electron Microscopy

Science, Hatfield, PA, USA). The loss of Nissl staining on six serial sections was quantified using the Cavelieri Estimator from non-biased StereoInvestigator software (MicroBrightField, Williston, VT, USA), as previously described, to determine infarct volume (mm^3) [10, 22].

Behavioral Testing.

All animal behavioral assessments were performed as previously described for pMCAO [10, 23, 24]. *Rotarod.* Mice were trained for 4 consecutive days prior to pMCAO or sham surgery, with baseline measurements recorded on day four and testing performed on days 3, 7, 14, 21, and 28. Four trials were performed per day at 4 rpm and an acceleration of 0.1rpm/sec, with two minutes of rest between trials. *Modified Neurological severity scoring (mNSS).* Deficit was graded on a 0-14 scale (0=normal function; 14=maximum deficit) based on motor, balance, and reflex tests. Baseline measurements were taken one day prior to pMCAO or sham surgeries and mice were tested on days 1, 3, 7, 14, 21, and 28 following the procedure. *Adhesive Tape Test.* A piece of 3mm x 4mm cloth adhesive tape was placed on each forepaw with equal pressure. The mice were returned to a transparent testing box, where the time-to-contact and the time-to-remove were recorded for the ipsilateral and contralateral forepaws. Prior to sham or pMCAO surgery, mice underwent four consecutive days of training and then were tested on days 1, 3, 7, 14, 21, and 28 following surgery. Scores were reported as asymmetry score, as previously published [25]. Asymmetry Score = (contralateral time to remove – ipsilateral time to remove)/(contralateral time to remove + ipsilateral time to remove)*100.

Cerebral blood flow

Analysis of blood flow was done using laser speckle contrast imaging (RFLSI III Laser Speckle Imaging System, RWD, China) through a thinned skull. Briefly, mice were anesthetized 2.5%isolfulane-30% oxygen, the skin was prepared, and a midline incision was made. A drill with a carbide bur was used to thin the skull as previously described [26]. Warmed saline was continuously applied to the thinned skull to keep it moist. Blood flow, via perfusion units, was assessed pre-injury and 10m, 6-hours, and 1-4 days

post-injury. A standardized region of interest (ROI) was used for each mouse and blood flow was calculated relative to the contralateral, uninjured hemisphere.

Vessel Painting and collateral quantification

Vessel painting was performed as previously described [10, 27]. Summarily, following pMCAO or sham procedures and five minutes prior to euthanasia via isoflurane overdose, mice were injected with heparin (2,000 units/kg), and sodium nitroprusside (SNP, 0.75 mg/kg). Following cessation of breathing, mice were perfused with 15mL of 1X phosphate buffered saline (PBS) with 20units/ml of heparin to remove blood. To label the artery/arteriole system (including pial collaterals), 10ml of DiI (0.01mg/ml, Invitrogen) in 4% sucrose-PBS-heparin was perfused followed by 50ml of cold 4% paraformaldehyde to fix the brain tissue. Whole brain tiled images were taken at 4X magnification using a Nikon C2 confocal (Tokyo, Japan). Fiji-ImageJ (NIH) was used for quantification of the number and diameter of intercollaterals.

Nitric Oxide Synthase Inhibitor Treatment

Following pMCAO surgery, mice were placed on L-NAME dissolved in drinking water (1g/L) or plain drinking water as previously described [28]. Mice were allowed ad libitum access to treated or untreated water for 24-hours, at which point they were euthanized and either vessel painted, or brains were snap frozen and serum was collected. Serum samples were processed in accordance with manufacturer guidelines for a nitrate/nitrite colorimetric analysis kit (Cayman Chemical, Ann Arbor, MI, USA) to quantify the end products of nitric oxide metabolism, nitrate (NO_3^-) and nitrite (NO_2^-).

Immunohistochemistry of cortical whole mounts

Whole cortical mounts were dissected, washed in 1xPBS, and placed in 2% Fish Gel with 0.4% Triton block for four hours. Samples were then incubated for two days in rabbit anti-smooth muscle actin (SMA) (Cell Signaling Technology, Danvers, MA, USA; 19245S), rat anti-CD11b (Abcam, Cambridge, UK; ab8878), or rabbit anti-Iba1 (FUJIFILM WakoPure Chemical Corporation, Osaka, Japan; 019-19741) primary antibodies in block at 1:200. Following washing with 1XPBS with 0.1% Tween 20, whole cortical

samples were incubated for two hours at room temperature with Alexa Flour 488 or Alexa Fluor 647 conjugated secondary antibodies (ThermoFisher, Waltham, MA). Samples were washed with 1XPBS + 0.1% Tween 20 and imaged on a Nikon C2 inverted confocal microscope (Tokyo, Japan). For PCNA staining, samples were first incubated for 1.5 hours in 6N HCl at 37°C, followed by a 30-minute incubation in sodium borate to neutralize the acid treatment. The samples were then washed before undergoing the same treatment as the described above using rabbit anti-PCNA (1:300; Cell Signaling Technology, Danvers, MA, USA; 13110).

Endothelial Cell Culture

Primary, brain derived murine endothelial cells were isolated, characterized, and cultured [9]. Briefly, endothelial cells were expanded and then plated in 24-well plates coated with 0.2% gelatin at a seeding density of 75,000 cells/well. The following day, wells were scratched with a 200μL pipette tip, washed twice with PBS, and then treated with Vasculotide or vehicle in base media. Cells were imaged using a Nikon Eclipse Ti2 inverted fluorescence microscope (Tokyo, Japan) at 0-, 12-, 24-, and 48-hours post-scratch. Distance from edge to edge of the scratch was assessed using ImageJ software and wound healing was determined relative to initial (0-hour) measurements. For western blot analysis, ECs were suspended in base media with 10nM Vasculotide or PBS and incubated for 5 minutes at 37°C. Cells were centrifuged, pellets were washed once with PBS, and then resuspended in RIPA buffer for western blot analysis.

Western Blot analysis.

EC or cortex was collected and immediately homogenized on ice in RIPA buffer containing proteinase and phosphatase inhibitors using a hand-held motorized tissue grinder (ThermoFisher, Waltham, MA, USA). Homogonates were spun at 4°C for 20 minutes at 15,000 x *g*, then stored at -80°C until use. Protein concentration was determined using the Pierce™ BCA Protein Assay Kit (ThermoFisher, Waltham, MA, USA) and read on the BioTek Synergy HTX multimode reader (Agilent, Santa Clara, CA, USA). Fifty micrograms of protein were run

per sample on an 8% gel for Tie2/pTie2 or 10% gel for Ang1/Ang2, then transferred onto a PVDF membrane. Membranes were blocked overnight using EveryBlot blocking buffer (Biorad, Hercules, CA, USA) then incubated at 4°C for 48 hours with primary antibody. Primary antibodies: pTie2 (ThermoFisher, Waltham, MA, USA), Tie2, Ang1(R&D Systems, Minneapolis, MN, USA), Ang-2 (Abcam, Cambridge, UK), and β-actin (Cell Signaling Technology, Danvers, MA, USA). Following incubation, membranes were washed in 1XTBST, incubated for 1hr in fluorescent secondary antibodies (LI-COR Biosciences, Lincoln, NE, USA) at room temperature. Imaging was performed on Odyssey Imaging System (LI-COR, Lincoln, NE, USA) and relative density analyzed using Fiji-ImageJ (NIH).

Sequencing

Mice were hand cardiac perfused with 0.9ml of RNAlater (Sigma Aldrich) with 0.1ml 2% Evans blue dye to flush blood, label vasculature, and preserve tissue. Brains were then frozen overnight in RNAlater and pial surfaces were removed the following day. Pial surfaces samples were pooled together from four mice and placed in TRIzol® reagent (ThermoFisher, Waltham, MA. USA). RNA was isolated using the Direct-zol RNA microprep kit (Zymo, Irvine, CA) and total RNA from the pial surfaces according to manufactures instructions and was quantified by absorbance with spectrophotometer ND-1000 (ThermoFisher, Waltham, MA. USA). 1000ng total RNA collected from each tissue sample was shipped to MedGenome Inc. (Foster City, CA, USA) for RNA-seq library construction.

The libraries were sequenced on Novaseq platform with 100 bp paired-end mode (Illumina). Data quality check was performed using FastQC (v0.11.8). The adapter trimming was performed using fastq-mcf program (v1.05) and cutadapt (v2.5). For the RNA-Seq analysis we begin by removing the unwanted sequences, including mitochondrial genome sequences, ribosomal RNAs, transfer RNAs, adapter sequences and others. Contamination removal was performed using Bowtie2 (v2.5.1). Clean reads were mapped to the GRCm38.p6 genome, and Alignment was performed using STAR (v2.7.3a) aligner. Reads

mapping to ribosomal and mitochondrial genomes were removed before performing alignment. The raw read counts were estimated using HTSeq (v0.11.2). R package DESeq2 was applied to get the normalized counts and downstream analysis. Gene with larger than 1.2-fold change and adjusted p-value less than 0.05 were considered significant.

Statistical analysis.

The data was analyzed and plotted with GraphPad Prism, version 9 (GraphPad Software, Inc., San Diego, CA, USA). To compare two experimental groups, the Student's two-tailed t-test was employed. For multiple comparisons, one-way or two-way ANOVA and repeated measures were used, followed by post hoc Tukey's analysis where appropriate. Changes were considered significant at a P-value < 0.05. Mean values, accompanied by the standard error of the mean (SEM), were reported.

Figures:

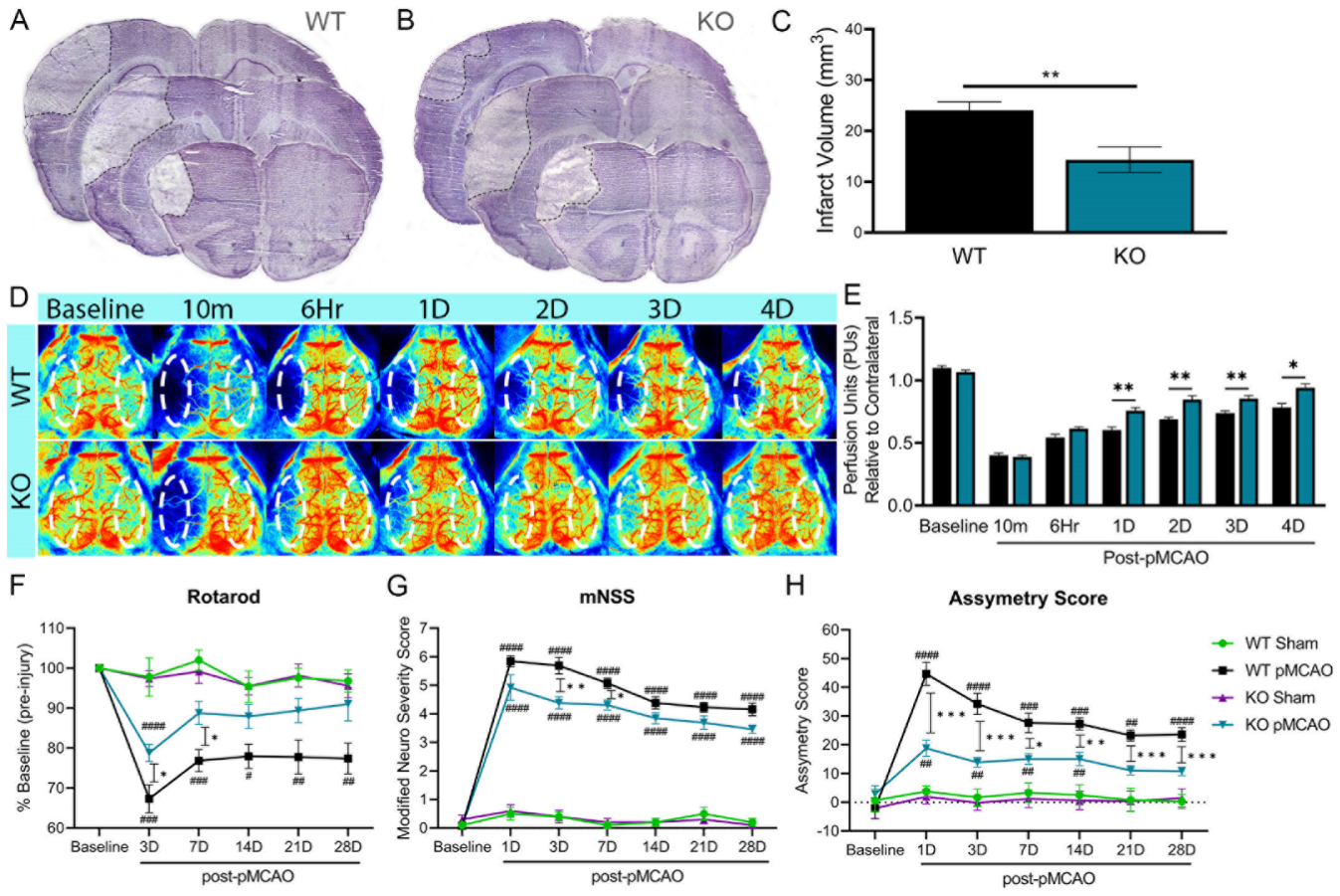

Figure 1. Loss of EC-specific EphA4 reduces infarct volume and improves functional outcome following pMCAO (A) Representative images of nissl stained sections from WT and (B) KO mice. (C) Quantified analysis of infarct volume showed neuroprotection in the KO mice compared to WT control mice at 24-hours post-pMCAO. N=9 (D) Laser speckle contrast images pre-and post=pMCAO of WT and KO mice. (E) Quantification of analysis shows increased CBF in KO mice compared to WT controls 1-4 days post-stroke. N=12-16 (F) Assessment of functional recovery using rotarod, (G) modified neurological severity score, and (H) adhesive tape test indicate improved performance by KO mice compared to WT animals post-pMCAO. N=10-13 *P<0.05; **P<0.01; ***P<0.001 compared to WT mice. #P<0.05; ##P<0.01; ###P<0.001; ####P<0.0001 compared to respective sham groups. Dotted oval in panel D=standardized ROI used to measure CBF.

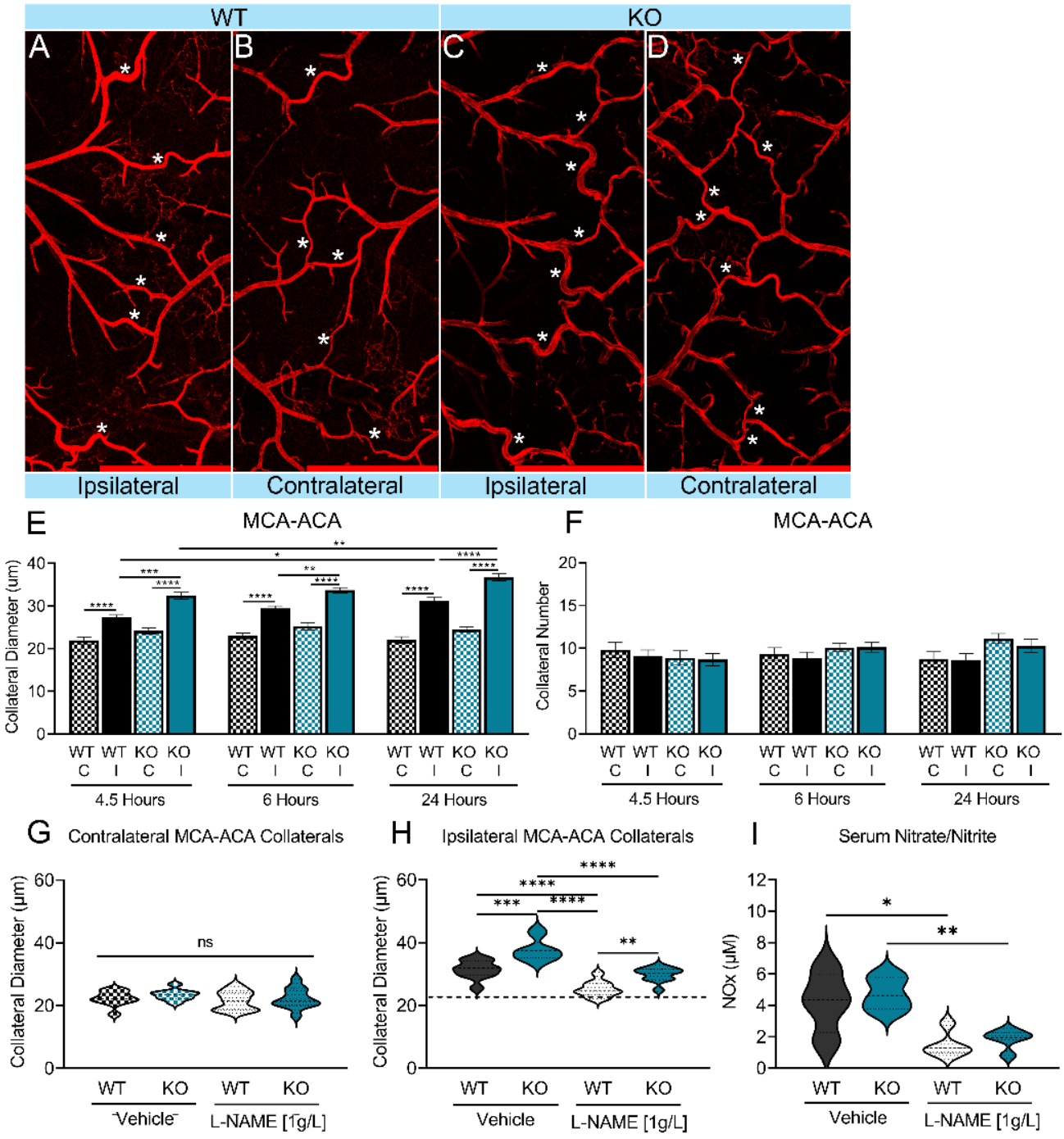

Figure 2. Increased collateral size in a select niche in the acute stages following pMCAO in KO mice. (A-B) Representative 4X tiled images of the MCA-ACA pial collateral niche in WT and (C-D) KO mice. (E) Quantification of collateral diameter in the MCA-ACA collateral niche shows increased vessel size at 4.5-, 6-, and 24-hours post-pMCAO in KO mice compared to WT controls. (F) No significant

differences are seen between genotypes in the number of MCA-ACA connecting pial collaterals present. N=15 (G) Mice were given plain drinking water or water treated with 1g/L of L-NAME immediately following stroke. No difference was seen in MCA-ACA collateral diameter in the contralateral hemisphere of control or L-NAME treated mice 24-hours post-pMCAO. (H) L-NAME treatment significantly decreased collateral diameter in both WT and KO mice compared to vehicle controls. However, MCA-ACA collateral diameter remained elevated in KO mice treated with L-NAME compared to L-NAME treated WT mice. N=9-11 (I) Serum NOx levels 24-hours post-pMCAO shows decreased nitrate/nitrite levels in mice treated with L-NAME compared to control mice. N=4-5. Dashed line in panel H = contralateral collateral diameter. Scale bars = 1mm. *$p<0.05$, **$p<0.01$, ***$p<0.001$, ****$p<0.0001$

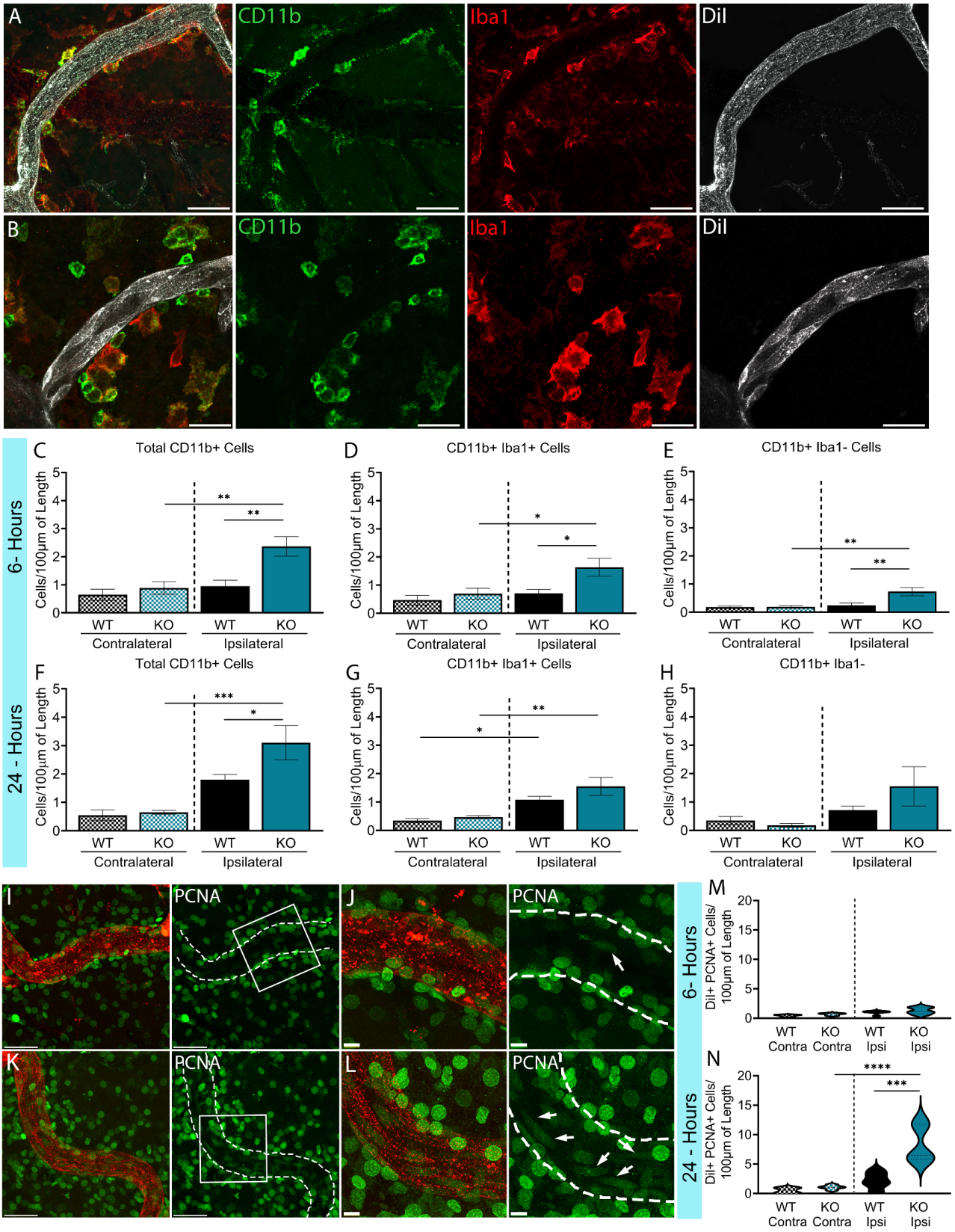
A
CD11b
Iba1
DiI
B
CD11b
Iba1
DiI
6- Hours
24 - Hours
C
Total CD11b+ Cells
D
CD11b+ Iba1+ Cells
E
CD11b+ Iba1- Cells
F
Total CD11b+ Cells
G
CD11b+ Iba1+ Cells
H
CD11b+ Iba1-
Cells/100µm of Length
WT
KO
Contralateral
Ipsilateral
I
PCNA
J
PCNA
K
PCNA
L
PCNA
M
DiI+ PCNA+ Cells/ 100µm of Length
N
DiI+ PCNA+ Cells/ 100µm of Length
WT Contra
KO Contra
WT Ipsi
KO Ipsi

Figure 3. Loss of EC-specific EphA4 results in increased immune cell recruitment EC proliferation. (A) Representative images of WT and (B) KO MCA-ACA pial collaterals at 24-hours post-pMCAO. (C) Quantification of total CD11b+, (D) CD11b+/Iba1+, and (E) CD11b+/Iba1- cells show increased recruitment to KO pial collaterals at 6-hours post-pMCAO, compared to WT controls. (F) Quantification of total CD11b+ cells show increased recruitment to KO vessels compared to WT mice at 24-hours. (G) No change between genotypes is seen in CD11b+/Iba1+, and (H) CD11b+/Iba1- cells being recruited at 24-hours post-pMCAO. N=5-7 (I-J) Representative 40X and 60X images of WT and (K-L) KO MCA-ACA pial collateral vessels at 24-hours post-pMCAO. (M-N) Quantification of PCNA positive endothelial cells determined by elongated nuclei embedded within the DiI vessel paint, shows increased cell numbers at 24 hours but not 6 hours in KO mice. N=5 cortical whole mounts with 4-10 collaterals/whole mount. Scale = 40um for 40X images (A-B, I, K) and 10um for 60X (J, L) *$p<0.05$, **$p<0.01$, ***$p<0.001$, ****$p<0.0001$

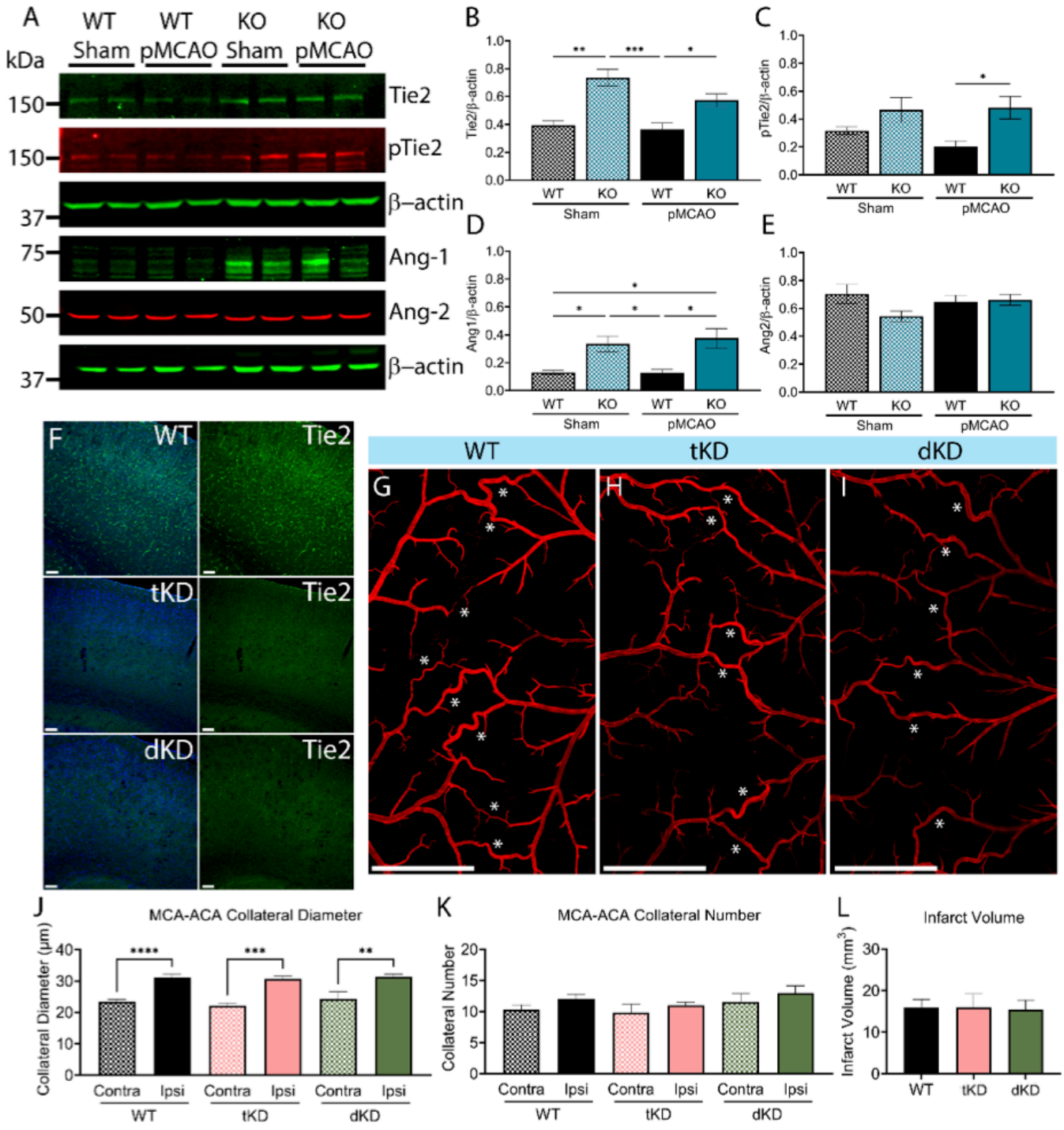

Figure 4. Deletion of Tie2 in endothelial cells fails to alter collateral size or tissue damage. (A) Western blot analysis of cortex samples 24-hours post-pMCAO. (B) Densitometric analysis shows increased Tie2, (C) p-Tie2, and (D) Ang-1 in KO cortex compared to WT after stroke. (E) No differences are seen in Ang-2 expression. N=4 (F) Representative 10X confocal images of Tie2 staining. (G)

Representative 4X tiled confocal images of the ipsilateral MCA-ACA pial collaterals in WT, (H) tKD, and (I) dKD vessel painted brains. (J) Quantification of MCA-ACA diameter and (K) number shows no changes between genotypes. (L) No differences are seen in infarct volume between groups. N=4-7 Scale bars = 100um for 10X images (F) and 1mm for 4X tiles (G-I). *p<0.05, **p<0.01, ***p<0.001, ****p<0.0001

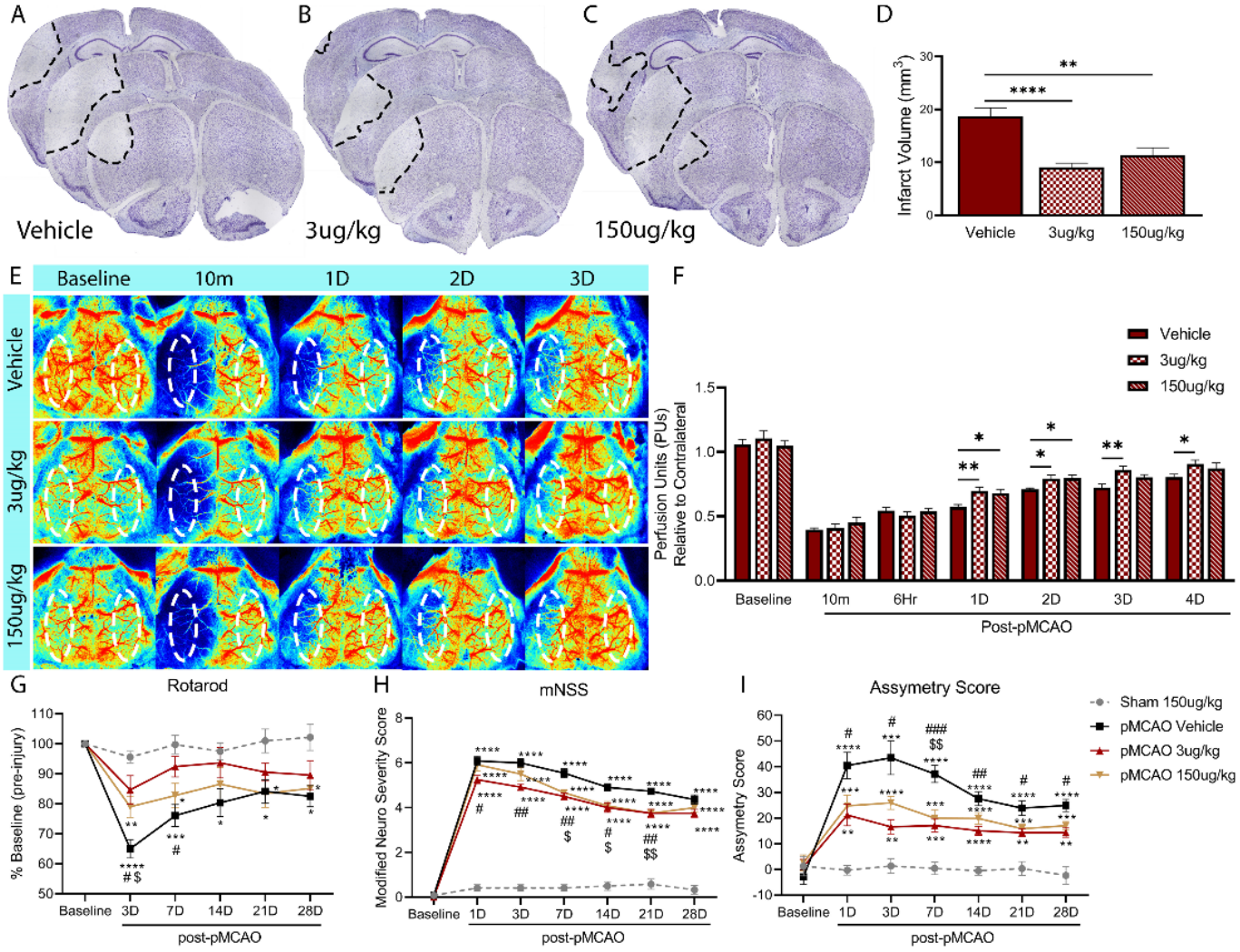

Figure 5. Angiopoetin-1 memetic peptide, Vasculotide, confers neuroprotection and improves functional recovery in *EphA4*$^{fl/fl}$ mice. (A) Representative images of nissl stained sections 24-hours post-pMCAO of WT mice treated with saline (vehicle control), (B) 3µg/kg-VT, or (C) 150µg/kg-VT. (D) Quantitative analysis of infarct volume indicates Vasculotide confers neuroprotection. N=9-10 (E) Representative laser speckle contrast images of CBF in vehicle and Vasculotide treated mice. (F) Quantified CBF analysis pre- and post-pMCAO. N=12-13 (G) Rotarod, (H) modified neurological severity score, and (I) adhesive tape test showed improved performance in Vasculotide treated mice, notably the 3µg/kg-VT group, compared to vehicle controls. N=11-12 Dotted oval in panel

E=standardized ROI used to measure CBF. *= compared to Sham 150µg/kg-VT mice. # = pMCAO 3µg/kg-VT vs pMCAO Vehicle mice. $ = pMCAO 150µg/kg-VT vs pMCAO Vehicle mice. $^{*,\#,\$}p<0.05$, $^{**,\#\#,\$\$}p<0.01$, $^{***,\#\#\#}p<0.001$, $^{****}p<0.0001$

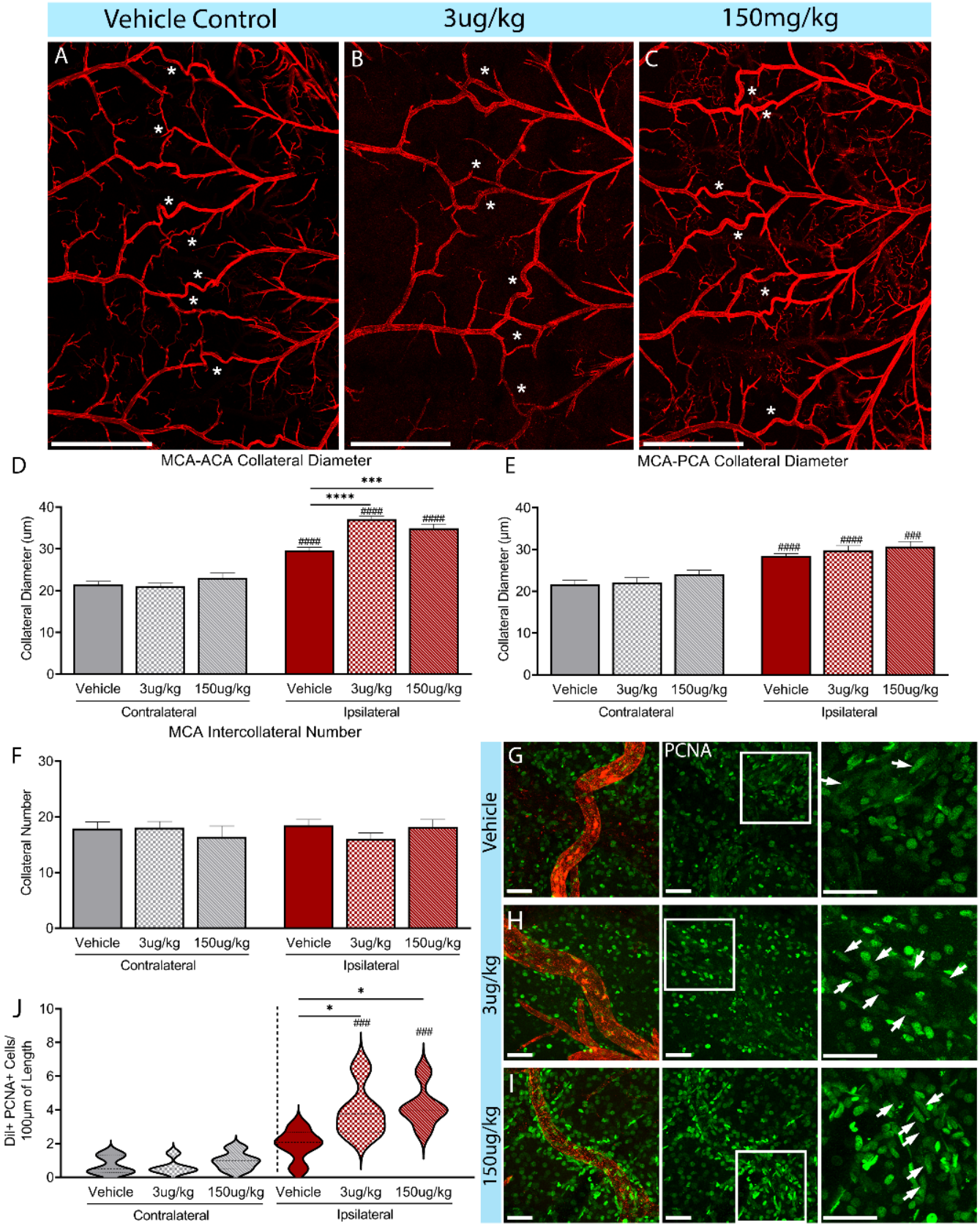
Vehicle Control
3ug/kg
150mg/kg
A
B
C
D
MCA-ACA Collateral Diameter
Collateral Diameter (um)
Vehicle
3ug/kg
150ug/kg
Contralateral
Ipsilateral
E
MCA-PCA Collateral Diameter
Collateral Diameter (µm)
MCA Intercollateral Number
F
Collateral Number
J
Dil+ PCNA+ Cells/ 100µm of Length
G
PCNA
H
I
Vehicle
3ug/kg
150ug/kg

Figure 6. Stimulation of Tie2 via Vasculotide leads to increased collateral size and endothelial cell proliferation. (A) Representative tiled 4X confocal images of vessel painted brains 24-hours post-pMCAO that received vehicle, (B) 3μg/kg-VT, or (C) 150μg/kg-VT. (D) Quantification of the MCA-ACA connecting collateral niche shows VT treatment at either dosage increases collateral diameter at 24-hours post-injury. (E) Vasculotide did not alter size of MCA-PCA connecting collateral vessels or (F) the total number of MCA intercollaterals. N=9-11. (G) Representative 40X images of PCNA stained MCA-ACA pial collateral vessels at 24-hours post-pMCAO from mice receiving vehicle, (H) 3μg/kg-VT, or (I) 150μg/kg-VT. (J) Quantification of PCNA positive ECs indicates Vasculotide treatment at either dose increases proliferation of ECs at 24-hours post-injury. N=5. Scale Bar = 1mm (A-C) or 50um (G-I). #=compared to respective contralateral hemisphere. $^{*,\#}p<0.05$, $^{**,\#\#}p<0.01$, $^{***,\#\#\#}p<0.001$, $^{****}p<0.0001$

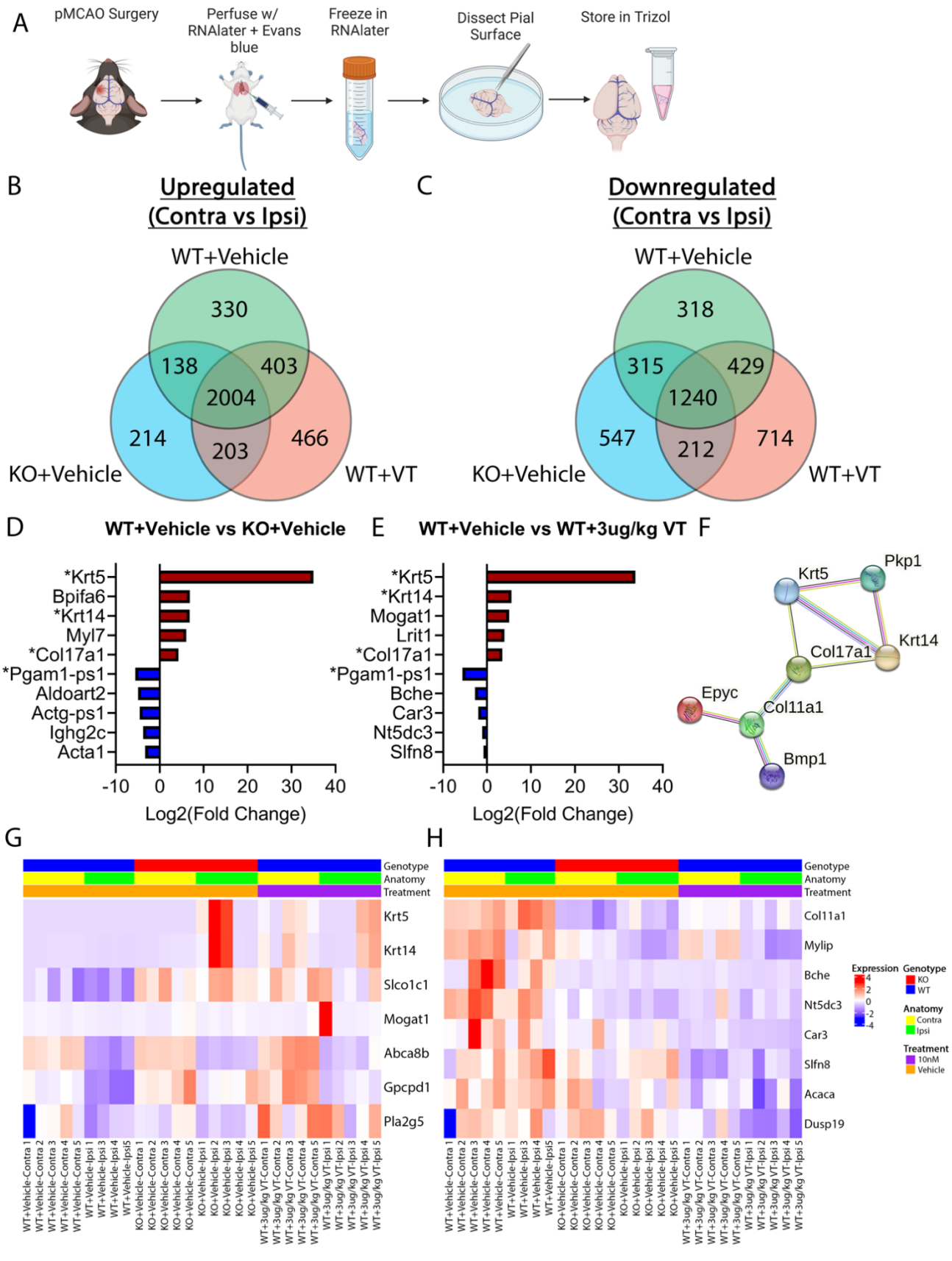
A
pMCAO Surgery
Perfuse w/ RNAlater + Evans blue
Freeze in RNAlater
Dissect Pial Surface
Store in Trizol
B
Upregulated (Contra vs Ipsi)
WT+Vehicle
330
138
403
2004
214
203
466
KO+Vehicle
WT+VT
C
Downregulated (Contra vs Ipsi)
WT+Vehicle
318
315
429
1240
547
212
714
KO+Vehicle
WT+VT
D
WT+Vehicle vs KO+Vehicle
*Krt5
Bpifa6
*Krt14
Myl7
*Col17a1
*Pgam1-ps1
Aldoart2
Actg-ps1
Ighg2c
Acta1
-10 0 10 20 30 40
Log2(Fold Change)
E
WT+Vehicle vs WT+3ug/kg VT
*Krt5
*Krt14
Mogat1
Lrit1
*Col17a1
*Pgam1-ps1
Bche
Car3
Nt5dc3
Slfn8
-10 0 10 20 30 40
Log2(Fold Change)
F
Krt5
Pkp1
Krt14
Col17a1
Epyc
Col11a1
Bmp1
G
Genotype
Anatomy
Treatment
Krt5
Krt14
Slco1c1
Mogat1
Abca8b
Gpcpd1
Pla2g5
H
Genotype
Anatomy
Treatment
Col11a1
Mylip
Bche
Nt5dc3
Car3
Slfn8
Acaca
Dusp19
Expression
Genotype
KO
WT
Anatomy
Contra
Ipsi
Treatment
10nM
Vehicle

Figure 7. RNA sequencing analysis displays altered pial surface transcriptomics in EphA4 KO and Vasculotide treated mice. (A) Schematic of pial surface isolation for bulk RNA sequencing. (B) Venn diagrams of upregulated and (C) downregulated gene expression changes in ipsilateral vs contralateral pial surfaces 24-hours post-stroke. (D) Top upregulated and downregulated genes in the ipsilateral hemisphere of KO-Vehicle or (E) WT-3ug/kg VT compared to WT-Vehicle. * represent genes upregulated by both KO and Vasculotide treated mice. (F) String plot of differentially expressed genes in the KO-Vehicle compared to WT-Vehicle pial surfaces in the Krt5-Krt14 pathway. (G) Heatmap of upregulated and (H) downregulated genes compared to WT-Vehicle contralateral hemisphere.

Genes	WT-PBS v KO-PBS	WT-PBS v WT-3ug/kg	Protein Name	Function
Krt5	*34.9500286	*33.7844355	Keratin 5	Dimerizes with keratin 14 to form keratin intermediate filaments
Krt14	*6.80941442	*5.60230665	Keratin 14	K5/14 filaments support stable desmosomes via protein kinase c alpha
Pkp1	*-0.873522	-0.1659545	Plakophilin-1	Interacts with Keratin 5 and 14; regulates desmosome formation and stability
Prkca	-0.1967567	-0.3824723	Protein kinase C alpha	Phosphorylates keratin 5 to regulate adhesion and migration.
Col17a1	*4.26572569	*3.51790395	Collagen Type XVII Alpha 1 Chain	Coordinates actin and keratin networks; connects to keratin filaments via plectin
Plec	-0.251231	-0.0447901	Plectin	Intracellular protein scaffold that connects Col17a1 to keratin intermediate filaments
Col11a1	*-0.6370792	*-0.5644451	Collagen Type XI Alpha 1 Chain	Component of extracellular matrix (ECM); contributes to ECM rigidity
Bmp1	*-0.3421163	-0.119285	Bone Morphogenetic Protein 1	Metalloproteinase enzyme; Cleaves C-propeptides of type XI procollagen to allow for mature collagen fibril formation
Epyc	*-0.6784174	-0.3927127	Epiphycan	Extracellular proteoglycan; associates with Col11a1

Table 1. Differential Gene Expression in the *Krt5/Krt14* Pathway

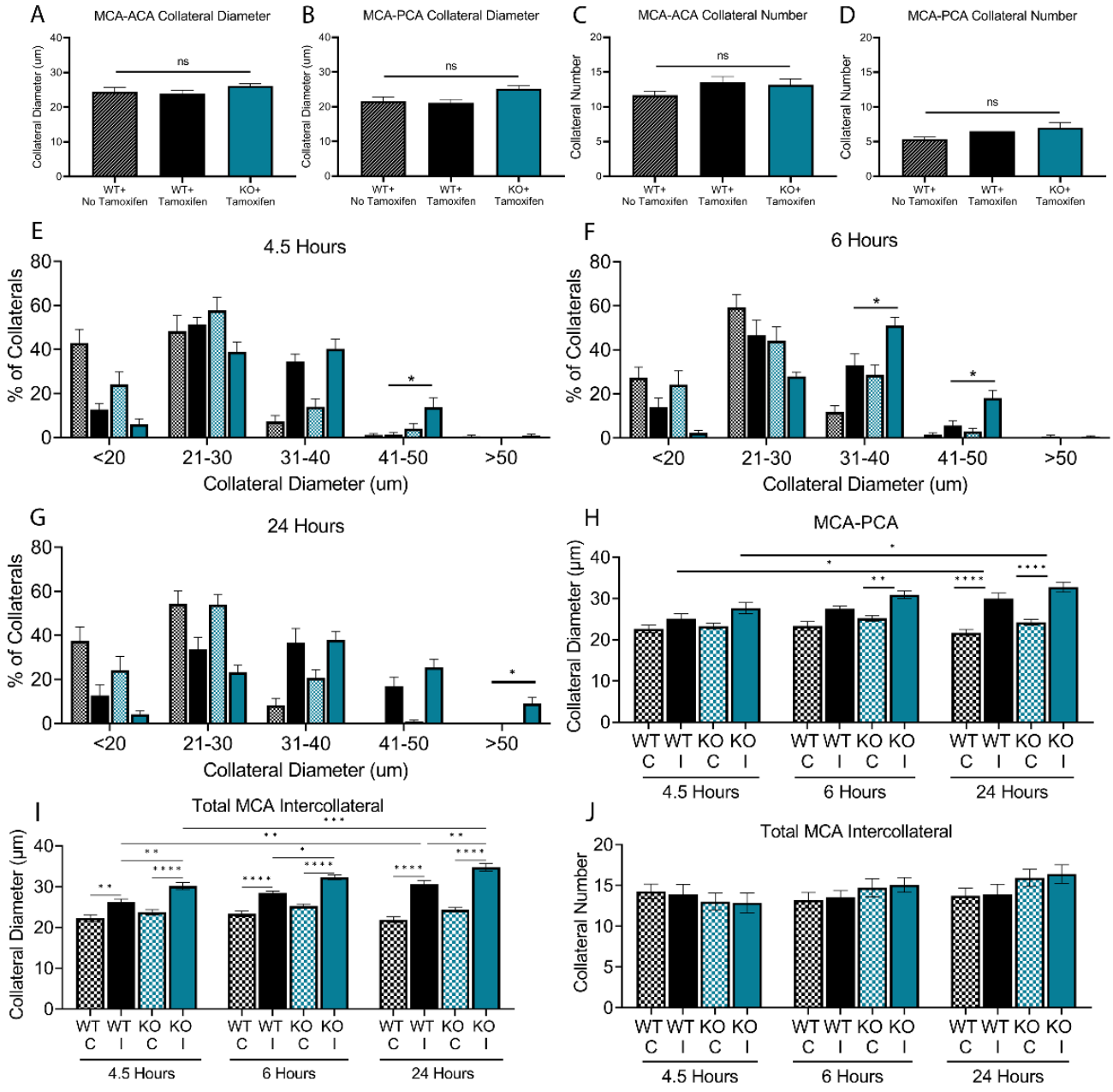

Supplemental Figure 1. Excision of EphA4 from ECs during adulthood does not influence collateral size or number pre-pMCAO. Naïve mice were vessel painted to assess how removal of EphA4 from endothelial cells effected collateral size. (A) Loss of EphA4 did not impact collateral size in either the MCA-ACA or (B) MCA-PCA collateral niches. (C-D) Collateral number was also not altered by tamoxifen injections and subsequent removal of EphA4 from ECs. N=3. (E) Distribution of MCA-ACA

connecting collaterals at 4.5, (F) 6, and (G) 24 hours indicates KO mice have a significantly higher percentage of collaterals in the 41-50 or >50-micron range compared to WT controls. (H) No difference was noted in collateral diameter of MCA-PCA connecting collaterals between WT and KO mice. (I) MCA intercollaterals, consisting of collateral vessels that connect the MCA-ACA and MCA-PCA arterial trees, are significantly larger in KO mice starting at 4.5 hours and going through 24-hours, compared to WT controls. (J) No difference was seen at any time point in the number of MCA intercolaterals between WT and KO mice. N=15. *$p<0.05$, **$p<0.01$, ***$p<0.001$, ****$p<0.0001$

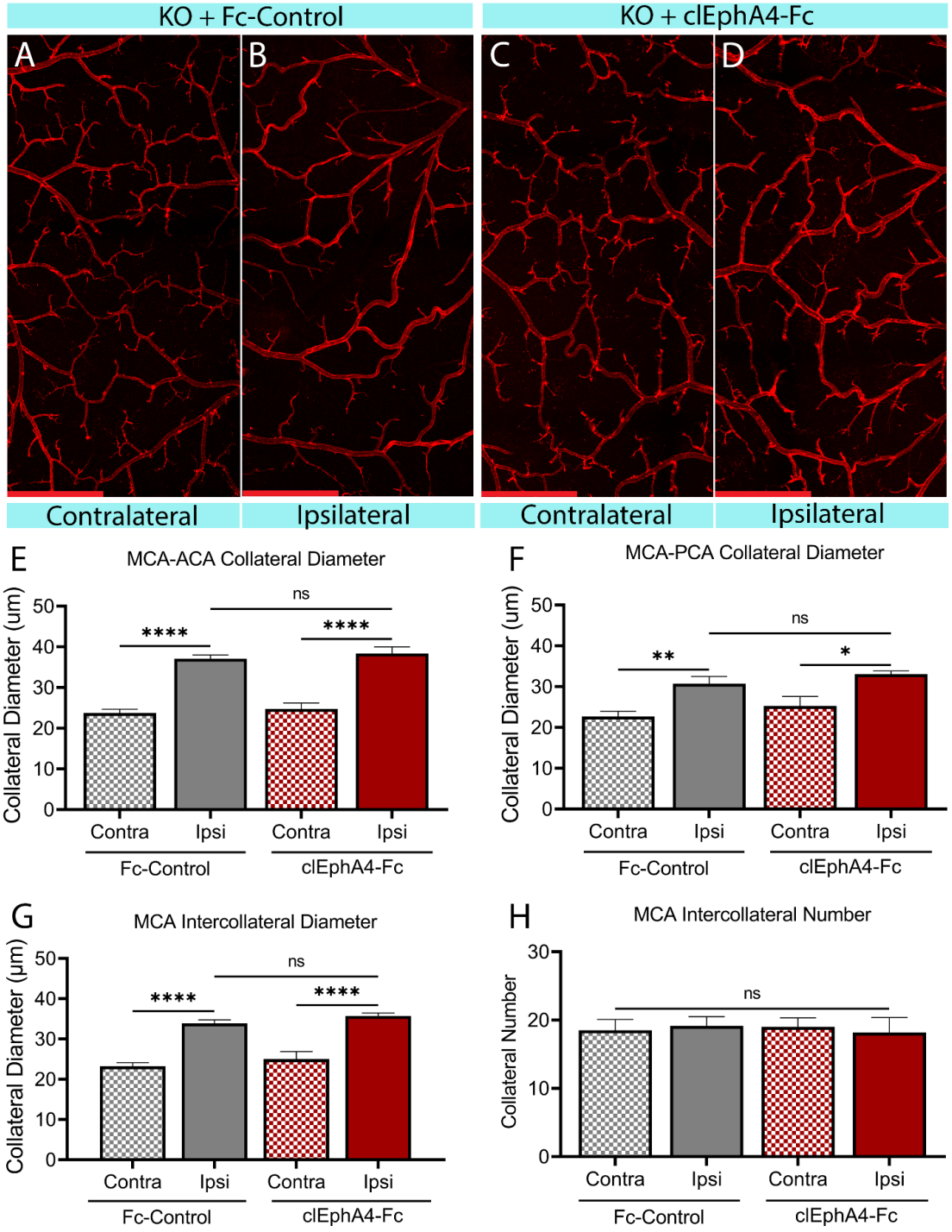

Supplemental Figure 2. EphA4 functions through forward signaling in endothelial cells to regulate collateral growth. (A-B) Representative confocal images of vessel painted MCA-ACA connecting pial collaterals in KO mice that received either clustered Fc-control or (C-D) clEphA4-Fc fusion proteins directly following pMCAO. (E) No differences are observed between the ipsilateral collateral size of KO

mice that received clEphA4-Fc or clustered Fc-control fusion protein in the MCA-ACA connecting or (F) MCA-PCA connecting pial collateral niches. (G) Neither MCA intercollateral diameter nor (H) number was not altered by treatment with clEphA4-Fc compared to Fc-control treated mice. N=5-6 mice. Scale bar = 1mm. *p<0.05, **p<0.01, ***p<0.001, ****p<0.0001

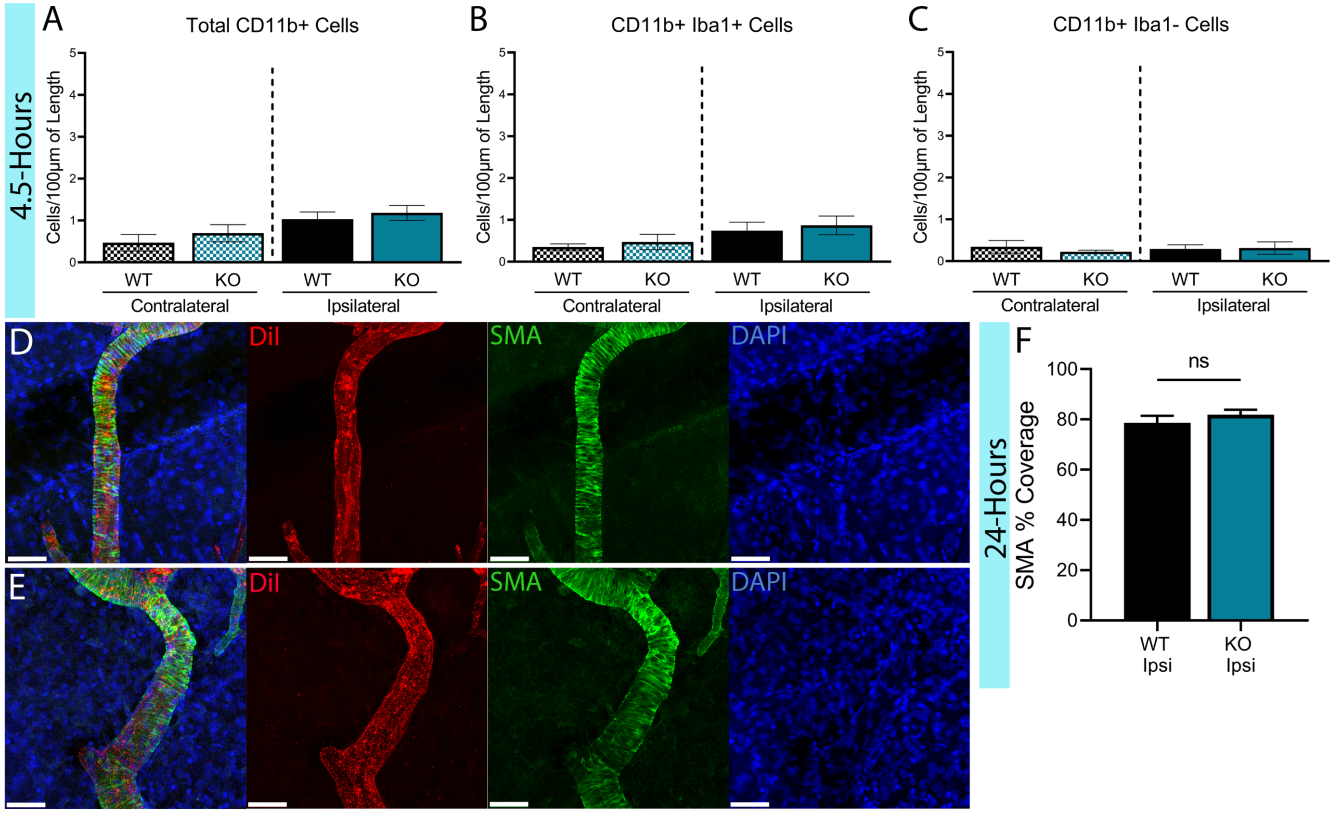

Supplemental Figure 3. EphA4 ablation does not alter early immune cell recruitment or change SMC coverage in the first 24-hours post-stroke. (A) Analysis of total CD11b+, (B) CD11b+/Iba1+, and (C) CD11b+/Iba1- immune cells shows no difference in immune cell recruitment between WT and KO mice at 4.5-hours post stroke. N=5 mice. (G-H) Representative images of MCA-ACA connecting collaterals stained with SMA to show SMCs. (F) Analysis of percent coverage of SMA with DiI indicates that there is no significant change in SMC reorganization at 24-hours post-pMCAO. N=4-5 mice. Scale bar = 50um.

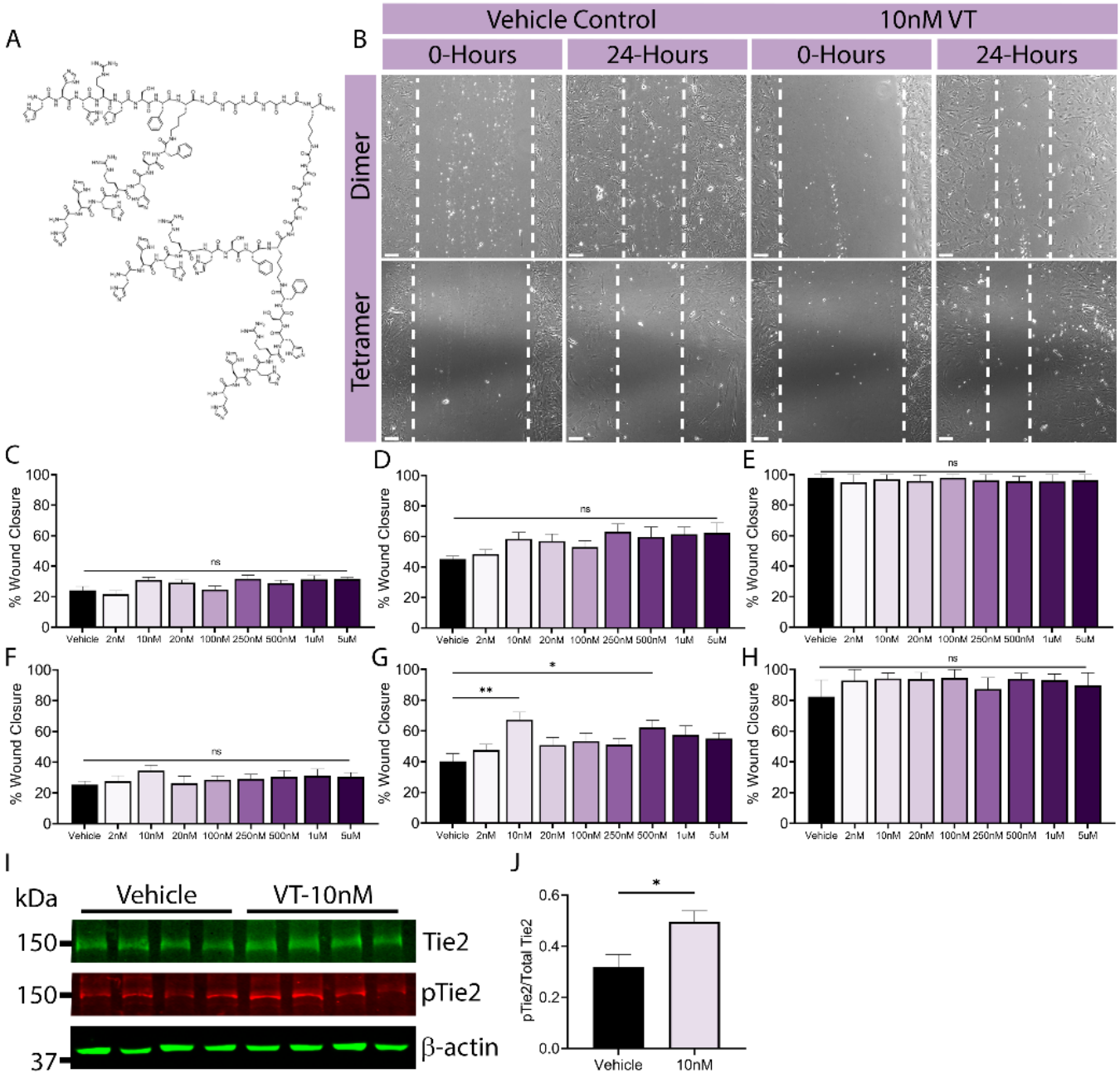

Supplemental Figure 4. Construct of Vasculotide, an angiopoetin-1 memetic peptide, influences endothelial cell response *in vitro*. (A) Schematic of tetrameric construct of the Vasculotide peptide. (B) Representative images of wildtype primary endothelial cells at 0hrs and 24hrs post-scratch treated with dimer or tetramer constructs of Vasculotide. (C) Dimer form of Vasculotide does not influence scratch healing at 12hrs, (D) 24hrs, or (E) 48hrs post-scratch. (F) Quantification of scratch healing after treatment with tetrameric Vasculotide at 12hrs, (G) 24hrs, and (H) 48hrs post-scratch indicates 10nM and 500nM

concentrations significantly improve scratch healing at 24-hours only, compared to vehicle (PBS) treated controls. N=4-5 (I) Western blot analysis of cells after treatment with 10nM Vasculotide or vehicle for 5 minutes. (J) Quantification of pTie2 normalized to Tie2 expression reveals increased pTie2 in Vasculotide treated cells. N=4 *P<0.05; **P<0.01

1. Agarwal, S., et al., *Collateral response modulates the time-penumbra relationship in proximal arterial occlusions.* Neurology, 2018. **90**(4): p. e316-e322.
2. Seker, F., et al., *Collateral Scores in Acute Ischemic Stroke : A retrospective study assessing the suitability of collateral scores as standalone predictors of clinical outcome.* Clin Neuroradiol, 2020. **30**(4): p. 789-793.
3. Zhang, H., D. Chalothorn, and J.E. Faber, *Collateral Vessels Have Unique Endothelial and Smooth Muscle Cell Phenotypes.* Int J Mol Sci, 2019. **20**(15).
4. Ma, T. and Y.P. Bai, *The hydromechanics in arteriogenesis.* Aging Med (Milton), 2020. **3**(3): p. 169-177.
5. Kaloss, A.M. and M.H. Theus, *Leptomeningeal anastomoses: Mechanisms of pial collateral remodeling in ischemic stroke.* WIREs Mech Dis, 2022. **14**(4): p. e1553.
6. Bai, J., et al., *Ephrin B2 and EphB4 selectively mark arterial and venous vessels in cerebral arteriovenous malformation.* J Int Med Res, 2014. **42**(2): p. 405-15.
7. Shin, D., et al., *Expression of ephrinB2 identifies a stable genetic difference between arterial and venous vascular smooth muscle as well as endothelial cells, and marks subsets of microvessels at sites of adult neovascularization.* Dev Biol, 2001. **230**(2): p. 139-50.
8. Jellinghaus, S., et al., *Ephrin-A1/EphA4-mediated adhesion of monocytes to endothelial cells.* Biochim Biophys Acta, 2013. **1833**(10): p. 2201-11.
9. Okyere, B., et al., *Endothelial-Specific EphA4 Negatively Regulates Native Pial Collateral Formation and Re-Perfusion following Hindlimb Ischemia.* PLoS One, 2016. **11**(7): p. e0159930.
10. Okyere, B., et al., *EphA4/Tie2 crosstalk regulates leptomeningeal collateral remodeling following ischemic stroke.* J Clin Invest, 2020. **130**(2): p. 1024-1035.
11. Pasquale, E.B., *Eph-ephrin bidirectional signaling in physiology and disease.* Cell, 2008. **133**(1): p. 38-52.
12. Saito, M., et al., *Remote Ischemic Conditioning Enhances Collateral Circulation Through Leptomeningeal Anastomosis and Diminishes Early Ischemic Lesions and Infarct Volume in Middle Cerebral Artery Occlusion.* Transl Stroke Res, 2022.
13. Chen, F., et al., *Activation of EphA4 induced by EphrinA1 exacerbates disruption of the blood-brain barrier following cerebral ischemia-reperfusion via the Rho/ROCK signaling pathway.* Exp Ther Med, 2018. **16**(3): p. 2651-2658.
14. de Boer, A., et al., *Environmental enrichment during the chronic phase after experimental stroke promotes functional recovery without synergistic effects of EphA4 targeted therapy.* Hum Mol Genet, 2020. **29**(4): p. 605-617.
15. Lemmens, R., et al., *Modifying expression of EphA4 and its downstream targets improves functional recovery after stroke.* Hum Mol Genet, 2013. **22**(11): p. 2214-20.
16. Venkat, P., et al., *Angiopoietin-1 Mimetic Peptide Promotes Neuroprotection after Stroke in Type 1 Diabetic Rats.* Cell Transplant, 2018. **27**(12): p. 1744-1752.
17. Venkat, P., et al., *Treatment with an Angiopoietin-1 mimetic peptide promotes neurological recovery after stroke in diabetic rats.* CNS Neurosci Ther, 2021. **27**(1): p. 48-59.
18. Jiang, S., et al., *Proteomic analysis of the cerebrospinal fluid in multiple sclerosis and neuromyelitis optica patients.* Mol Med Rep, 2012. **6**(5): p. 1081-6.
19. Richens, J.L., et al., *Practical detection of a definitive biomarker panel for Alzheimer's disease; comparisons*

between matched plasma and cerebrospinal fluid. Int J Mol Epidemiol Genet, 2014. **5**(2): p. 53-70.
20. Sathyanesan, M., et al., *A molecular characterization of the choroid plexus and stress-induced gene regulation.* Transl Psychiatry, 2012. **2**(7): p. e139.
21. Zhang, D., et al., *Proteomic Analysis of Brain Regions Reveals Brain Regional Differences and the Involvement of Multiple Keratins in Chronic Alcohol Neurotoxicity.* Alcohol Alcohol, 2020. **55**(2): p. 147-156.
22. Brickler, T.R., et al., *Angiopoietin/Tie2 Axis Regulates the Age-at-Injury Cerebrovascular Response to Traumatic Brain Injury.* J Neurosci, 2018. **38**(45): p. 9618-9634.
23. Bieber, M., et al., *Validity and Reliability of Neurological Scores in Mice Exposed to Middle Cerebral Artery Occlusion.* Stroke, 2019. **50**(10): p. 2875-2882.
24. Bouet, V., et al., *The adhesive removal test: a sensitive method to assess sensorimotor deficits in mice.* Nat Protoc, 2009. **4**(10): p. 1560-4.
25. Baek, H., et al., *Modulation of Cerebellar Cortical Plasticity Using Low-Intensity Focused Ultrasound for Poststroke Sensorimotor Function Recovery.* Neurorehabil Neural Repair, 2018. **32**(9): p. 777-787.
26. Winship, I.R., *Laser speckle contrast imaging to measure changes in cerebral blood flow.* Methods Mol Biol, 2014. **1135**: p. 223-35.
27. Hughes, S., O. Dashkin, and R.A. Defazio, *Vessel painting technique for visualizing the cerebral vascular architecture of the mouse.* Methods Mol Biol, 2014. **1135**: p. 127-38.
28. Lewis, C.V., et al., *Increasing nitric oxide bioavailability fails to improve collateral vessel formation in humanized sickle cell mice.* Lab Invest, 2022. **102**(8): p. 805-813.

Chapter 4

Noninvasive Low-Intensity Focused Ultrasound Mediates Tissue Protection following Ischemic Stroke

This chapter is published as a manuscript in Biomedical Engineering Frontiers

AAAS
BME Frontiers
Volume 2022, Article ID 9864910, 11 pages https://doi.org/10.34133/2022/9864910

BMEF
A SCIENCE PARTNER JOURNAL

Research Article

Noninvasive Low-Intensity Focused Ultrasound Mediates Tissue Protection following Ischemic Stroke

Alexandra M. Kaloss,[1] Lauren N. Arnold,[2] Eman Soliman,[1] Maya Langman,[2] Nathalie Groot,[1] Eli Vlaisavljevich,[2,3] and Michelle H. Theus[1,3]

[1] *Department of Biomedical Sciences and Pathobiology, Virginia Tech, Blacksburg, VA 24061, USA*
[2] *Department of Biomedical Engineering and Mechanics, Virginia Tech, Blacksburg VA 24061, USA*
[3] *Center for Engineered Health, Virginia Tech, Blacksburg Virginia 24061, USA*

Correspondence should be addressed to Michelle H. Theus; mtheus@vt.edu

Received 3 November 2021; Accepted 25 May 2022; Published 7 August 2022

Objective and Impact Statement. This study examined the efficacy and safety of pulsed, low-intensity focused ultrasound (LIFU) and determined its ability to provide neuroprotection in a murine permanent middle cerebral artery occlusion (pMCAO) model. *Introduction*. Focused ultrasound (FUS) has emerged as a new therapeutic strategy for the treatment of ischemic stroke; however, its nonthrombolytic properties remain ill-defined. Therefore, we examined how LIFU influenced neuroprotection and vascular changes following stroke. Due to the critical role of leptomeningeal anastomoses or pial collateral vessels, in cerebral blood flow restoration and tissue protection following ischemic stroke, we also investigated their growth and remodeling. *Methods*. Mice were exposed to transcranial LIFU (fundamental frequency: 1.1 MHz, sonication duration: 300 ms, interstimulus interval: 3 s, pulse repetition frequency: 1 kHz, duty cycle per pulse: 50%, and peak negative pressure: -2.0 MPa) for 30 minutes following induction of pMCAO and then evaluated for infarct volume, blood-brain barrier (BBB) disruption, and pial collateral remodeling at 24 hrs post-pMCAO. *Results*. We found significant neuroprotection in mice exposed to LIFU compared to mock treatment. These findings correlated with a reduced area of IgG deposition in the cerebral cortex, suggesting attenuation of BBB breakdown under LIFU conditions. We also observed increased diameter of CD31-postive microvessels in the ischemic cortex. We observed no significant difference in pial collateral vessel size between FUS and mock treatment at 24 hrs postpMCAO. *Conclusion*. Our data suggests that therapeutic use of LIFU may induce protection through microvascular remodeling that is not related to its thrombolytic activity.

1. Introduction

Ischemic stroke is a leading cause of death and disability that is often associated with a minimal degree of functional restoration. In the hyperacute phase of ischemic stroke, surgical thrombectomy following large vessel occlusion (LVO) is the optimal intervention to remove the primary obstruction and restore cerebral blood flow (CBF) to the penumbra [1, 2]. Because systemic treatment with IV rt-PA has shown little effect in the treatment of LVO, additional means of therapeutic intervention are needed to compliment current treatment options either prior to and/or following thrombectomy. Focused ultrasound (FUS) has been shown to provide good skull penetration, enhance thrombolytic effects, and reduce cerebral

infarction in rodent studies when applied under a range of parameters directly or in combination with t-PA or other therapeutics [3–5]. However, unexpected hemorrhagic complications have been observed in clinical trials testing transcranial low-frequency ultrasound mediated thrombolysis in brain ischemia (TRUMBI) trial, in which unfocused 300kHz ultrasound pulses were applied using long pulses [6, 7]. This trial was ultimately stopped before completion due to high rates of hemorrhage in patients, likely due to the low ultrasound frequency and long pulses used in these treatments. These findings suggest that additional testing for optimal energy levels under cerebral ischemic conditions is needed.

Ultrasound (US) is known to have several biological effects depending on its emission characteristics. Recently, there is growing evidence that US at lower intensities (<2W/cm^2) facilitates enzymatic mediated thrombolysis by breaking fibrin polymers which can increase the effectiveness of thrombolytic drugs. However, in addition to its perceived thrombolytic effects, more information is needed to improve our understanding of the mechanistic underpinnings that may drive acute neuroprotection. Notably, there are no reports in the preclinical literature about intracerebral bleeding or relevant cerebral cellular damage at energy levels up to 1W/cm^2. Additionally, the emitted US beam widens with decreasing frequency, insonating increased volumes of intracerebral vasculature with the low-frequency US therapy and potentially damaging off-target tissues. Therefore, additional studies are needed to confirm the safety and efficacy of US therapy for stroke. Among several ultrasound technologies, low-intensity focused ultrasound (LIFU) has emerged as a noninvasive therapy for several diseases. Previous studies have shown this therapy upregulates neurotrophins, including VEGF and endothelial nitric oxide synthase (eNOS), in animal models of heart disease, vascular dementia, and Alzheimer′s disease ([8, 9]; S. H. [10]). Moreover, additional long-term functional benefits have been shown in models of stroke, with changes suggested to be mediated through angiogenesis and neurogenesis [11, 12].

In the present study, we examined the use of LIFU for the treatment of ischemic stroke using a 1.1MHz single element FUS transducer designed to deliver transcranial LIFU in a murine model. Specifically, we evaluated whether directed LIFU could promote acute neuroprotection in a nonthrombotic murine model of permanent middle cerebral artery occlusion (pMCAO). Another important objective of this study was to verify the absence of adverse effects of LIFU (e.g., hemorrhage) on the brain under ischemic conditions. First, a pilot experiment was conducted to assess the safety of the LIFU therapy applied under two peak negative pressures conditions: ~2.0 MPa and 3.5MPa. Then, additional experiments were completed at a peak negative pressure of 2.0MPa to determine a mechanism of action unrelated to thrombolytic effects. The efficacy and safety of LIFU under the experimental ultrasonic conditions for ischemic stroke therapy were evaluated using a series of postmortem analyses, while closely monitoring for adverse effects of FUS treatment (e.g., hemorrhage) on the brain under ischemic conditions.

2. Results

2.1. Transcranial LIFU Safety and Efficacy. LIFU was applied transcranially for 30 minutes using a 1.1MHz single element FUS transducer following pMCAO for all groups (Figure 1). To determine the safety of transcranial LIFU under the experimental ultrasonic parameters, a pilot study was first conducted comparing two peak negative pressures (*p*−) (1.8 MPa and 3.5MPa). Sham or pMCAO (i.e., stroke) adult, male CD1 mice in the pilot group were exposed to 30 minutes of LIFU at a peak negative pressure of either 1.8MPa or 3.5MPa, with an ultrasonic pulse applied every three seconds (interstimulus interval ðISIÞ = 3s) (*n* = 3-4 mice per group). A pulse repetition frequency (PRF) of 1kHz, duty cycle (DC) per pulse of 50%, sonication duration (SD) of 300ms, and tone-burst duration (TBD) of 0.5ms were used in all experiments. Throughout the surgery and LIFU treatment, the animal was anesthetized using isoflurane and monitored for signs of distress or changes in temperature and respiration rate. After LIFU treatment,

the animal's behavior was noted during recovery, and the treated region was monitored for hemorrhage. Mortality occurred in one of three sham mice and one of four pMCAO mice in the 3.5 MPa treated group. Additionally, hemorrhaging occurred in one of two remaining sham mice and one of three remaining pMCAO mice treated with 3.5 MPa LIFU (Figures 2(a) and 2(b) and 2(d) and 2(e)). The destruction of cerebral arteries and connecting pial arteries was appreciable in the vessel-painted images in the area of 3.5MPa LIFU treatment where hemorrhaging occurred (Figures 2(c) and 2(f)). No mortality or hemorrhage was noted in the sham or pMCAO groups treated with 1.8MPa LIFU. Based on the results from the pilot study, a peak negative pressure of 2.0MPa was chosen for neuroprotection experiments to maximize the potential effects of the LIFU treatment while minimizing any risk to the subjects.

2.2. LIFU Prevents Cortical Tissue Damage and BBB Permeability following pMCAO. Utilizing the pMCAO model of ischemic stroke [13], adult male CD1 mice were first subjected to stroke surgery followed by 30-minute exposure to 1.1 MHz, 2.0MPa peak negative pressure LIFU, or mock LIFU. In the mock LIFU group, the mice were still placed under the transducer and exposed to isoflurane for 30 minutes but did not receive any ultrasound treatment. As seen in the pilot experiment, mice were maintained at $37 \pm 0.5^{\circ}$C and were monitored for changes in respiratory rate or signs of distress. No distress, changes in respiration rate, or hemorrhage were noted in any of the mice. Mice were recovered for 24 hours (hrs) then were euthanized and evaluated for infarct volume. Using 6 Nissl-stained coronal serial sections, we quantified the infarct volume using the Cavalieri probe in MBF StereoInvestigator [14] and observed that mice receiving the LIFU therapy showed a significant reduction in infarct volume compared to mock LIFU ($7.51 \pm 1.44 mm^3$ vs. $19.62 \pm 3.68 mm^3$, respectively, $n = 8$-9 per group $^{**}P = 0.005$) (Figures 3(a)–3(c)). Next, we stained serial coronal sections with anti-mouse-488 antibodies to identify and quantify the area of IgG deposition in the brain at 24hrs post-pMCAO. Compared to mock LIFU (23.77 ± 4.43 mm^3, $n = 5$), we observed a significant reduction in LIFU-treated mice (7.29 ± 2.56 mm^3, $n = 7$, $^{**}P = 0.0016$) (Figures 4(a)–4(c)). IgG deposition was seen in anterior to posterior ipsilateral cortical hemisphere of mock-treated pMCAO mice (Figure 4(a)) which was substantially attenuated in LIFU-treated mice (Figure 4(b)).

2.3. LIFU Increased Microvessel Size in the Ischemic Cortex following pMCAO. To determine if LIFU-mediated neuroprotection is correlated with the microvascular remodeling, we stained coronal sections with a vascular marker, CD31, and measured the microvessel diameter in the ipsilateral cortex. We found that LIFU treatment significantly increased the vessel diameter ($7.07 \pm 0.17 \mu m$, $n = 5$) when compared to mock control ($4.06 \pm 0.11 \mu m$, $n = 4$) (Figures 5(a)–5(e)). This observation suggests a vasodilatory effect of ultrasound which may contribute to the protection against pMCAO induced ischemic stroke.

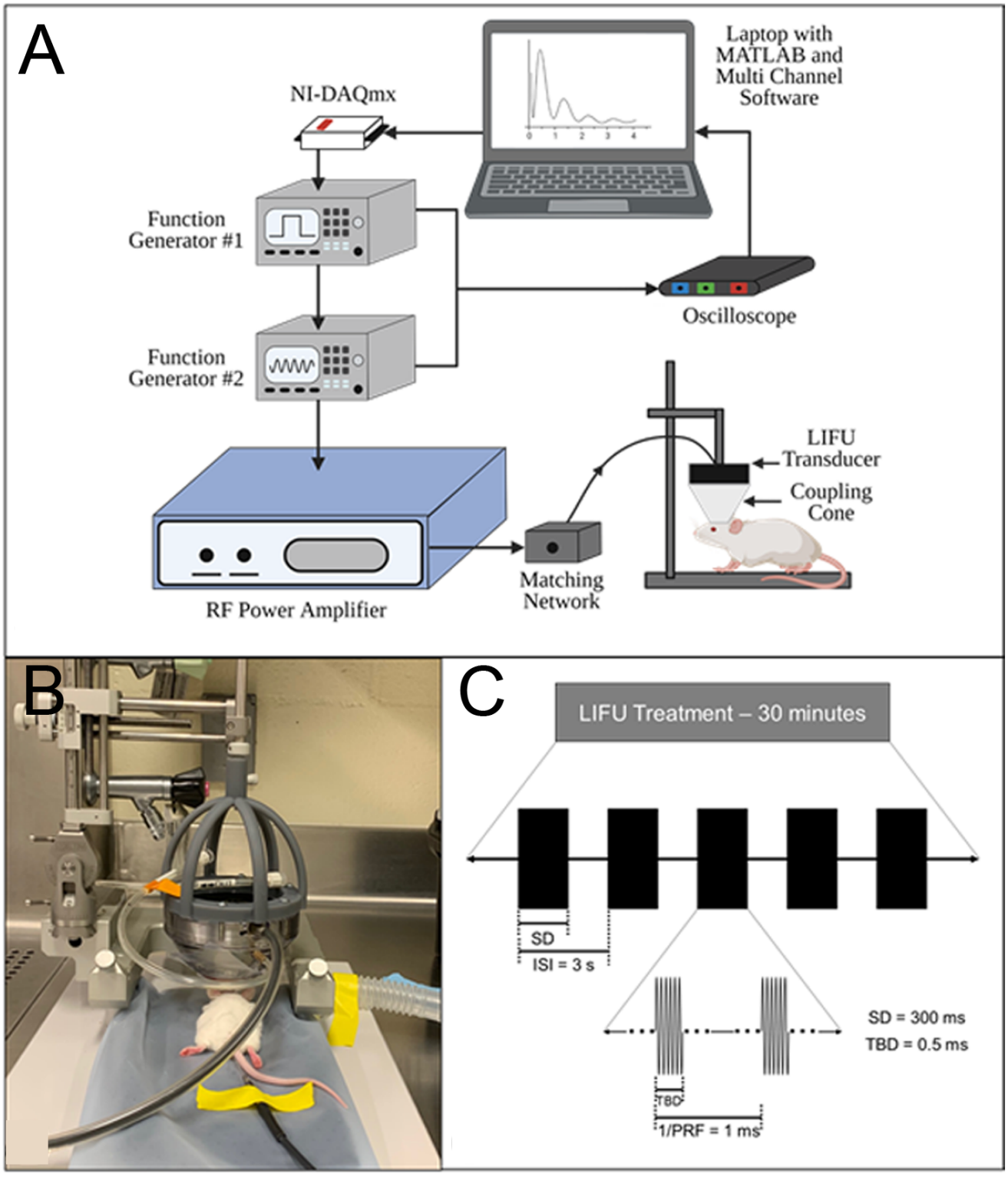

Figure 1. Experimental setup for focused ultrasound treatment following ischemic stroke. (A) Two connected function generators were driven by a custom MATLAB computer program to generate a pulsing signal amplified by a linear power amplifier and transmitted to the FUS transducer. (B) Transcranial focused ultrasound was applied to the cerebral vasculature of an adult, male CD1 mouse using a 1.1 MHz single element transducer coupled to the skull with a coupling cone filled with degassed water. (C) Mice were treated with LIFU at a peak negative pressure of either -1.8 MPa, -2.0 MPa or -3.5 MPa and PRF = 1 kHz, SD = 300 ms, ISI = 3 s, and TBD = 0.5 ms for 30 minutes. Figure 1A created in part with Biorender.com.

2.4. No Change in Leptomeningeal Anastomoses in Response to LIFU Treatment following pMCAO. Leptomeningeal anastomoses or pial collateral vessels are *anastomotic* vessels that provide alternative routes for retrograde cerebral blood flow into the occluded territory following stroke and have a role in preserving the penumbral tissue. Due to the proximity of these vessels to the cranial LIFU treatment, we evaluated whether tissue protection may be due, in part, to their functional remodeling. Using our established vessel painting technique [13, 15, 16], we sought to quantify the diameter and number of pial collaterals at 24hrs post-pMCAO in the ipsilateral and contralateral hemispheres of mock LIFU ($n = 12$) and LIFU-treated mice ($n = 11$). As we previously demonstrated [13, 16], we observed a significant increase in the diameter (μm) of ipsilateral MCA-ACA

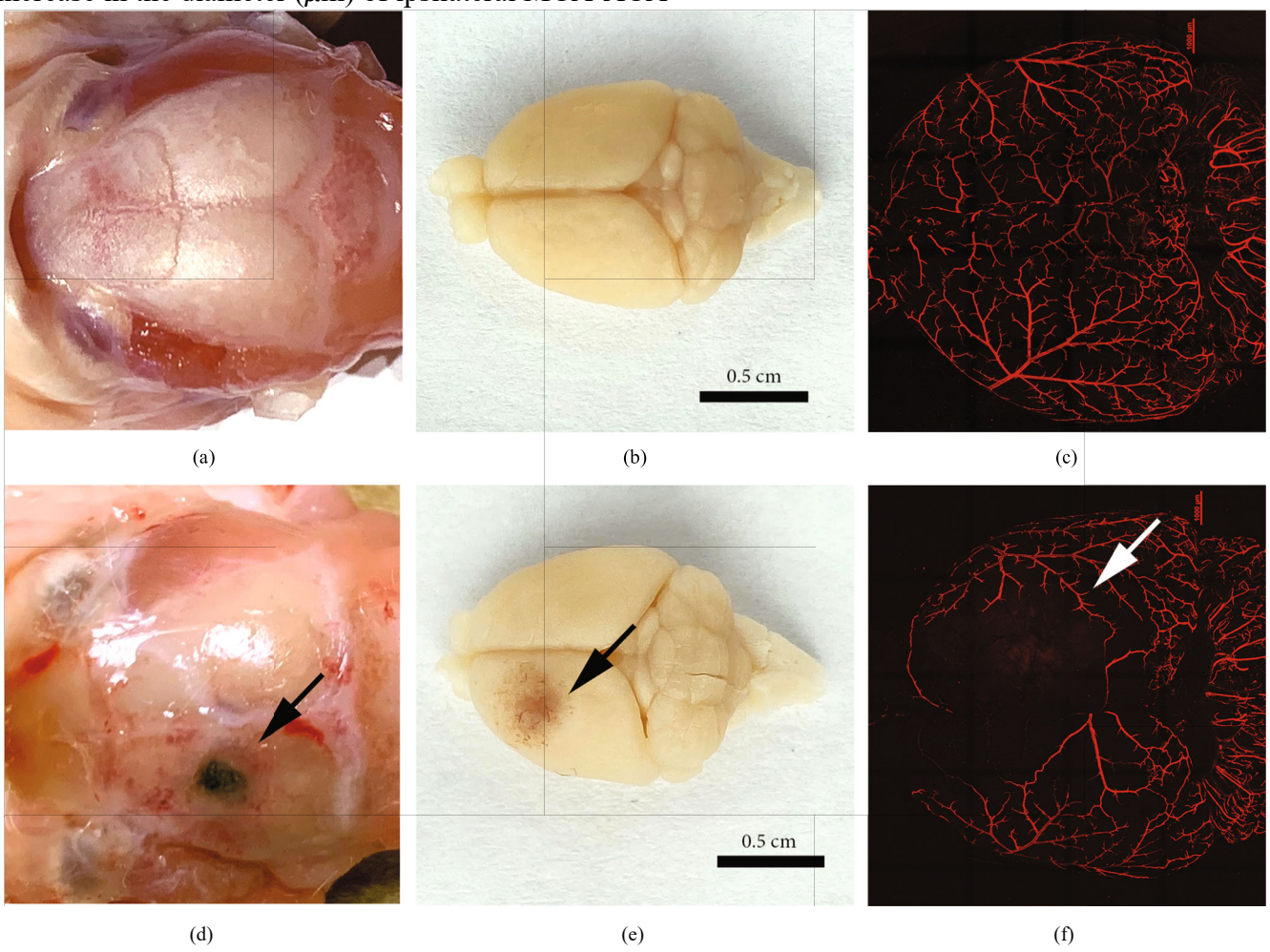

Figure 2: Atypical tissue damage and mortality observed after LIFU treatment at $p-$ 3.5 MPa. (a, b) Representative images of nonhemorrhagic sham brain after LIFU treatment at $p-$ 1.8 MPa. (c) Example of a vessel-painted confocal image after sham surgery and LIFU treatment without ultrasound-induced damage at $p-$ 1.8 MPa. (d, e) Representative images of hemorrhage observed on the brain surface of sham animal after LIFU treatment at $p-$ 3.5 MPa (arrow). (f) Example of a vessel-painted confocal image of tissue damage after sham surgery and LIFU treatment at $p-$ 3.5 MPa (white arrow). Scale = 1000μm.

intracollaterals (30:98 ± 3:75μm) compared to contralateral (24:44 ± 2:80μm; $P = 0:0039$) in the control mock FUS mice(Figures 6(a), 6(b), and 6(e)). Similarly, we found LIFU treated (-2 MPa, 1.1MHz) mice also showed a significant increase in collateral size in the ipsilateral (33:04 ± 4:26μm) vs. contralateral (24:75 ± 6:24μm, $P = 0:004$) hemispheres (Figures 6(c)–6(e)); however, no difference was observed between mock- and LIFU-treated mice. These changes were also observed in the MCA-PCA collaterals

(Figure 6(f)) and in all MCA intercollaterals (Figure 6(g)). No difference in collateral number was seen across groups (Figure 6(h)). Lastly, the size distribution for pial collaterals was assessed. For all MCA intercollaterals (Figure 6(i)), we observed an increase in collateral size in the ipsilateral hemisphere of LIFU-treated mice, with 33.2% of collaterals ranging from 31 to 40 microns and 15.7% from 41 to 50 microns compared to 15.9% and 4.25% in the contralateral hemisphere, respectively. Conversely in mock LIFU mice, a significant increase was seen only in the 31-40-micron range, which contained 38.4% of ipsilateral collaterals but only 16.5% of collaterals in the contralateral hemisphere. Both mock- and LIFU treated mice had significantly fewer collateral vessels ranging less than 20-micron range on the ipsilateral hemisphere (mock: 11.6% and LIFU: 10.2%), compared to the contralateral (mock: 32.4% and LIFU: 40.2%). For pial collaterals connecting the MCA-ACA (Figure 6(j)), the previous trends for LIFU-treated mice remain unchanged with significantly more ipsilateral pial collaterals in the 31-40 and 41-50 range (34.2% and 17.9%) compared to contralateral collaterals (14.9% and 4.2%). Significantly more ipsilateral collaterals were only observed in 31-40-micron range for the mock LIFU group (Ipsi: 35.4% and Contra: 13.6%). Lastly, the LIFU-treated mice also had significantly fewer ipsilateral collaterals in the <20-micron range, with 14.3% of ipsilateral and 31.2% of contralateral collaterals in this range. Although no significant changes were seen in pial collateral size in the LIFU-treated group at 24 hrs, it does not rule out the ability for LIFU treatment to improve or alter vasodilation within the pial collateral niche, which could influence neuroprotection. Overall, these findings suggest LIFU may offer significant neuroprotection through alternative mechanisms to arteriogenesis.

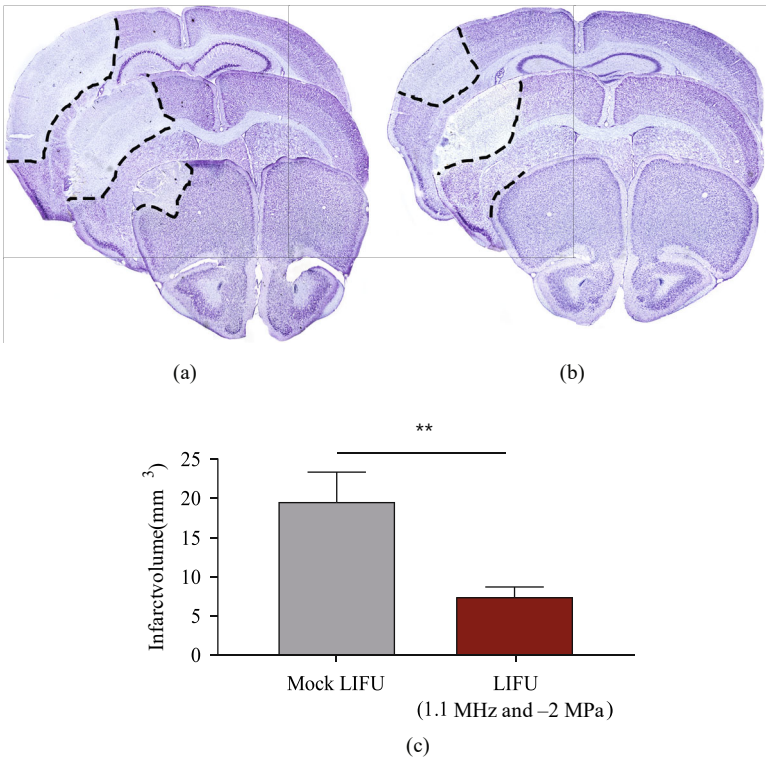

Figure 3: Infarct volume reduced in mice treated with LIFU following ischemic stroke. (a) Representative images of serial Nissl-stained sections at 3 bregma levels in mock-treated and (b) LIFU-treated mice, 1-day post-pMCAO. (c) Quantified data shows a significant reduction in infarct volume in FUS-treated mice compared to mock-treated controls; $n = 8$-9. $^{**}P < 0{:}005$.

3. Discussion

The current study provides further evidence of the safety and neuroprotective properties of LIFU in a murine model of pMCAO. We observed a ~2.5-fold decrease in the infarct volume induced by pMCAO at 24hrs post-pMCAO, and this result correlated with reduced area of IgG deposition in the ipsilateral cortex. Vasogenic edema is a major concern following ischemic stroke and is due to the disruption of the blood-brain barrier (BBB). The decrease in IgG deposition observed indirectly measures BBB function and suggests LIFU may function to prevent the accumulation of extracellular fluid. A decrease in edema following surgically induced ischemic stroke with LIFU treatment has been shown by multiple groups, further supporting this hypothesis [17–19].

We further demonstrate that microvascular remodeling may influence LIFU-mediated protection. LIFU-treated mice showed a significant increase in CD31-positive vessel diameter, which may indicate acute vasodilatory effects of ultrasound. Indeed, previous findings in humans show noninvasive transcutaneous low-frequency ultrasound causes vasodilation in brachial arteries [20]. Focused ultrasound has been shown to trigger the endothelium to release nitric oxide resulting in dilation of blood vessels [21]. Activation of the endothelial cells by focused ultrasound treatment supports VEGF signaling, angiogenesis, and restoration of the BBB, most notable under the anesthetic isoflurane, which was used in the present study [22]. These changes may play a central mechanistic role in the neuroprotective properties of LIFU under ischemic stroke conditions. The sustained vasodilation in the microvessels may also explain, at least in part, the increase in cerebral blood flow by roughly 20% seen in other studies at least 30 minutes posttranscranial focused ultrasound treatment [19]. Transcranial LIFU was applied to the cerebral vasculature, including the MCAACA pial collateral niche, after ischemic stroke using a 1.1 MHz single element transducer. Pulsed LIFU was delivered to the affected cerebral tissue at a PRF of 1kHz, a duty cycle per pulse of 50%, a sonication duration of 300ms, and an interstimulus interval of 3s (Figure 1(c)). However, no change in pial collateral vessel size was noted. The lack of enlargement of these vessels could be due to the short duration of LIFU treatment and indicates neuroprotection is likely linked to the vasodilation of smaller caliber capillaries rather than growth of the pial collateral arterioles.

Histological findings confirm microvascular changes in the penumbra of transcranial LIFU-treated mice compared to mock treatment. Although not evaluated in the current study, previous work has highlighted the importance of blood-brain barrier (BBB) permeability in tissue damage following stroke [23]. Our findings suggest that the use of transcranial LIFU at a fundamental frequency of 1.1MHz and a peak negative pressure of 2.0MPa for 30 minutes after ischemic stroke at defined pulsing parameters can mediate tissue protection compared to previous studies. Indeed, issues have been raised regarding the use of low frequency ultrasound causing increased blood-brain barrier disruptions and intracerebral hemorrhage—particularly in the presence of recombinant tissue plasminogen activator—which was corroborated in rat experiments using 20 kHz ultrasound [24]. We also observed cortical hemorrhagic

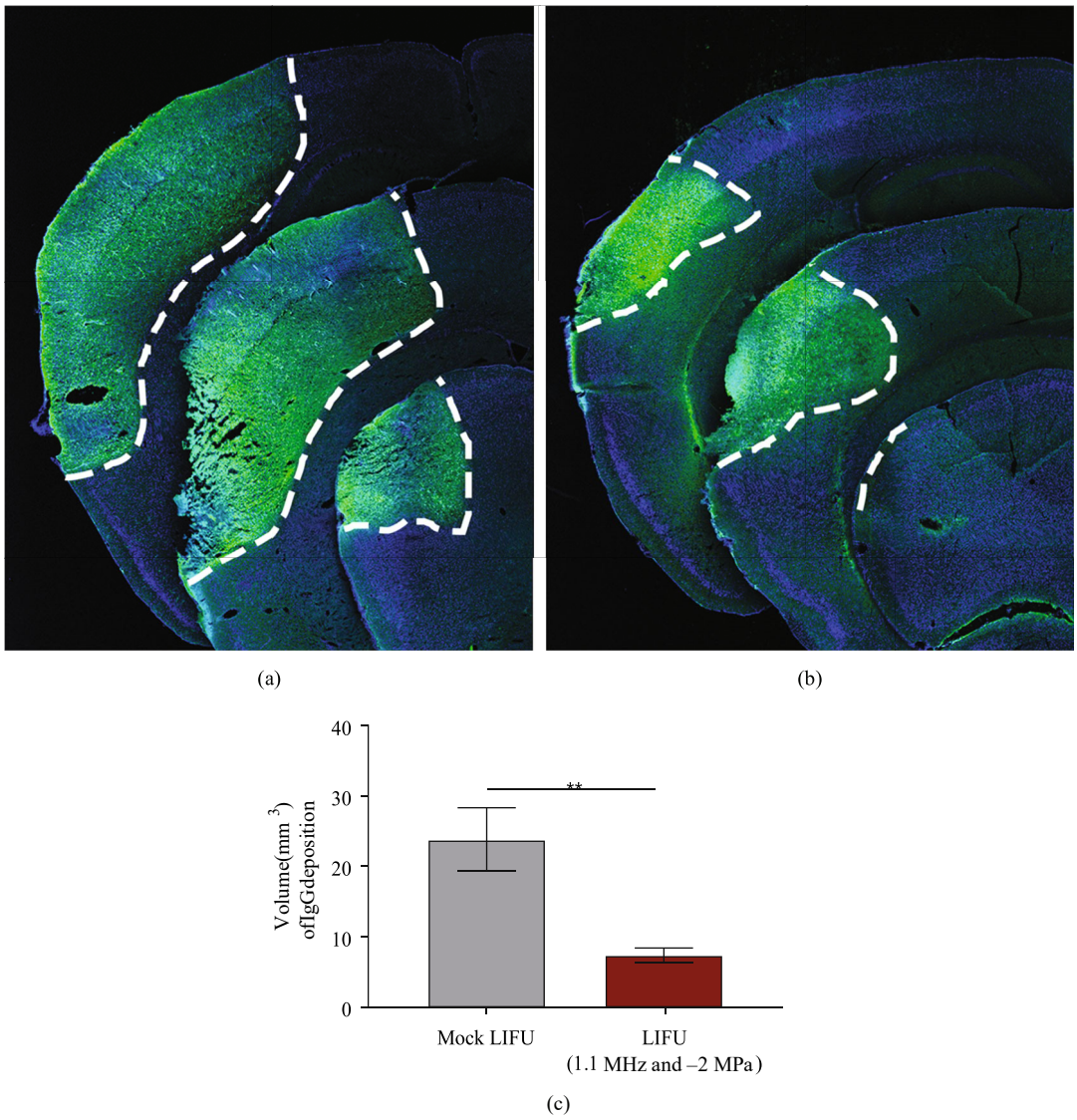

Figure 4: IgG deposition reduced in LIFU-treated mice after pMCAO. (a) Representative confocal images of sections immunolabeled with anti-IgG (green) and counterstained with DAPI (blue) from mock-treated and (b) LIFU-treated mice 1-day after pMCAO. (c) Quantified analysis showing reduced deposition of IgG in LIFU-treated animals compared to mock-treated controls. $n = 5\text{-}7$. $^{**}P < 0.005$.

lesions that appeared like traumatic cerebral contusions on gross morphology and increased mortality when increased ultrasonic pressures were applied to subjects using the same FUS system and pulse schema, but at a peak negative pressure of approximately 3.5 MPa.

Our findings demonstrate the critical need for extensive preclinical evaluation of new devices that can deliver optimal ranges of transcranial LIFU as a therapeutic strategy for ischemic stroke. In this study, we show that our 1.1 MHz system was capable of delivering transcranial LIFU in order to safely induce significant neuroprotection when applied for 30 minutes after the onset of ischemic stroke. Further studies are needed to test the therapeutic window, for example, application up to 6-8hrs postonset of stroke, using large animal models to adjust for skull thickness, as well as uncovering the cellular and molecular mechanisms underlying neural tissue protection that may include microvascular remodeling. Additional modes of action may include modulation of BBB, edema, vasospasms, tissue permeability, interstitial flow, and innate immune regulation [22, 25–27]. Overall, this work demonstrates the neuroprotective properties of LIFU in a murine model of stroke and provides insight into its possible role as a novel neural therapeutic for the treatment of cerebral ischemia.

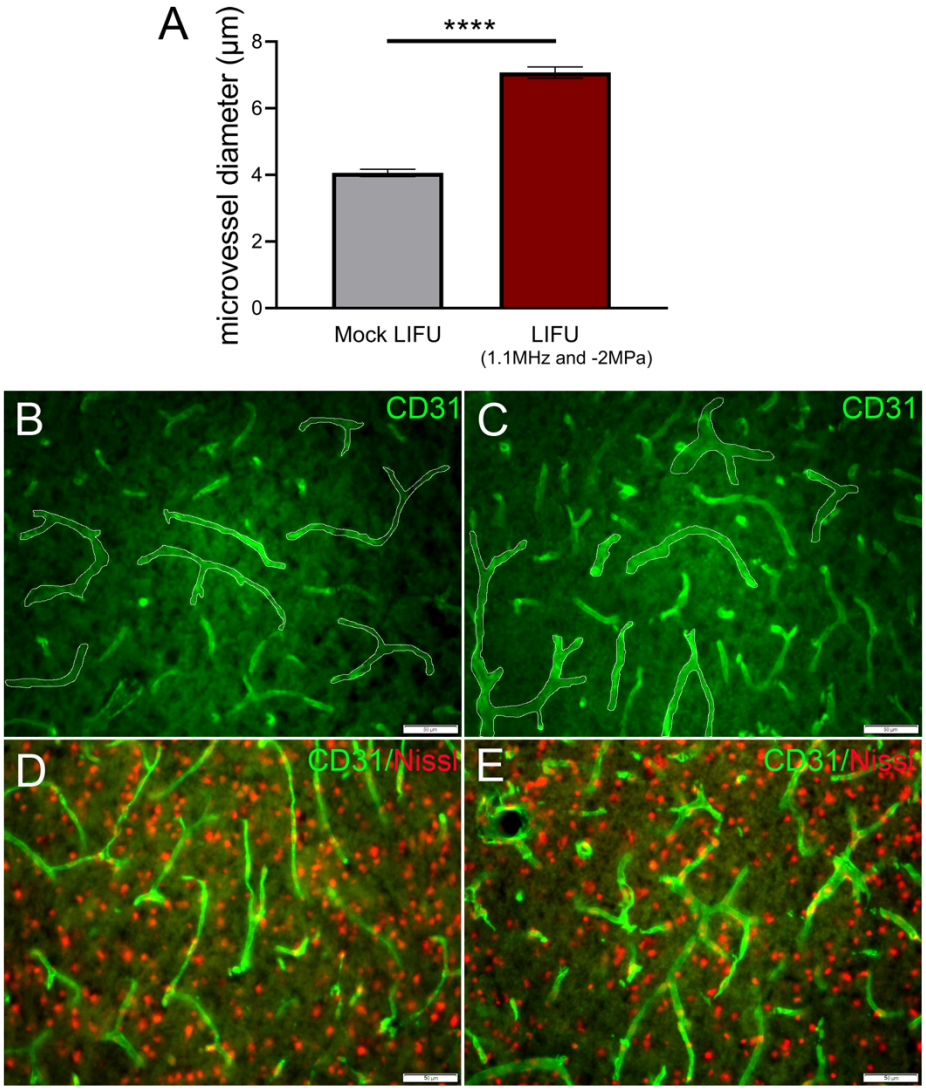

Figure 5: Microvessel size increased in mice treated with LIFU following ischemic stroke. (a) Quantified analysis showing increased microvessel diameter in LIFU-treated animals compared to mock-treated controls. $n = 4$-5. $^{****}P < 0{:}0001$. (b–e) Representative images for IHC staining of CD31 (microvessels, green) and Nissl (neurons, red) in the ipsilateral cortex of (b, d) mock-treated and (c, e) LIFU-

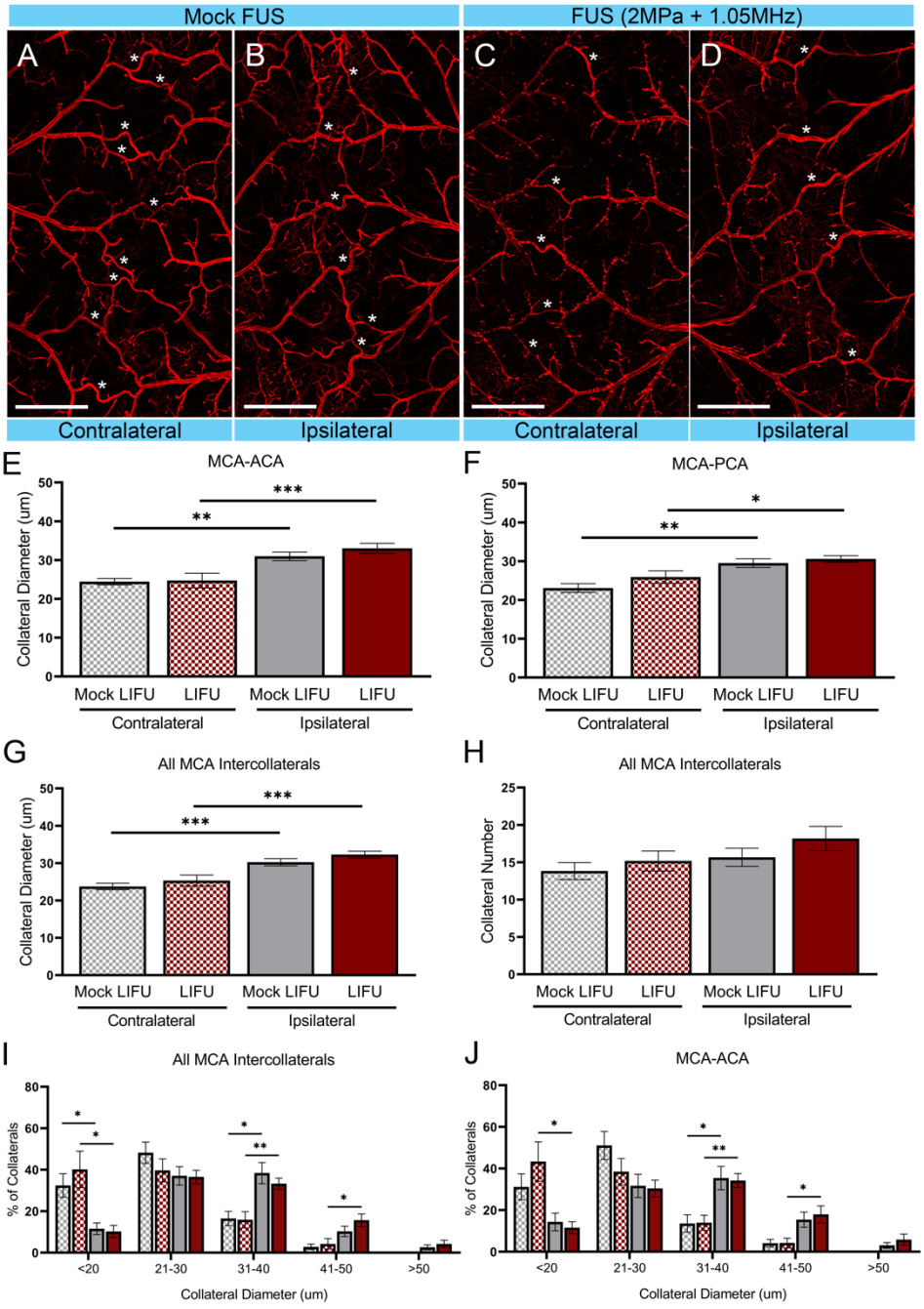

Figure 6: LIFU treatment does not significantly alter pial collateral size. (a, b) Representative vessel-painted confocal images of pial collaterals (stars) in both mock LIFU and (c, d) LIFU-treated brains 1-day post-pMCAO. (e) MCA-ACA, (f) MCA-PCA, and (g) average MCA intercollateral diameters 1-day post-pMCAO. Ipsilateral collaterals were significantly larger than the contralateral collaterals in both groups. No significant difference was seen in collateral diameter size between mock- and LIFU-treated groups. (h) Intercollateral counts show no significant difference in the number of pial collaterals in the control and treated groups. (i) Breakdown of MCA intercollateral and of (j) MCA-ACA collateral diameters after pMCAO. n = 11-12. $^{*}P < 0{:}05$; $^{**}P < 0{:}005$; $^{***}P < 0{:}001$

4. Methods

4.1. Animals. All rodents were bred and housed in an AAALAC accredited, virus/antigen-free facility with a 12 hrs light-dark cycle; food and water were provided *ad libitum*.

treated mice 1-day after pMCAO.

Male CD1 mice ages 8-12 weeks were purchased from Charles River, Durham, NC. All mice were given defined codes prior to pMCAO surgery to enable double-blinded experimentation. A total of fourteen mice were used for the initial safety testing, and 23 mice were used for the final study.

4.2. Surgical Procedures. The murine model of pMCAO was performed as previously described. Briefly, 8-12-week old male mice were given Buprenorphine-SR (0.15mg/kg, ZooPharm, Laramie, WY); then, anesthesia was induced using 2% isoflurane-30% oxygen. During the procedure, mice were maintained at 37 ± 0.5˚C and monitored for changes in respiratory rate. The skull was thinned to expose and cauterize the main and two distal branches of the left middle cerebral artery (MCA). Sham mice received identical procedures and skull thinning, without ligation using cauterization. Transcranial FUS was performed immediately following pMCAO procedures for 30 minutes as detailed below. For mock LIFU-treated animals, the mice were placed under the transducer for 30 minutes, but the ultrasound system was not turned on. During the procedure and recovery, mice were monitored for signs of distress and hemorrhage. Mice were euthanized by vessel painting at 24 hours post-pMCAO.

4.3. Focused Ultrasound System and Treatment Parameters. The transcranial focused ultrasound (FUS) system used in this study is depicted in Figure 1. Two connected function generators were controlled via a current-generation data acquisition driver (NI USB-6501, National Instruments Corp., Austin, Texas, USA) interfacing with a custom MATLAB (The MathWorks, Natick, MA, USA) script using the Data Acquisition Toolbox (MATLAB Data Acquisition Toolbox, The MathWorks, Inc., Natick, MA, USA). MATLAB was used to trigger the first function generator by sending a current signal to the generator at the interstimulus interval (ISI = 3s) for 600 stimulations, resulting in a total sonication time of 30 minutes. The first function generator (SDG5082, Siglent Technologies, Solon, OH, USA) generated a square wave used to trigger the second function generator (SDG1025, Siglent Technologies, Solon, OH, USA) and controlled the pulse repetition frequency (PRF = 1kHz), the duty cycle per pulse (DC = 50%), and the sonication duration (SD = 300ms). The second function generator was used to control the ultrasound fundamental frequency (FF = 1.1MHz), the tone-burst duration (TBD = 0.5ms), and the peak negative pressure ($p-$). All pulsing parameters were chosen after a thorough review of published studies investigating LIFU for neuromodulation and neuroprotection ([17, 28]; L. [29, 30]). The pulsed signal from the second function generator was amplified by a linear power amplifier (2100L, Electronics and Innovation, LTD, Rochester, NY, USA) and transmitted to a 1.1MHz single element focused ultrasound transducer with estimated focal dimensions of 10.21 mm in length and 1.37 mm in diameter (H-101, Sonic Concepts, Inc., Bothell, WA, USA) through its corresponding matching network (Sonic Concepts, Inc., Bothell, WA, USA). The output from both function generators was verified and monitored in real time during treatment using a 2-channel oscilloscope (Handyscope HS5, TiePie engineering, Sneek, Friesland, The Netherlands) and Multi-Channel Software (TiePie Multi Channel Version 1.42.3.1000/0.9.7.3, TiePie engineering, Sneek, Friesland, The Netherlands). The FUS ultrasound transducer was coupled to the mouse skull using a conical coupling device (C-101, Sonic Concepts, Inc., Bothell, WA, USA) filled with degassed water. Ultrasound coupling gel was placed between the membrane of the coupling cone and the animal's skull to further reduce signal attenuation. The components of the FUS system are summarized in Figure 1(a), and a picture of this setup is shown in Figure 1(b). The pulsing regime employed in these studies is pictured in Figure 1(c).

Transcranial FUS was applied to each subject immediately following the pMCAO cauterization procedure (i.e., stroke) for 30 minutes using the pulsing parameters listed above. Focal pressures were measured prior to experiments using a high-sensitivity calibrated rod hydrophone (HNR0500, Onda Corp., Sunnyvale, CA, USA). Before treatment, the FUS transducer was positioned over on the lest

parietal bone 4mm rostral of bregma and 2mm lateral of midline (sagittal suture) on all treated mice and two studies were completed. First, a safety study was conducted on fourteen adult, male CD1 mice with experimental groups as follows. Three sham mice (i.e., mice with craniotomy but without MCA ligation) were treated with 30 minutes of LIFU therapy at $p-$ -1.8MPa, three sham mice were treated with LIFU at $p-$ -3.5 MPa, and two sham mice were left untreated. Four pMCAO (i.e., stroke) mice were also treated with LIFU at $p-$ 3.5MPa, and two pMCAO mice were left untreated. Mice included in the pilot study were monitored for the appearance of gross hemorrhage in the treatment area immediately after treatment and for 24 hours posttreatment. Mortality of each group was also recorded.

Based on the results of the pilot study, eleven adult, male CD1 mice were subjected to the LIFU treatment at a peak negative pressure of -2 MPa. Twelve additional mice were used as an experimental control by applying mock ultrasound where the FUS transducer was positioned over the same region as the treated mice, and anesthesia was maintained for 30 minutes without turning on the ultrasonic device.

4.4. Vessel Painting and Pial Collateral Quantification. The vessel painting technique was performed as previously described [15, 31]. Briefly, male mice were injected with heparin (2,000 units/kg) and sodium nitroprusside (SNP, 0.75 mg/kg) five minutes prior to euthanization, using an overdose of isoflurane. Mice were then perfused with 10 ml of 1X phosphate buffered saline (1X PBS) containing 20 units/ml heparin and then 10 ml DiI (0.01mg/ml, Invitrogen) -4% sucrose-PBS-heparin mixture at a flow rate of 2ml/min followed by 50 ml of cold 4% paraformaldehyde (PFA). Fixed brains were imaged and tiled at 4x magnification on an inverted Nikon C2 confocal microscope. Images were imported into ImageJ (NIH) for quantification of the number and diameter of intercollaterals, as described [13, 16].

4.5. Infarct Volume, IgG Deposition Volume, and CD31 Immunostaining. Perfused fixed brains were cryopreserved in 25% sucrose and then embedded in OCT and serial cryosectioned. Infarct volume (mm^3) was assessed by the Cavalieri Estimator probe using the StereoInvestigator software (MicroBrightField, Williston, VT, USA), as previously described. Briefly, six serial coronal sections, cut at 30 μm, were stained using a 0.2% Cresyl violet solution (Electron Microscopy Science, Hatfield, PA) or anti-mouse IgG-488 (Invitrogen, Waltham, MA). The total volume of infarct was quantified by estimating the area of tissue loss in the ipsilateral cortical hemisphere using six, serial coronal sections. A 100μm spaced grid was placed over the ipsilateral hemisphere in the Cavalieri probe and infarcted area scored. The coronal sections were used for immunohistochemical (IHC) staining of CD31. Sections were blocked with 2% cold water fish skin gelatin (Sigma, Inc., St. Louis, MO) in 0.2% Triton-X100, incubated with goat anti-CD31 (1 :100, R&D systems, Minneapolis, MN, USA) overnight at room temperature (RT), washed with 1X PBS, and then incubated with donkey anti-goat 488 (1 :250, Thermofisher, USA) for 1 hour at RT. Slides were then mounted with DAPI counterstain (SouthernBiotech, Birmingham, AL), and images were acquired using Olympus fluorescence microscope. Microvessel diameters were measured using ImageJ.

4.6. Statistical Analysis. Data was graphed using GraphPad Prism, version 9 (GraphPad Software, Inc., San Diego, CA). Where appropriate, Student's two-tailed t-test was used for comparison of two experimental groups and multiple comparisons by one-way or two-way ANOVA followed by *post hoc* Bonferroni test. Changes were identified as significant at $^{*}P < 0.05$, $^{**}P < 0.01$, and $^{***}P < 0.001$. Each mean value was reported together with the standard error of mean (SEM). An experimenter blinded to the conditions performed all lesion volume and IgG deposition quantifications.

4.7. Study Approval. All procedures were conducted in accordance with the NIH Guide for the Care and Use of Laboratory Animals, the Virginia Tech Institutional Animal Care and Use Committee (IACUC; #18-088).

Abbreviations

VP: Vessel painting
pMCAO: Permanent middle cerebral artery occlusion LIFU: Low-intensity focused ultrasound.

Data Availability

The datasets generated during and/or analyzed during the current study are available from the corresponding author on reasonable request.

Conflicts of Interest

Dr. Eli Vlaisavljevich has an ongoing research partnership and financial relationship with HistoSonics, Inc. Lauren Arnold has an ongoing consulting relationship with Theraclion. No other authors have a conflict of interest to report.

Authors' Contributions

A.K., L.A., N.G., and E.S. performed research and analyzed data. A.K., L.A., M.L., E,V., E.S., and M.T. wrote and edited paper, designed research, and contributed reagents/analytic tools. Alexandra M. Kaloss and Lauren N. Arnold contributed equally to this work.

Acknowledgments

We recognize the Institute for Critical Technology and Applied Science and the Center for Engineered Health for seed grant support. This work was also supported by the National Institute of Neurological Disorders and Stroke of the National Institutes of Health, R01NS112541 (MHT). Lauren Arnold was supported by the Virginia Tech ICTAS Doctoral Scholars Program throughout the duration of this work.

References

[1] M. Goyal, B. K. Menon, W. van Zwam et al., "Endovascular thrombectomy after large-vessel ischaemic stroke: a metaanalysis of individual patient data from five randomised trials," *Lancet*, vol. 387, no. 10029, pp. 1723–1731, 2016.

[2] R. G. Nogueira, A. P. Jadhav, D. C. Haussen et al., "Thrombectomy 6 to 24 hours after stroke with a mismatch between deficit and infarct," *The New England Journal of Medicine*, vol. 378, no. 1, pp. 11–21, 2018.

[3] S. Datta, C. C. Coussios, L. E. McAdory et al., "Correlation of cavitation with ultrasound enhancement of thrombolysis," *Ultrasound in Medicine & Biology*, vol. 32, no. 8, pp. 1257– 1267, 2006.

[4] C. A. Molina, A. D. Barreto, G. Tsivgoulis et al., "Transcranial ultrasound in clinical sonothrombolysis (TUCSON) trial," *Annals of Neurology*, vol. 66, no. 1, pp. 28–38, 2009.

[5] A. Zafar, S. A. Quadri, M. Farooqui et al., "MRI-guided highintensity focused ultrasound as an emerging therapy for stroke: a review," *Journal of Neuroimaging*, vol. 29, no. 1, pp. 5–13, 2019.

[6] A. V. Alexandrov, C. A. Molina, J. C. Grotta et al., "Ultrasound-enhanced systemic thrombolysis for acute ischemic stroke," *The New England Journal of Medicine*, vol. 351, no. 21, pp. 2170–2178, 2004.

[7] M. Daffertshofer, A. Gass, P. Ringleb et al., "Transcranial lowfrequency ultrasound-mediated thrombolysis in brain ischemia: increased risk of hemorrhage with combined ultrasound and tissue plasminogen activator: results of a phase II clinical trial," *Stroke*, vol. 36, no. 7, pp. 1441–1446, 2005.

[8] S. L. Huang, C. W. Chang, Y. H. Lee, and F. Y. Yang, "Protective effect of low-intensity pulsed ultrasound on memory impairment and brain damage in a rat model of vascular dementia," *Radiology*, vol. 282, no. 1, pp. 113–122, 2017.

[9] W. T. Lin, R. C. Chen, W. W. Lu, S. H. Liu, and F. Y. Yang, "Protective effects of low-intensity pulsed ultrasound on aluminum-induced cerebral damage in Alzheimer's disease rat model," *Scientific Reports*, vol. 5, no. 1, p. 9671, 2015.

[10] S. H. Liu, Y. L. Lai, B. L. Chen, and F. Y. Yang, "Ultrasound enhances the expression of brain-derived neurotrophic factor in astrocyte through activation of TrkB-Akt and calciumCaMK signaling pathways," *Cerebral Cortex*, vol. 27, no. 6, pp. 3152–3160, 2017.

[11] C. M. Gorick, J. C. Chappell, and R. J. Price, "Applications of ultrasound to stimulate therapeutic revascularization," *International Journal of Molecular Sciences*, vol. 20, no. 12, p. 3081, 2019.

[12] A. M. Shah, S. Ishizaka, M. Y. Cheng et al., "Optogenetic neuronal stimulation of the lateral cerebellar nucleus promotes persistent functional recovery after stroke," *Scientific Reports*, vol. 7, no. 1, p. 46612, 2017.

[13] B. Okyere, M. Creasey, Y. Lebovitz, and M. H. Theus, "Temporal remodeling of pial collaterals and functional deficits in a murine model of ischemic stroke," *Journal of Neuroscience Methods*, vol. 293, pp. 86–96, 2018.

[14] T. R. Brickler, A. Hazy, F. Guilhaume Correa et al., "Angiopoietin/Tie2 axis regulates the age-at-injury cerebrovascular response to traumatic brain injury," *The Journal of Neuroscience*, vol. 38, no. 45, pp. 9618–9634, 2018.

[15] R. A. Defazio, S. Levy, C. L. Morales et al., "A protocol for characterizing the impact of collateral flow after distal middle cerebral artery occlusion," *Translational Stroke Research*, vol. 2, no. 1, pp. 112–127, 2011.

[16] B. Okyere, W. A. Mills, X. Wang et al., "EphA4/Tie2 crosstalk regulates leptomeningeal collateral remodeling following ischemic stroke," *The Journal of Clinical Investigation*, vol. 130, no. 2, pp. 1024–1035, 2020.

[17] H. Baek, K. J. Pahk, M. J. Kim, I. Youn, and H. Kim, "Modulation of cerebellar cortical plasticity using low-intensity focused ultrasound for poststroke sensorimotor function recovery," *Neurorehabilitation and Neural Repair*, vol. 32, no. 9, pp. 777–787, 2018.

[18] H. Baek, A. Sariev, S. Lee, S. Y. Dong, S. Royer, and H. Kim, "Deep cerebellar low-intensity focused ultrasound stimulation restores interhemispheric balance after ischemic stroke in mice," *IEEE Transactions on Neural Systems and Rehabilitation Engineering*, vol. 28, no. 9, pp. 2073–2079, 2020.

[19] L. D. Deng, L. Qi, Q. Suo et al., "Transcranial focused ultrasound stimulation reduces vasogenic edema after middle cerebral artery occlusion in mice," *Neural Regeneration Research*, vol. 17, no. 9, pp. 2058–2063, 2022.

[20] K. Iida, H. Luo, K. Hagisawa et al., "Noninvasive lowfrequency ultrasound energy causes vasodilation in humans," *Journal of the American College of Cardiology*, vol. 48, no. 3, pp. 532–537, 2006.

[21] A. Maruo, C. E. Hamner, A. J. Rodrigues, T. Higami, J. F. Greenleaf, and H. V. Schaff, "Nitric oxide and prostacyclin in ultrasonic vasodilatation of the canine internal mammary artery," *The Annals of Thoracic Surgery*, vol. 77, no. 1, pp. 126–132, 2004.

[22] A. S. Mathew, C. M. Gorick, E. A. Thim et al., "Transcriptomic response of brain tissue to focused ultrasound-mediated blood-brain barrier disruption depends strongly on anesthesia," *Bioengineering & translational medicine*, vol. 6, no. 2, article e10198, 2021.

[23] X. Jiang, A. V. Andjelkovic, L. Zhu et al., "Blood-brain barrier dysfunction and recovery after ischemic stroke," *Progress in Neurobiology*, vol. 163-164, pp. 144–171, 2018.

[24] T. Gerriets, M. Walberer, M. Nedelmann, G. Bachmann, and M. Kaps, "Blood-brain barrier disruption by low-frequency ultrasound," *Stroke*, vol. 38, no. 2, p. 251, 2007, author reply 252.

[25] P. Y. Chen, K. C. Wei, and H. L. Liu, "Neural immune modulation and immunotherapy assisted by focused ultrasound induced blood-brain barrier opening," *Human Vaccines & Immunotherapeutics*, vol. 11, no. 11, pp. 2682–2687, 2015.

[26] C. T. Curley, A. D. Stevens, A. S. Mathew et al., "Immunomodulation of intracranial melanoma in response to blood-tumor barrier opening with focused ultrasound," *Theranostics*, vol. 10, no. 19, pp. 8821–8833, 2020.

[27] B. P. Mead, C. T. Curley, N. Kim et al., "Focused ultrasound preconditioning for augmented nanoparticle penetration and efficacy in the central nervous system," *Small*, vol. 15, no. 49, article e1903460, 2019.

[28] T. Guo, H. Li, Y. Lv et al., "Pulsed transcranial ultrasound stimulation immediately after the ischemic brain injury is neuroprotective," *IEEE Transactions on Biomedical Engineering*, vol. 62, no. 10, pp. 2352–2357, 2015.

[29] L. Liu, J. Du, T. Zheng et al., "Protective effect of low-intensity transcranial ultrasound stimulation after differing delay following an acute ischemic stroke," *Brain Research Bulletin*, vol. 146, pp. 22–27, 2019.

[30] S. Wu, T. Zheng, J. du et al., "Neuroprotective effect of lowintensity transcranial ultrasound stimulation in endothelin1-induced middle cerebral artery occlusion in rats," *Brain Research Bulletin*, vol. 161, pp. 127–135, 2020.

[31] B. Okyere, K. Giridhar, A. Hazy et al., "Endothelial-specific EphA4 negatively regulates native pial collateral formation and re-perfusion following hindlimb ischemia," *PLoS One*, vol. 11, no. 7, article e0159930, 2016.

Chapter 5

Conclusion and Future Directions

Summary of Findings

The novel ability of pial collateral vessels to remodel into conductance arteries and reroute blood flow back to the ischemic area makes them a novel therapeutic target. Despite substantial research done in various collateral niches, including leptomeningeal anastomoses, much of this research fails to translate into successful clinical trials. This dissertation work begins to elucidate the temporal cellular response of pial collaterals after ischemic stroke and identifies therapeutic options to enhance pial collateral growth.

Previous research has implicated the receptor tyrosine kinase, EphA4, in the restriction of pial collateral vessel growth. In chapter 3, we utilize EC-specific EphA4 KO mice to elucidate the cell specific role of this receptor in collateral vessels after stroke. During the initial hours after stroke, we find that immune cell recruitment precedes endothelial cell proliferation, and both events occur before robust smooth muscle cell reorganization. These responses are accelerated in mice lacking EC-specific EphA4, correlating with increased pial collateral size during the first 24-hours after injury. EphA4 KO mice also exhibited decreased tissue damage and improved functional recovery. Protein analysis indicates EphA4 KO mice express higher Tie2, p-Tie2, and Ang-1 levels than wildtype counterparts. Taken together with results from Tie2 and EphA4/Tie2 genetic knockdown mice, we ascertained that EphA4 restricts collateral growth by suppressing the Tie2 signaling axis.

As Ang-1 was more highly expressed in KO mice, we employed Vasculotide, an Ang-1 memetic peptide, with the aim of recapitulating the results seen in the EphA4 KO experiments using a potentially clinically relevant pharmacological agent. A single bolus, 3ug/kg dose of Vasculotide after pMCAO resulted in decreased infarct volume, as well as enhanced collateral size, endothelial proliferation, decreased infarct volume, and functional recovery. EphA4 KO and 3ug/kg Vasculotide treated mice both displayed similar transcriptomic alterations in the Krt5/Krt14 pathway within the ipsilateral pial surface compared to WT controls after stroke. Conversely, mice treated with a single 150ug/kg dose of Vasculotide were able to recapitulate the increased collateral size and neuroprotection of EphA4 KO mice but failed to robustly enhance CBF recovery and performance on behavioral testing.

In addition to pharmacological targeting of pial collaterals, in chapter 4, we explored a device driven therapeutic to enhance pial collateral growth. Since low-intensity focused ultrasound (LIFU) has been shown to enhance cerebral blood flow in other models, we employed it directly after stroke with the objective of stimulating blood flow through pial collateral vessels and enhancing arteriogenesis. Despite significant neuroprotection, potentially due to microvascular remodeling and modulation, it failed to stimulate pial collateral vessel growth. These findings indicate that while Vasculotide provides a novel therapeutic option for enhancing the pial collateral niche post-stroke, LIFU as a device-driven therapy can offer neuroprotection via a mechanism other than pial collateral enhancement.

Future Directions and Concluding Remarks

Considerable work is still needed to understand the mechanism of collateral growth in the initial 24 hours following an ischemic stroke and of EphA4/Tie2 signaling in this niche. Further studies should focus on determining the intermediary proteins that dictate the interaction between EphA4 and the Tie2/Ang signaling cascade. This information may offer other therapeutic targets outside of the Tie2 receptor, which could lead to enhanced specificity, safety of treatment, or novel combination therapies.

Regarding Vasculotide treatment, one important question remains to be answered. In chapter 3, we delivered Vasculotide directly following pMCAO. Despite being important preliminary work for determining the peptide's efficacy, the timing is next to impossible in a clinical setting. Continued work needs to be performed to determine the optimal timeframe of administration after stroke to achieve the greatest collateral enhancement. Additionally, more information on how Vasculotide impacts other vascular beds, such as capillaries, will assist in elucidating if its neuroprotective effects are due to mechanisms outside of enhanced arteriogenesis. This information may also shed light on other disease and injury models in which Vasculotide treatment may be beneficial.

Lastly, LIFU treatment offered significant neuroprotection after stroke. Like Vasculotide, more research needs to be performed to determine if LIFU remains effective if given at later timepoints after stroke. Similarly, the treatment duration was 30 minutes in the experiments performed in chapter 4, testing alternative treatment durations could elucidate if shorter treatment regimens offer equal efficacy. Lastly, work to discover the mechanism of neuroprotection, such as modulation of the blood brain barrier, should be pursued.

Collectively, the research in this dissertation highlights multiple avenues for neuroprotection after stroke and begins to unravel the temporal cellular mechanism of pial collateral remodeling in the clinically relevant first 24 hours after an ischemic stroke. We have also provided compelling evidence that EphA4 restricts collateral remodeling by hindering Tie2 signaling and that activating this cascade is a novel pharmacological target for enhancing arteriogenesis. Continued research on target therapies aimed at amplifying collateral response is necessary, potentially leading to the extension of the stroke treatment window beyond 24 hours and to improved quality of life in stroke patients.